Delft University of Technology

Final Thesis Geo-Energy Engineering
AESM2310

Storage Performance Analyses of Underground Hydrogen Storage in Depleted Gas Reservoirs

A.G. Ocampo Mendoza (4646347)
To obtain the degree of Master of Science in Applied Earth Sciences
at Delft University of Technology
To be defended publicly on 2 November 2022, at 11:00

Committee:

Hadi Hajibeygi	TU Delft	Supervisor
Walter Eikelenboom	EBN	co-Supervisor
Thijs Huijskes	EBN	Committee member
Maartje Boon	TU Delft	Committee member
Raymond Godderij	EBN	Committee member
Sebastian Geiger	TU Delft	Committee member

Abstract

Overcoming the intermittency problem of renewable energy is an issue that has to be addressed in order to achieve an efficient energy system. Hydrogen has been gaining interests, as green energy carrier, which is included in the energy transition plans of not only the Netherlands, but worldwide. Due to its physical characteristics, large scale storage of hydrogen requires volumes that can only be provided by porous media in the subsurface. Underground Hydrogen Storage (UHS) in depleted gas fields is a large scale storage possibility that is generating attention and increased research. However, it is currently in a Low Technology Readiness Level, meaning that more research, and especially field scale projects are necessary. There is very few literature that tries to use alternative gases as a cushion gas for a UHS. Therefore, this investigation is relevant for the future development of UHS. This investigation will use CMG GEM, a commercial compositional reservoir simulator to model the fluid interactions in the subsurface when hydrogen is stored in depleted gas fields. This will be done by means of a sensitivity analysis, where the hydrodynamic behaviour between hydrogen and possible alternative cushion gases, such as methane, carbon dioxide and nitrogen are studied. Apart from the technical analysis, a simplified economic evaluation is used to calculate a levelized cost to store hydrogen, which will allow for an economic optimized selection of cushion gases in an UHS. The two main constraints for an UHS system are the purity of the extracted hydrogen and the rate at which it is extracted from the subsurface. The results of this investigation show that the mixing of hydrogen with an alternative cushion gas will change drastically based on the degree of the reservoir heterogeneity and the location of the perforated interval. This ever-increasing mixing will have an effect on the capability of the system of delivering pure hydrogen for the expected time.

Acknowledgements

Not surprisingly, I have procrastinated the writing of these acknowledgments to almost the very last moment. With a bit of melancholy, I slowly realize that the writing of this thesis (almost) marks an end to my student life at the TU Delft. These five years abroad have been tough in the academic and personal sense, but they have taught me great life lessons, such as not planning anything on Thursday mornings.

First of all, big shoutout to the Mijnbouwkundige Vereeniging. It has made me feel at home, and has connected me with incredible people with whom I have shared endless committee time, trips, and a couple of study pilsjes. Thank you MV for the unlimited chococinos, for all the activities, and for the endless Glück Aufs.

I would like to thank EBN for the opportunity to write my thesis with them. I have met very knowledgeable, passionate, and helpful colleagues throughout my internship. I also very much enjoyed sharing this time with Bouke and Toon, my fellow interns. Needless to say, I will definitely miss the lunch.

This investigation would not have been possible without the great guidance of my daily EBN supervisor, Walter Eikelenboom. Your advice and remarks mentored and motivated me through this investigation process. I managed to reflect and constantly assess my work with your knowledge of not only Reservoir Engineering, but also of the entire E&P industry. I enjoyed working with you very much. Thanks to Hadi Hajibeygi for your guidance throughout the process of this thesis, your precise feedback strengthened this report. Special mention to Maartje Boon and Sebastian Geiger for joining the grading committee and for providing feedback in the last stages of this investigation.

Thanks to my closest friends, to my current and old roommates, and to Julia for being there for me, especially in these past months. I am forever in your debt. Thanks to my aunt for being the first (and probably last) non-scientist person to read and check the grammar of my thesis. Last, but definitely not least, an eternal thanks to my parents for encouraging me to go abroad and fulfil my dreams. Gracias.

Glück Auf!

G.A Ocampo Mendoza
Delft, November 2022

Contents

List of Tables

List of Figures

1 Introduction

Commitments by different countries, including the Netherlands, to achieve net zero by 2050 imply the decrease in the use of energy systems that mostly or solely rely on hydrocarbons, which are emitters of greenhouse gases. This reduction of the use in coal, gas and oil point towards an increased use of renewable energy sources in the global and the different local energy mixes.

There is, however, a slight inconvenience with major renewable systems and that is their intermittency in power generation. Power systems such as wind power depend on the local wind conditions. Solar energy is dependent on cloud coverage, snow, frost, and, of most importance the hours of daylight during different times of the year. The effectiveness of these systems can be largely hindered by factors that humans cannot control, which gives them volatility and variability. Consumption of energy has a baseline during the summer and has a peak during the winter. The intermittency of solar and wind energies cannot accommodate for the seasonal variability. Therefore, the society needs to look for a way to store surplus energy that cannot immediately go to the grid. Moreover, both of these have peaks of production even in a daily scale, meaning that in case of a lack of an appropriate electricity grid, some of the electricity generated can be lost. It is therefore crucial to find a way to store this surplus electricity, as this would eliminate the variability of production of renewable resources Thaysen et al., 2021.

1.1 Hydrogen and the Dutch Energy System

Despite being the most abundant element in the universe, except a very few cases, the diatomic molecule of hydrogen is not commonly found on Earth as a free element McCay, 2014. Hydrogen must be produced via chemical reactions from other substances that have hydrogen in their composition, such as water and natural gas. The most common method of creating hydrogen is Steam Methane Reformation (SMR) where natural gas is heated with a catalyst to produce carbon monoxide and hydrogen. Hydrogen is commonly classified with colours (grey, blue and green) depending on the technique used to generate the hydrogen. This, however, has nothing to do with the purity of the created hydrogen. SMR generates 'grey' hydrogen, as it also releases greenhouse gases. Another type of hydrogen is 'blue', which is also created by means of SMR, but the majority of the carbon dioxide generated during the process is captured, occasioning that this process becomes more environmentally sustainable. Last but not least, comes 'green' hydrogen, which is generated by means of the electrolysis of water using renewable power as an energy source. This process splits water molecules to generate hydrogen and oxygen without any harmful by-product. Therefore, this production of hydrogen has very little impact on the atmosphere in terms of greenhouse gas emissions compared to the 'blue' and 'grey' types. Green hydrogen is of interest to this report and is important in the context of the Dutch energy system, which will be discussed in the following sections.

According to IEA 2019, only 0.1% of the world's current hydrogen production currently comes from electrolysis, meaning that most of it come from the polluting SMR. This indicates that there is still a lot of work to enable large-scale production of hydrogen via the electrolysis of water. This processes splits water into is constituent elements, hydrogen and oxygen. This method is quite advantageous as the hydrogen produced has a very high purity, so that it can be used in fuel cells or electronics. Because of the fact that renewable energy is becoming cheaper due to technological advances, it will be increasingly more viable to generate hydrogen from electrolysis.

The concept of using (surplus) renewable energy to use electrolysis into hydrogen is called Power-to-Gas Hashemi et al. 2021a. As mentioned earlier, due to the variability of power generation by renewable energy sources and local patterns of consumption, there is a need of converting this electricity into another form, such as hydrogen. This hydrogen can be injected into the gas network or be stored for later use. This of course, requires the availability of different storage facilities, an interconnected energy grid and some economic incentive to use hydrogen as a fuel.

Hydrogen has been gaining traction during the past years as a possible low carbon energy carrier. It is important to state that hydrogen is an energy *carrier* which is a molecule or phenomenon (molecule in this case) that meaning that it takes more energy to separate it from other molecules than the energy that it produces as a fuel. This however does not mean that it is not useful, as it can be used as a fuel for transportation, power generation, heating, agriculture among other industries. Hydrogen has the highest energy content of any particle by weight but its low ambient temperature density makes it have a low energy content per volume.

The United Nations Industrial Development Organisation has defined hydrogen as "a true paradigm shift in the area of more efficient energy storage, especially for renewable energy on industrial scale" Heinemann et al. 2021. Hydrogen will be of great importance in the energy systems of the future as an alternative to polluting fossil fuels and its roll-out in the energy grid will depend on laws and regulations that aim at achieving climate neutrality. After the Paris Agreement of 2015, countries have built roadmaps to achieve climate neutrality by 2050. The 'Klimaatakkoord', Rijksoverheid 2019 is the Dutch set of legislation that draws the plan to reduce carbon dioxide levels by 49%, compared to 1990 levels by the year 2030. This plan also includes hydrogen as an essential carrier of energy. Also under the statutes of this document, a roadmap for offshore wind power has been brought up (and quite recently increased further upwards by the Esbjerg Wind Declaration to 21GW). This, in turn, means that the production capacity for hydrogen will also increase.

Apart from this international agreement, in response to the unprovoked invasion of Ukraine by Russia, the European Commission drafted the REPowerEU plan. This is due to the need of the EU states to be less dependent on Russian fossil fuels, which will bring security of supply of energy to EU countries. By diversifying energy supplies, especially from renewable sources, countries will be less dependent on one single potentially unreliable energy producer. This plan includes a target of 10 million tonnes of domestic renewable hydrogen production EuropeanCommission.

These two ambitious plans for the production of hydrogen can only be possible with the storage of hydrogen in the subsurface Hashemi et al. 2021b, 2022. Small-scale storage such as tanks will of course help storing some of this hydrogen. However, the physical space needed to hold billion of cubic meters of hydrogen at surface conditions is extremely high. It is therefore more sensible to store it under high pressure in the subsurface.

Based on an operational range between 150-250 Bar and the availability of data, a recent study by EBN and TNO concluded that there is a 194bcm theoretical working volume capacity for offshore underground hydrogen storage. This conclusion, however, does not consider the technical feasibility of these fields, implying that this value will decrease. These technical details include cap rock integrity specially under cyclic loading Ramesh Kumar et al. 2021; Ramesh Kumar and Hajibeygi 2021, microbiology, general flow properties van Rooijen et al. 2022; Boon and Hajibeygi 2022 among others. Nevertheless, the data shows that there is no shortage for storage space. Despite not being the target of our investigation, it is good to mention that the theoretic capacity of offshore salt caverns is $163.5 Mm^3$. This offers even more storage capacity in the subsurface van Gessel et al. 2022.

However, the Technology Readiness Level (TRL) of hydrogen storage in depleted gas fields is still low. This means that it needs more laboratory, in-situ testing and dynamic modelling to be ordered to see the feasibility of a system like this. It is important to conduct more research on the physical and chemical reactions as well as the multi-component and phase flow that will occur in the porous media. It would be, of course, ideal to have field data to be able to history match and understand the influence of reservoir characteristics. It is important to increase the TRL of hydrogen storage in porous media by the understanding of the physical processes that govern it, and therefore it is important to conduct numerical investigations, such as this one, as well as laboratory and field experiments.

1.2 Literature Study

A literature review has been conducted in order to construct a relevant and insightful research question and derived sub questions. This review will look into the knowledge gaps in the concept of UHS, the physical processes that govern the single-phase multi component flow and more specifically how this translates the dynamic simulation of hydrogen in porous media. As mentioned in the previous section, the TRL of this system is still low, meaning that this investigation will want to fill in some of the knowledge gap as well as raising points for further investigation and dynamic modelling.

The current knowledge of Underground Hydrogen Storage comes from simulations or small-scale lab experiments given that there is almost no real life experience with UHS in depleted fields or aquifers. However, this small pool of knowledge is crucial in terms of simulation dynamics and to our better understanding in the physical processes that dominate gases in a UHS.

There are very few measurements for contact angle related to UHS. Experiments done by Hashemi et al. 2021c quantify the contact angle of hydrogen in a brine rock system in in-situ conditions using a captive bubble cell. The results show that the system is water wet after the drainage and imbibition, which means that water will

preferably occupy smaller pores. This was the case for different temperatures, pressures and salinities, which is advantageous for UHS. Experiments like this are important as they will lead to better understanding of capillary pressure and relative permeability curves, which are important reservoir simulator parameters.

Jangda et al. 2023 performed x-ray scans of the flow of hydrogen in a brine saturated sandstone sample. In the case of the non-hydrogen-equilibrated brine, the dissolution of hydrogen is slightly higher, than in the case of a hydrogen-equilibrated brine. As the brine in the subsurface will not be saturated with hydrogen, this may be an issue when assessing the recovery of hydrogen.

All of the real life experience related to UHS are the injection of a mixture of gas that contains hydrogen into the subsurface. Although the purpose of these experiments are not the cyclic storage and production of hydrogen, these can give us clue on potential safety and especially technical aspects that could hinder or prevent a successful UHS operation.

Within the reviewed literature, there are some 'town gas' storage projects, which is a gas produced by the strong heating of coal in the absence of air. The composition of the produced gas contains about 50–60% hydrogen, 15–20% carbon dioxide, 10–20% methane and traces of nitrogen Panfilov and Panfilov 2010. Although these were not 100% hydrogen storage projects, the gases that were stored contained a considerable amount of hydrogen.

The town gas storage near the city of Lobodice in Czech Republic reported a decrease in hydrogen content and increase in methane content in the extracted gas. The initial injected composition consisted of 55% H2, 20% CO2 + CO and 20% CH4. After several months of injection and storage, the extracted gas contained 37% H2, 12% CO2 + CO and 40% CH4. An initial attribution by gas leakage was discarded after it was found out that the produced methane had been formed during the cyclicity process and was not the one in-situ or injected. This conversion from hydrogen to methane in reservoir conditions was caused by a bacterial process called methanogenesis Kopal et al. 2016. Although the production of methane would increase the calorific density of the produced gas, the intention is to retrieve as much hydrogen as possible, meaning that this bacterial effect is a risk to a UHS system. Strobel et al. 2020

Apart from the town gas project, there have been two storage projects that a combination of hydrogen and methane has been injected into a depleted gas field, this is the project Hychico in Argentina Perez and Dupraz 2016 and the ongoing Underground Sun Storage 2030 project in Austria RAG 2021. The latter is planning to inject pure hydrogen into a depleted field in the next years, which will give a much better insight in the behaviour of hydrogen in the subsurface.

There is a limited number of numerical simulations dealing with the storage of hydrogen in porous media. I will subdivide these studies in four different categories, as they involve different reservoir settings. These are simulations of hydrogen storage in: condensate fields, aquifers, oil fields and gas fields. The latter is the category that is we are mostly interested in this investigation, however, knowledge and findings from the all categories could provide some better insight in this investigation.

Feldmann et al. 2016 shows an increased hydrogen purity through different cycles. This paper consists of a numerical simulation in a depleted gas field using hydrogen as a cushion gas in a real reservoir model. In this paper, the reservoir was loaded with hydrogen for 5 years, followed by a cyclic operation of six months. This operation is done in four separate permeable layers that have tight clay layers. There are no flow boundary conditions in the simulation. The main findings of the investigation, as shown in prodcyle show that the purity of the extracted hydrogen is never 100% and that it slightly increases on each cycle.

The investigation by Hagemann 2017 uses the open source software $DuMu^x$, which is used for dynamic reservoir simulation. They state that the mixing zone between the initial gas and the injected hydrogen becomes much larger when mechanical dispersion is included. This implies that effects that they see in most of their simulations are due to numerical dispersion. As a consequence, the predicted hydrogen concentration in the produced gas stream is around 15 percentage points less than in the simulation without mechanical dispersion.

This study also states that bio-chemical reactions lead to considerable production of CH4 and H2S in the reservoir, this was mostly due to bacteria. Consequently, the hydrogen concentration in the produced gas stream is much lower than in the simulation without bio-chemical effects.

The research by Lysyy et al. 2021 is a numerical simulation where the recovery of hydrogen is evaluated when being injected in a gas, oil and water zone that occur in the same reservoir model. This investigation uses different volumes of formation gas as a cushion their sensitivity analysis.

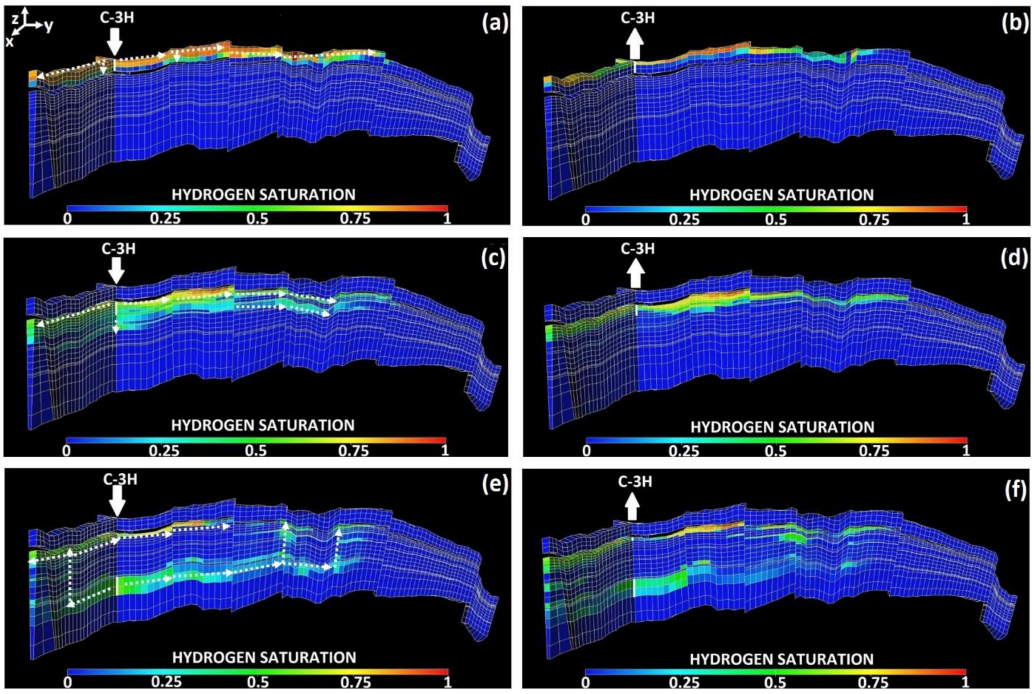

Figure 1: Hydrogen Saturations. A,B Gas Zone. C, D Oil Zone, E, F Water Zone. Pictures on the left show the saturation at the end of the initial injection of hydrogen (where saturation is at its maximum). Pictures on the right show the saturation at the end of a prolonged withdrawal. It is clear that the recovery in the water zone is much less than the one in the gas and oil zones

When the ratio of hydrogen to formation gas was the lowest, the volume of hydrogen recovered was the highest. However, the purity of this extracted gas was the lowest. From the three zones that have been tested out (water, gas and oil), the purity is the lowest in the water zone. On the prolonged withdrawal, higher percentage of recovery was obtained at the cost of hydrogen purity.

Cai et al. 2022 developed a numerical dynamic simulator to model UHS in an aquifer, salt cavern, methane saturated aquifer and depleted gas field with carbon dioxide as a cushion gas. All these models were history matched as a benchmark. Their model extends the structure of the Rio Vista gas field in California, USA to create an anticline structure. This is shown in Figure 2.

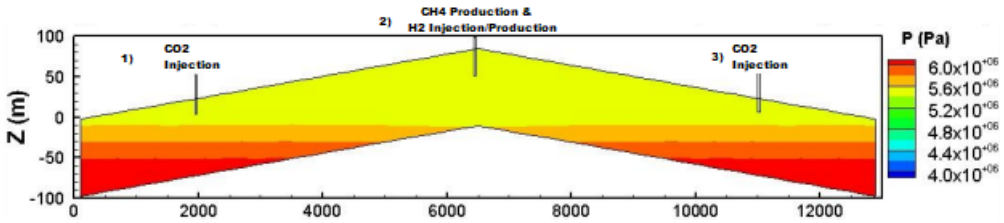

Figure 2: Simplifed model used in Cai et al. 2022. The well names were added to the figure.

Wells 1 and 3, the wells on the bottom part of the anticline, inject CO2 for the first 10 years. This is portrayed with the rising light blue line seen in Figure 3. There is extraction of pure methane from Well 2, which is the blue block. After this, there is injection of hydrogen ino the reservoir and then the injection-production cycles of hydrogen start at a rate of 1 kg/s for 6 months, shut-in for 3 months and a production rate of 1 kg/s for 3 months each year. The remaining methane in the reservoir is acting here as a cushion gas. There are two main

observations. First, within each cycle, the percentage of methane produced increases. Secondly, throughout the multiple cycles, the percentage of methane extracted rises up to a plateau of around 40% after some cycles.

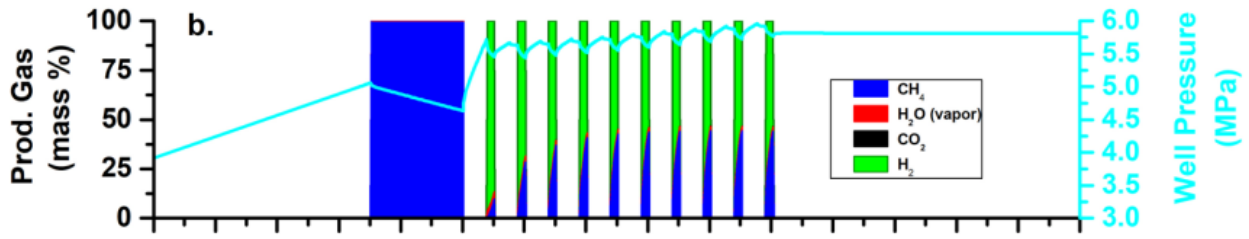

Figure 3: Purity of extracted hydrogen. Adaptation

The results of these three papers show that the purity of the extracted hydrogen rapidly decreases, especially in the case where heterogeneities are present, which is detrimental to the system efficiency. In all cases, the purity of the extracted hydrogen levels off at a certain purity.

Finally, there was a review on Dispersion. This is characterized by the dispersivity value. Soil and porous rock have a degree of randomness, where fluids will take different pathways when they are being transported. Wang et al. 2021. Compilations of dispersivity related studies conclude that dispersion increases with the length of measured scale. Gutierrez 2009, Gelhar et al. 1992, Molz 2015, Arya et al. 1988.

However, there is no clear relation between the scale and the dispersivity of the porous media. Some of the points of the data set are core-scale experiments, others are small scale field experiments and others are simulations. None of the large scale results are real life experiments. Many methods for obtaining the data have been used meaning that the results may not be consistent. Figure 4 comes from the study of Gelhar et al. 1992 and shows the reliability of the dispersivity experiments that his study analyzed. As seen, the bigger scale projects have low reliability based on his established parameters.

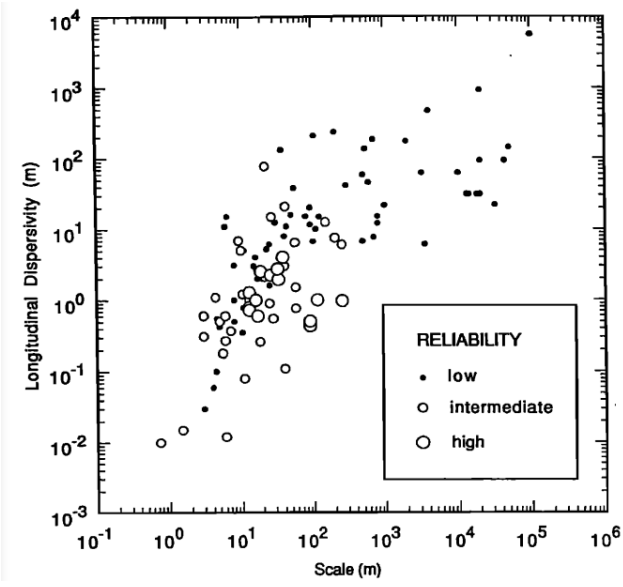

Figure 4: Longitudinal dispersivity versus scale

1.3 Project Description & Research Question

As seen in the literature study, there are still some knowledge gaps in the topic of hydrogen storage in gas fields. There seems to be only a couple of dynamic modelling investigations concerning the use of alternative cushion gases for underground hydrogen storage in porous media. Therefore, one of the main purpose of this thesis is to produce meaningful simulations that show the multi-component displacement that will occur in the reservoir when a UHS system has an alternative cushion gas. This is a prediction of the interactions with the

connate water, residual methane and the different gas used as a cushion. These flow interactions and patterns are controlled by fluid parameters such as viscosity, density, compressibility, relative permeability, as well as rock properties such as porosity, tortuosity, permeability and higher order parameters such as heterogeneity and vertical horizontal connectivity.

This dynamic flow prediction of gases in the reservoir will be done numerically by means of a commercial EP simulator. However, this simulator is not optimized, or made, for hydrogen storage. It is therefore important to assess the accuracy of the results, which entails understanding the individual physical processes that occur and how they affect the behaviour of the gases. CMG GEM, an Equation-of-State (EoS) compositional simulator that applies the finite difference method to perform flow simulations in porous media, will be used as a tool to predict and analyse gas-gas interactions.

The results of the commercial simulator can be predicted by means of an analytical solution, which can be implemented in a programming language such as python. Although there is a series of assumptions in the analytical solution, it will be able to predict the behaviour of the physical and transport processes occurring in this system.

The first step will be to grasp the underlying physics of the multi-component flow in the reservoir. This would entail a literature review on the gas-gas interaction between different possible cushion gases on the one side and the natural gas left in place and the hydrogen on the other side. This will allow to discern how different gas properties affect the interaction between the injected hydrogen and the cushion gas in the reservoir.

As mentioned earlier, one of the main constraints is the purity of the extracted hydrogen. This purity will depend on how much the hydrogen mixes with the cushion gas and residual methane. Although the economic and technical feasibility of gas separation are out of the scope of this investigation, it would be wise to optimize the production of hydrogen at a high purity. Therefore, it is of particular importance to be able to qualitatively and quantitatively describe and explain the degree of mixing in the reservoir. By testing one injection-production cycle, a better understanding of the processes can be achieved. With this acquired knowledge, simulations with multiple cycles can be better understood in terms of the input parameters. This first step would provide a set of guidelines and observations for a preferred type of cushion gas.

After the multi-component flow is properly understood, the second step would be to test the effect of heterogeneities. The heterogeneity of the model is varied to see the behavior of gas in the presence of heterogeneities. The effect of heterogeneities is analyzed with the use of a pancake layer model.

The third and final step is to test the effect of perforation intervals. At first, the perforations for both injection and production are located throughout the entire reservoir column. By modifying the perforation interval, the effect of heterogeneity is seen and can be therefore optimized for production purposes. The buoyancy of the different gases, as well as the reservoir pressure due to injection are taken into consideration for the analysis. Although the geomechanics of cyclic loading are not within the scope of this investigation, it is important to have realistic working pressure in the reservoir during injection and production. This is to ensure well and reservoir integrity, which are needed to ensure a safe subsurface project.

If the optimal perforation intervals for different heterogeneities are better known, the choice of cushion gas can be established with more ease knowing the operational constraints of the reservoir. The subsurface is a heterogeneous media and the knowledge obtained from these simple tests can be used to analyze the multi-component flow in the reservoir. Understanding these tests are the starting point for a full analysis of realistic reservoir models, as they will give insights into the .

Therefore, the main research question is:

What is the most ideal cushion gas that can be used in an Underground Hydrogen Storage system in depleted gas reservoir?

1. How will the working volume/cushion gas ratio be with different gases?
2. What is the optimal perforation interval depending on the cushion gas?
3. How do heterogeneous rock properties affect the multi-component flow?
4. Is there an optimal injection rate to ensure the maximum purity of hydrogen?

1.4 Thesis outline

In order to fully answer the research question and its derived sub-questions, the thesis has been divided into different chapters, which will guide the reader throughout the reconstruction of the thought process and investigation. This first chapter has highlighted the importance of hydrogen in the Dutch energy system, as well as formulating a set of research questions based on a literature research. Chapter two will give background information on the physical properties of hydrogen as well as an introduction to Underground Hydrogen Storage systems. The next chapter will delve into the physical processes that drive the flow and mixing of gases in porous media. Chapter four will present the modelling tools used in this investigation, as well as presenting the methodology and the base case scenario. The following chapter will discuss the results of the investigation. Chapter six will give the limitations of this investigation and finally, chapter seven will wrap up the results and give recommendations based on the findings.

2 Background

2.1 Hydrogen properties

It is important to understand the properties of the element hydrogen itself, because the implications of its physical and chemical properties will reverberate throughout the many topics that we will discuss throughout this investigation.

Hydrogen is a colourless, odourless, tasteless, highly combustive gaseous substance and is the lightest element in the periodic table. A hydrogen atom consists of a proton and an electron, and because of stability in electron arrangement, it is found as a diatomic molecule H^2. Tarkowski 2019

Hydrogen has a very low boiling and melting point, as shown in Table 1 which are due to small intermolecular forces. This low boiling point implies that hydrogen will be stored in the subsurface as a gas. The diatomic molecule of hydrogen has a weight of 2.016Da, and is also the smallest existing molecule, which implies that it is able to diffuse more easily than other gases. This will have an effect in the subsurface, as a higher diffusion coefficient will possibly lead to a higher mixing in the subsurface. However, as we will explore later, this effect is quite subtle. The fact that it is the smallest particle in existence means that it could potentially leak through cap rocks such as shale, despite their extremely low permeability.

Property	**Value**
Density (kg/m3)	0.04281
Volume (m3/kg)	23.359
Internal Energy (kJ/kg)	5474.9
Enthalpy (kJ/kg)	7810.7
Entropy (J/g*K)	62.705
Cv (J/g*K)	10.41
Cp (J/g*K)	14.534
Joule-Thomson (K/bar)	-0.05369
Viscosity ($\mu Pa \cdot s$)	13.892
Critical Temperature (C)	-240.005 C
Critical Pressure (Bar)	12.964 bar
Critical density (kg/m3)	31.262
Acentric factor	-0.219
Normal Boiling Point (C)	-252.781
Normal Melting Point (C)	–259.14

Table 1: Thermodynamic properties of hydrogen at Standard Temperature and Pressure

The properties of hydrogen will be compared to some gases that are relevant within the context of underground storage, such as methane (CH4), carbon dioxide (CO2) and nitrogen (N2). The viscosity of a fluid is determined by the strength of its intermolecular forces. Figure 5 shows the isothermal viscosity of these four different gases. At atmospheric pressure the ratio between the isothermal viscosity of any of the three gases and hydrogen is barely more than 2. The viscosity of hydrogen does not increase significantly However, as pressure increases, this ratio becomes slightly higher for nitrogen and methane. However, the viscosity of carbon dioxide increases to 50 $\mu Pa \cdot s$ at 250 Bar, which makes this ratio much higher.

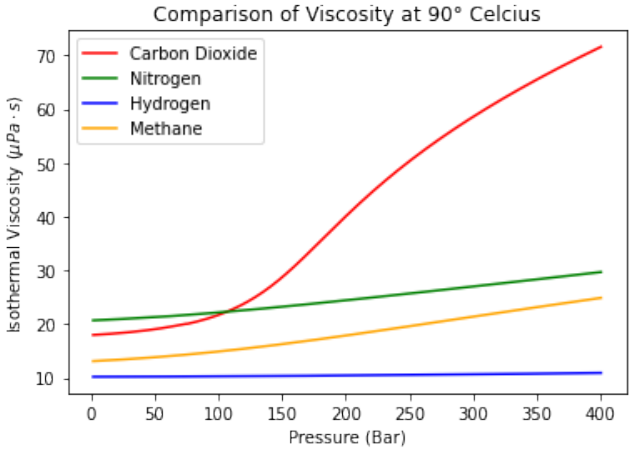

Figure 5: Isothermal Viscosity as a function of pressure

The injection of a low viscosity (or highly mobile) substance, such as hydrogen, at a constant flow rate, will lead to a reduced sweep efficiency of the fluids present in the reservoir. This would especially be the case in a brine saturated rock. In terms of an aquifer in porous media, this could potentially lead to viscous fingering, due to the high difference in mobility between H2 and the brine. This unstable displacement or viscous fingering can lead to unstable fronts between the displacing and displaced substances, which in turn can reduce the amount of hydrogen that can be recovered, or lead to a loss of hydrogen by lateral extent. This effect is less present in the context of a depleted gas field, as most of the water present will be irreducible.

Figure 6 shows the isothermal Density of the above-mentioned gases. The densities of the four gases are around $0.05\frac{kg}{m^3}$ at atmospheric pressure. The density of hydrogen is at 90° Celsius and 400 Bar is $22\frac{kg}{m^3}$. On the other hand, the density of carbon dioxide is $788\frac{kg}{m^3}$, which is almost 40 times bigger hydrogen density. Although the density of nitrogen and methane are not as high at that certain pressure, they are, respectively, approximately 15 and 10 times larger.

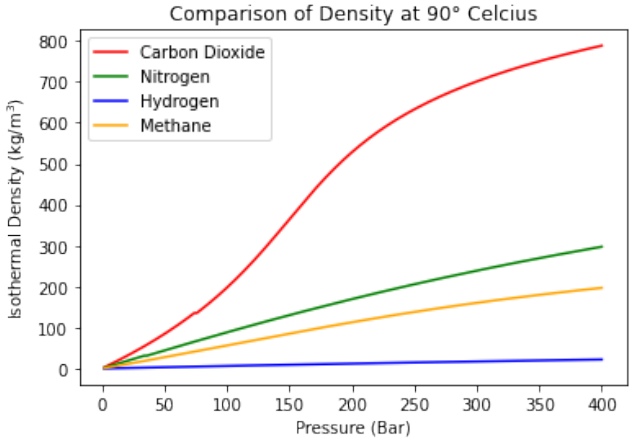

Figure 6: Isothermal Density as a function of pressure

The density of all the alternative gases increase as pressure increases. As seen, this increase is not linear or uniform between gases. This means that there will be a dynamic ratio between the densities of the injected and existing gases in the reservoir. This can influence the degree of mixing in the reservoir. The full effects and implications of these properties will be evaluated throughout the report, as they will explain some of the movement and mixing effects in the reservoir simulations.

2.2 Underground Gas Storage

Underground Gas Storage (UGS) is a process where methane is stored in different geologic, or man-made subsurface formations. These include salt caverns, aquifers and (depleted) oil/gas fields. Reservoir rocks, that were once saturated with hydrocarbons, are stratigraphically and/or structurally bounded, which allowed them to contain these fluids for prolonged periods of time. These same structures can be used for the storage of hydrogen, which can be used seasonally for industry and fuel. Given that this report will only deal with the storage of hydrogen in gas fields, we will skip the explanation of the process of storage in salt caverns.

The first UGS project took place in Ontario, Canada in 1915. In 2018, there were 689 UGS facilities in operation worldwide while there are only pilot projects being developed with hydrogen. UGS is a working concept and all the research done on it during the past decades makes this a well understood process.

To fully understand Underground Hydrogen Storage (UHS), we must first identify the similarities and differences between UGS and UHS in porous media, as it is a technology that is already being used and is relevant to the current Dutch energy portfolio. This comparison bases itself on Figure 7, which shows the Norg field average reservoir pressure during the operation of the field.

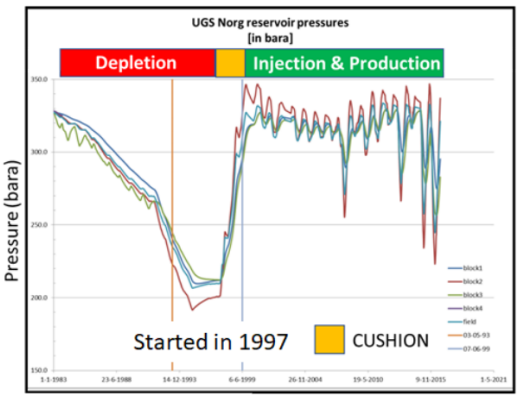

Figure 7: Reservoir pressure over time in the Norg UGS project NAM 2016. Adaptation

The process of storage in gas reservoirs begins after, or during, the depletion of the reservoir, highlighted in red. The average reservoir pressure will progressively decrease as gas is extracted. This drop in pressure, which in turn implies further and further reduction in production rate will continue while recovery of the extracted hydrocarbons is still economically feasible.

The second part of the process is the cushion phase, highlighted in yellow. For this depleted reservoir to become an UGS facility, a Cushion Volume 'CV' has to be injected into the reservoir to partially restore the pressure lost which is needed to drive the production and have a working pressure that is able to deliver gas at a certain rate. It is important to ensure that this cushion gas is permanently kept in the reservoir during the storage project and of course during the cyclic production and injection stages.

Finally, there is the green section, the Injection & Production phase. The amount of gas injected and produced during this period is called working volume 'WV'. As seen from this example, the cushion phase achieved almost the same pressure as the initial reservoir pressure. This, however, is not the case in every reservoir. This is a function of the volumes of gas to be stored, volume of the reservoir and technical and safety limits. Once a desired pressure is achieved, there will be cycles of injection and storage, which will increase and decrease the reservoir respectively. Natural gas is stored during the summer and extracted during the winter, which often leads to yearly cycles. However, there can be shorter or longer periods of cyclicity, depending on the intended use of the storage system. It is common to have higher production that injection rates as peak demand is concentrated on a shorter period. The variation in reservoir pressure depends on the volume of gas that has been extracted or injected in the reservoir. Juez-Larré et al. 2019

2.3 Underground Hydrogen Storage

This investigation however, is focused on Underground Hydrogen Storage (UHS) systems. The same principle of depletion, cushion and injection and production phases can be applied to UHS. However, the subsurface processes are not entirely the same, which will be explored in the following chapters.

The process of hydrogen storage into subsurface geological formations includes pre-injection of a certain cushion gas, such as nitrogen, methane, carbon dioxide or hydrogen itself, followed by hydrogen injection, which would form part of the working volume throughout the different cycles.

Within the UHS, there must be a balance between the Working Volume (WV), which is the volume of hydrogen that will be stored and produced cyclically, and the Cushion Volume (CV), which is a gas that stays permanently in the reservoir. These two volume will mainly depend on the size of the reservoir and on the operational constraints of the field. In an economic sense, this cushion will be a sunken cost that the operator will have to incur on the operation. Considering that hydrogen is an expensive gas to produce, it would be desirable to find an alternative cushion gas with a lower price.

However, an alternative cushion gas than hydrogen itself means that there will be more mixing of gases in the subsurface. In a system where hydrogen is also the cushion gas (referred to hydrogen-hydrogen from now on), there will be mixing of hydrogen with the residual methane in the reservoir. If methane is used as a cushion gas (methane-hydrogen system), there will be a mixing zone between the cushion gas and the hydrogen. Lastly, in the case of an alternative gas as a cushion gas (carbon dioxide/ nitrogen) there will be a mixing zone between the hydrogen, cushion gas and residual gas in the reservoir respectively.

Different industrial processes require a certain purity of hydrogen, which implies that sometimes it cannot come together with a specific percentage of impurities. It is good to note that this minimum purity is not known at present, so an assumption of 98% is used until more information becomes available. To give an example, fuel cells require a high, almost 100%, purity of hydrogen, while a gas turbine used for electricity generation can be modified to run on a wider range of hydrogen purity.

Apart from this, there is still ongoing research on separation techniques for hydrogen. If this separation turns out to be economically and technically feasible, then the stringent hydrogen purity threshold could be reduced. However, this investigation will base itself on an extracted purity of hydrogen of 98%. This sets the first constraint for this hydrogen underground storage simulation.

In an UGS, the cushion gas used is methane and the produced gas is methane. The WV:CV ratio is therefore straightforward to establish. In an UHS that uses hydrogen as a cushion gas, this ratio can be also obtained easily. However, if an alternative gas is used as a cushion, this definition does not hold entirely true. This will be further discussed in the Methodology.
Finally, fbfore starting a UHS project, there must be a definition of the minimum injection and production rates that want to be achieved with a certain reservoir. Dynamic modelling will try to predict if these rates can happen within the safe operating constraints. There must be sufficient facilities to process and transport hydrogen in and out of the reservoir. A project must consider infrastructure as well as the technical characteristics of the reservoir.

3 Physics

In the context of flow through porous media for UHS, mixing happens when a viscous and miscible substance travels and displaces another. This mixing translates into a so called 'mixing zone' or 'transition zone' that develops at the front, or boundary of both substances. This mixing zone grows as the displacement of the injected fluid progresses. Its extent is derived from two processes: the process of advection and of the combined effect of mechanical dispersion and molecular diffusion. These two will be briefly analysed in the following subsections.

As a note, we define the mixing zone as being the distance between 0.9 to 0.1 solvent concentration. This is shown in Figure 8. This zone will be useful to assess the degree of mixing in the reservoir.

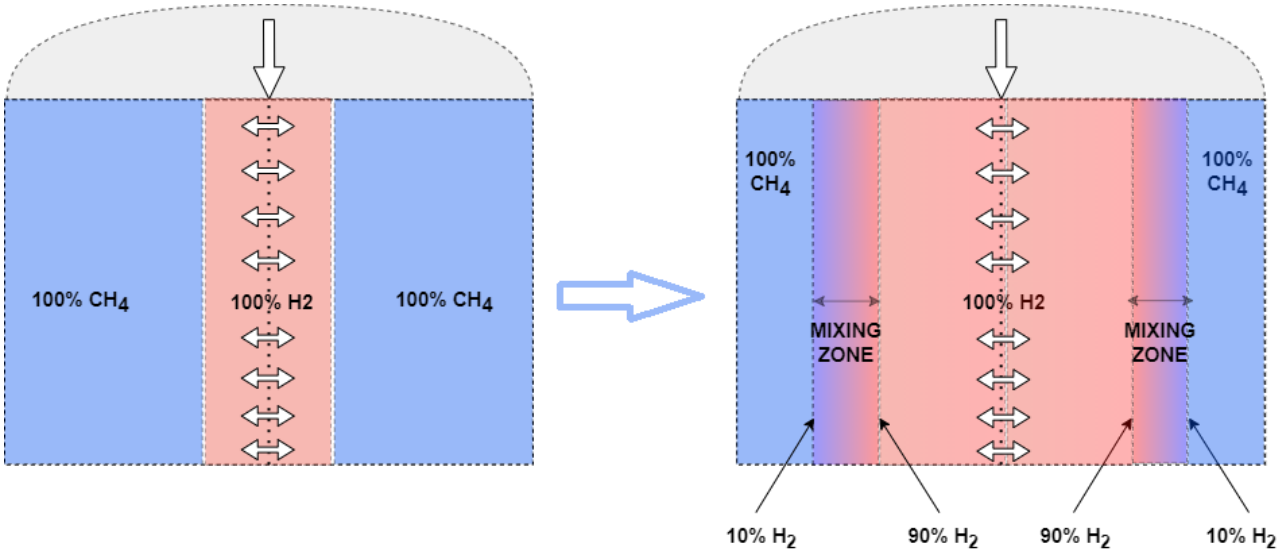

Figure 8: Development of mixing zone along time. Terstappen 2021

3.1 Advective-Dispersive equation

3.1.1 Advection

One source of mass transport is by advection. This arises due to particle movement by flow in a solution. In terms of this system, cushion gas and hydrogen are being transported through the reservoir in the injection cycles and production. This concentration C of a certain of a given substance will travel through the medium with Darcy velocity $\vec{u}$.

This physical movement of concentration due to flow is the mass of the substance which is carried over a certain control volume through time. This is comes from the injection and production of hydrogen from the well.

3.1.2 Mechanical Dispersion

Mechanical Dispersion arises during the physical transport of particles through porous media. Particles will be distributed unevenly due to the intrinsic complexity of porous media . The pore network will have dead ends, passages of variable aperture, among other differences that will result complicated streamlines within the porous medium. This non uniform flow will result in varying local velocities, will lead in the substance moving at different speeds at variable directions.

Despite the fact that different porous media may have similar effective porosities and permeabilities, the pathways for flow through their pore network will vary. This variability applies to all the different Representary Elementary Volume (REV) scales that there are. In the simplest scale, the pore scale, we have primary porosity, which is related to the original deposition, as well as secondary porosity, which is due to dissolution, precipitation and small scale fracturing withing and between grains. As shown in Figure 9, there will be differences in flow due to pore size, where higher apertures will allow a faster flow. Differences in path lengths will arise due to tortuosity. This means that certain paths will take longer to transport the solute from point A to B in the direction of travel. Finally, in the case of flow in viscous fluids, no slip conditions at the boundaries will

imply that there are local small variations in velocity through the pores, which will in turn imply the uneven distribution of the solution because of the creation of small internal back-flowing currents.

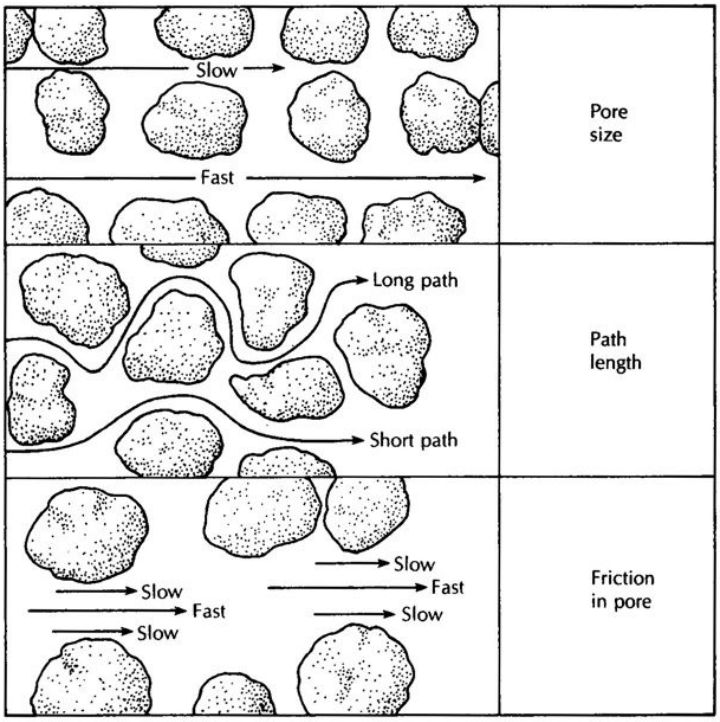

Figure 9: Flow paths due to distribution of grains

3.1.3 Molecular Diffusion

Molecular diffusion is caused by the Brownian or random motion of fluid due to their internal energy. The higher the temperature of the fluid, the higher the particle velocity, which would lead to more diffusion of the particles. This movement causes clashes between particles of the solute and in our case, the pore walls of our reservoir rock.

This diffusion is independent of flow, as it is driven by changes in concentration within the host medium. The solutes will move from areas of high concentration to low concentration, with decreasing speed as the differences in concentrations reduce. Given enough time, the space containing two different components will mix homogeneously solely due to this random motion of particles. This diffusion effect will occur slower in a porous media compared to an open space.

3.1.4 Derivation

The governing equations for the entire mixing process are derived from the effects described in the previous section. On one hand you have mass transport by advection, which is driven by the velocity of the solute in the medium and the Brownian motion of particles. Both of these will redistribute the different components on the system.

The effect of both of these can be summarized with the Diffusion tensor. In this case, for single-phase multi-component compressible flow, this tensor is represented by $\mathbf{D}_g$ (as we are dealing with only the gas phase) and is defined as:

$$\mathbf{D}_g = \begin{bmatrix} D_{ik,11} & D_{ik,12} & D_{ik,13} \\ D_{ik,21} & D_{ik,22} & D_{ik,23} \\ D_{ik,31} & D_{ik,32} & D_{ik,33} \end{bmatrix} \tag{1}$$

The tensor components are in the x, y and z directions are given by

$$D_{ik,mm} = \frac{D^*_{ik}}{F_k \phi S_k} + \frac{(\alpha_{kl} - \alpha_{kt})}{\phi S_k \left| u_k \right|} u^2_{km} + \alpha_{kt} \frac{|u_k|}{\phi S_k} \tag{2}$$

The remaining tensor components are given by

$$D_{ik,mn} = \frac{(\alpha_{kl} - \alpha_{kt})}{\phi S_k \left| u_k \right|} u_{km} u_{kn} \tag{3}$$

Where α_{kl} is the longitudinal and α_{kt} is the transverse dispersivity, S_k is the saturation and F_k is the formation resistivity factor, a function of the tortuosity of the medium.

This Diffusion tensor $\mathbf{D}_g$ forms part of the linear Fickian diffusion flux given by:

$$\overrightarrow{J}^z_g = -\rho_g S_g \mathbf{D}^z_g \nabla c^z_g \tag{4}$$

where c^z_g is the mass fraction of component z in the gas phase, ρ_g is the density of the gas phase, S_g is the saturation of the gas phase, and $\mathbf{D}^z_g$ is the diffusion tensor for component z in the gas phase.
The mass conservation for a system with M chemical species and only the gas phase, the mass conservation equation for component z = 1,...,M is defined as

$$\frac{\partial}{\partial t} \left(\phi \sum_g c^z_g \rho_g S_g \right) + \nabla \cdot \left(\sum_g c^z_g \rho_g \vec{v}_g + \vec{J}^z_g \right) = \sum_g c^z_g \rho_g q_g \tag{5}$$

where $\vec{v}_g$ is the superficial phase velocity and $q_g$is the source term.

3.2 Wettability & Capillary Forces

Wettability is defined as "The tendency of one fluid to spread on, or adhere to, the solid's surface in the presence of another immiscible fluid." (Zolotuchin, 2000). If fluid X preferably spreads in a surface, it means that the surface is wet by that particular fluid. Depending on the contact angle, it could also be neutral wet, meaning that it does not have a preference for a particular fluid. This preference depends on the mineral composition of the reservoir rock.

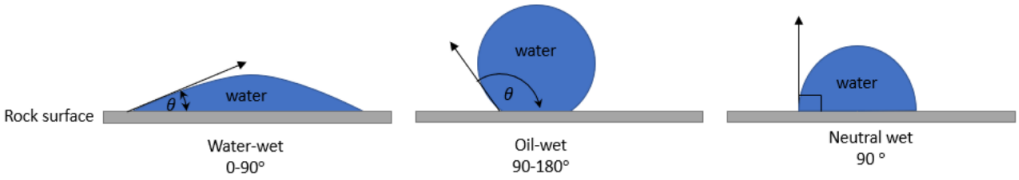

Figure 10: Relation contact angle and wettability for a water-oil system

In the context of porous media, it is useful to find out if the degree of wettability of the surfaces and if they are water or oil wet, as it will directly affect production. The wettability will have an effect on the saturation of fluids through the pores which will in turn affect the capillary pressure.

The capillary pressure is the pressure required for the non-wetting (nw) phase to displace the wetting (w) phase inside the porous media. This effect is present in the case of two immiscible fluids. When dealing with a water-wet system, this pressure is defined as following:

$$P_C = P_{nw} - P_n \tag{6}$$

In the context of UHS, capillary pressure is important because it will determine the irrecoverable hydrogen that is left on the system after a cycle of injection and production. Determining the drainage and imbibition curves, and therefore the relative permeability of the system can be derived from knowledge of the capillary forces.

3.3 Gravity Forces

As a brief introduction to this chapter, an explanation of buoyancy will be given, in order to have a reference to the similar processes that will occur in the subsurface. If there are two mixed immiscible fluids in a closed system, the system will tend to separate only based their denisty difference. The fluid with the higher density will sink while the lighter will rise, eventually separating completely. The rate at which separation happens depends on the density difference between the two.

If an object, or gas in the context of this investigation, has a lower density than the one overlying it, this will rise due to buoyant forces. The higher the difference in density between the two phases, the faster the displacement process will be. This will happen at the same time as the two gases mix due to advection and because of random motion.

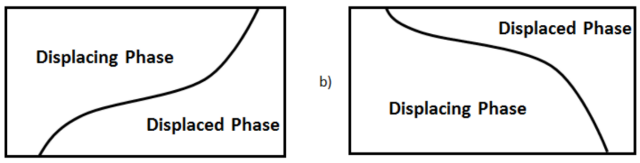

Figure 11: Gravity Segregation in displacement processes. a) Gravity Override where the displacing phase is denser than the displaced phase. b) Gravity Underride, the opposite effect than override.

To analyse the effect of buoyancy in the reservoir and its effect on mixing in the reservoir, the gravity number N can be defined. The term $\frac{Q_0}{2\pi k d^2 g}$ is the viscous force, or horizontal pressure gradient, which is exerted by the injection of fluid while the $\delta\rho g$ term is the buoyancy term.

$$N = \frac{k\Delta\rho g \rho_c 2\pi r_c d}{\mu_c Q_m} \tag{7}$$

where ρ is the difference between the fluids density, ρ_c is a characteristic density, r_c is a characteristic length in the reservoir and Q_m is the mass flow rate of hydrogen. This is the gravity number for incompressible flow. Large gravity numbers (N » 1) indicate that gravity forces dominate at that point in the reservoir. Small gravity numbers (N « 1) indicate that viscous forces are dominating. Gravity numbers close mean that this ratio is similar, and neither of these is dominant (however they both act on the system).

However, this formulation does not take into account the fact that there are density and viscosity changes as we inject hydrogen into the reservoir. This is due to the fact that density is dependent on pressure, meaning that there will be a variable density during injection periods.

The injection of hydrogen towards a gas of different composition (in this case either cushion gas or the residual methane), will create an interface between the both. This interface will have a certain width, as defined earlier as the mixing zone, and it will have a certain shape. This shape will be dependent on the rate of injection, the viscosity and density of the two gases that are mixing together and the reservoir permeability.

$$\gamma_{cw} = \frac{Q_0}{2\pi k d^2 g}\frac{\Delta\mu}{\Delta\rho} \tag{8}$$

As seen in equation Equation 8, this factor is inversely dependant on the distance from the well to the certain point in the reservoir. The farther away the gas is from the well, the lower its velocity will be, meaning that gravity forces will dominate in that area.

Although a full analysis of this dynamic viscosity change would require an extensive analysis of its own, the calculation for the parameter ζ is straightforward if done at individual snapshots of the injection and production phases. As shown in Figure 12, we can estimate the shape of the interface by calculating this parameter at a certain point in time. Note that both of the axis in the figure are in dimensionless lengths. This can serve as reference to be able to predict the shape of the interface based on basic information such as the reservoir permeability, and gas viscosity & density.

The interface can be described as a function of the radial distance away from the injection well

$$\zeta'(r') = \gamma_{cw}\left\{\ln(r') + \frac{1}{2}\ln\left[\frac{\gamma_{cw}}{2}\left(e^{2/\gamma_{cw}} - 1\right)\right]\right\} \tag{9}$$

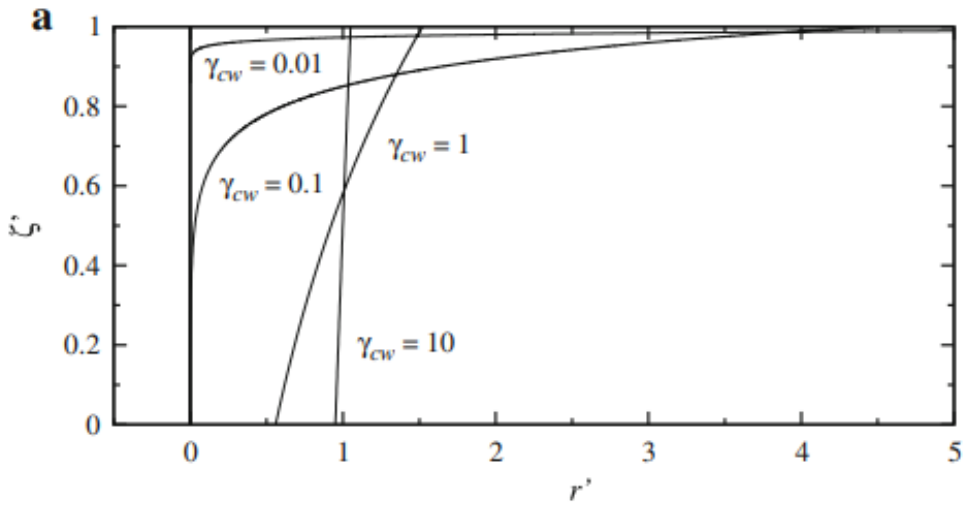

Figure 12: Prediction of interface shape depending on ζ factor Dentz and Tartakovsky 2008

Although the injection and production periods occur one after the other, there is still a dependence on the distance from the well bore, which still implies a dynamic interface between hydrogen and the cushion gas.

4 Modelling & Methods

4.1 CMG GEM

This research will use the different modules provided by Computer Modelling Group (CMG). The three modules that have been used are BUILDER, GEM and RESULTS.

The base case scenario, described in detail in the next section, has been created using the BUILDER module. This module allows the user to decide the grid type (radial, cartesian, CPG), the grid size properties as well as the basic reservoir parameters such as porosity and permeability. The user is guided in a step by step method through its Graphical User Interface (GUI), through the various required reservoir & rock parameters, numerical, geomechanical and production data that has to be inputted in order to be able to simulate any kind of dynamic flow problem. Group 2022

This input data is depends on the type of numerical simulator that is intended on using; in this case, GEM. This simulator is an efficient, multidimensional, equation-of-state (EOS) compositional simulator which can simulate all the important mechanisms of a miscible gas injection process, i.e. vaporization and swelling of oil, condensation of gas, viscosity and interfacial tension reduction, and the formation of a miscible solvent bank through multiple contacts. It uses the Peng-Robinson EOS to predict phase equilibrium in the various oil and gas phases. Group 2022

CMG GEM uses the finite difference method to solve partial differential equations. This is done by a discretization of a continuous process and space into a finite, smaller number of blocks. This discretization into smaller parts allows to approximate partial differential equations by solving a large amount of linear equations with matrix algebra. This discretization assigns reservoir characteristics to each of the individual blocks, which will be taken as input parameters for the different flow equations that are being used and solved.

As described in the Physics section, dispersion is the mixing of miscible components due to advection and convection. This however, the addition of dispersion is an optional term in the simulator. This implies that the smearing of the fronts between gases is not caused by a physical effect, but rather by the effect of using a finite difference scheme. This smearing is called numerical dispersion.

The simulator default value for dispersivity is 0. A dispersivity value of 0 implies that there is no advective or diffusive mixing. This would imply a sharp front between miscible fluids. However, this is not the case, there is always a smeared interface between the components, which is arises due to approximation mistakes derived from the finite difference method when solving partial differential equations.

This effect can be controlled, or reduced, by various methods, such as the ones described by Shrivastava 2003. The most accessible ones in this investigation are a control in the time step and cell size as well as the use of higher order schemes under a Total Variation Diminishing (TVD) flux limiter.

4.2 Dispersivity value

The Physics section refers to α_{kl} being the longitudinal and α_{kt} the transverse dispersivity. These are two parameters that are input in the simulator. The literature study shows that it is quite troublesome to calculate a dispersivity value for a porous medium. The trends shown by literature show a loose correlation between the longitudinal dispersivity value and the scale at which it is measured. The bigger the reservoir scale, the higher the dispersivity value.

The Physics section delves briefly over the small, pore scale mechanics of mechanical dispersion. Literature however, does not consider, or mention, the heterogeneities of the porous medium at any scale. It is also seen that most of the results for very high scale porous media are not tracer tests but simulations.

It is important to tackle the reason why this dispersivity value would increase as the measuring scale increases, as literature does not seem to approach it very often.

As mentioned, no-slip boundary conditions, variable pore openings and path lengths will have an effect in the mechanical dispersion. On a slightly higher scale, the lithofacies scale, we can recognize small depositional structures and layers of different characteristics. A cross-stratified sandstone would be an example of this. These

will be small scale heterogeneities between the different units, and depending on their mineral composition, will have different porosities and permeabilities.

In a facies scale, we will see more developed structures such as point bar deposits. These will be characterized by a certain depositional sequence and some stacked layers with certain thicknesses due to old paleocurrents and paleo flows. This is marked as b) in Figure 13

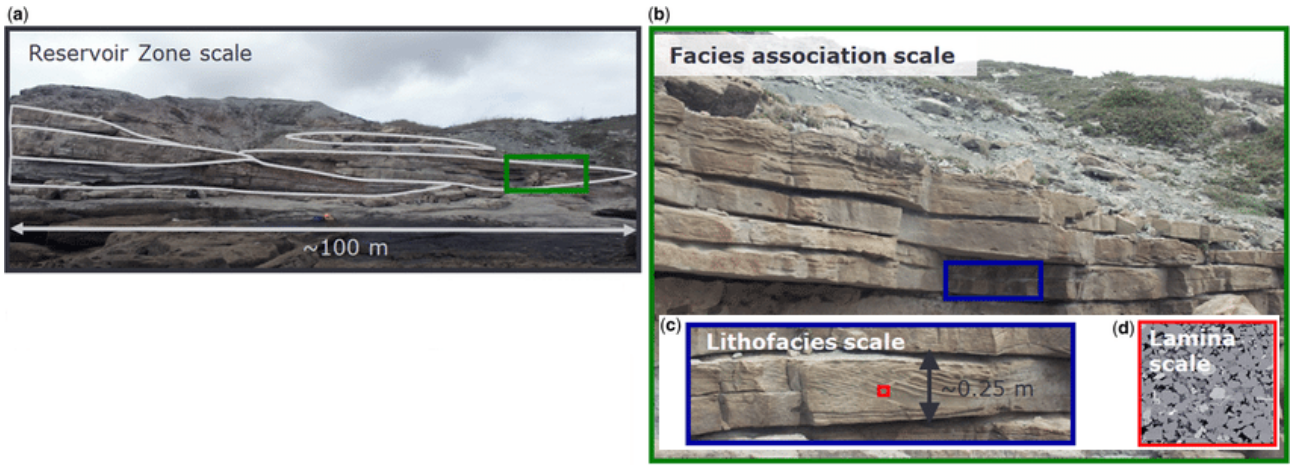

Figure 13: (a) Reservoir zone scale-the white lines outline the channel sandstones. (b) Facies association scale showing a point bar deposit. (c) Lithofacies-scale image showing a trough cross-stratified sandstone. (d) Lamina scale. Modified from Nordahl et al. 2014

In the lithofacies and facies scale, dispersion will be governed by mechanisms on a different length scale. The pore scale will of course have an influence within the different strata, however, low permeable strata will have a bigger impact on the streamlines of flow..

Finally, in a reservoir scale, there will be third order sequences, where, for example, there are deposits ranging from coastal deposits to deep marine ones. This is portrayed in part a) of Figure 13. Grid sizes of tens to hundreds of meters in the horizontal and lateral extent and a couple of feet high are commonly used in reservoir modelling. This means that the grid blocks will try to capture the small scale variabilities in porosity and permeability described above.

Apart from this, the horizontal and lateral extent of these layers and their connectivity have to be estimated, which in turn adds layers of uncertainty and complexity to an estimate for a 'unique' dispersivity value of a reservoir. This dispersivity can change in matter of meters because of the geology in place.

The main takeaway is that there are multiple scales of variabilities and heterogeneities in rocks, which means that characterizing parameters such as tortuosity, porosity, and permeability can be tricky and highly uncertain.

As mentioned in the literature review, and based on the reasoning above, it is no surprise that there is not a specific number for dispersivity. The compilations of studies on a dispersivity value agree that there is an increasing longitudinal dispersivity value as the scale of the experiments became larger. From a geological point of view, the larger the scale the higher the uncertainty. There are larger pathways for flow as the scale of experiment increases, which drives the uncertainty higher.

Establishing one single value for the dispersivity of an entire reservoir would also not be entirely accurate. Certain parts of the reservoir will have different permeability and connectivities which are great contributors to this so called dispersivity. It would be wiser to provide a static model that also include dispersivity values on every cell, however this is not the case in any reservoir simulator.

4.3 Analytical Solution

As mentioned in the above section, CMG is a commercial simulator, meaning that most operations are done in the back end of the simulator and cannot be accessed by the user. This poses some problems when trying to analyse with strict detail the convergence and numerical issues that come with a numerical simulator.

This simulator is not optimized for a hydrogen storage operation, meaning that we have to use some tools in order to benchmark the results given by the simulator. As we will discuss later, the results between the simulator and the analytical solutions are not exactly the same due to some of the assumptions done by these kind of mathematical solutions. However, the results of changing certain parameters can be seen in the numerical simulation, which will indicate how sensitive the simulator is. This can help us predict some of the behaviour that is happening in the porous media as well as having some reference point on our results.

This short investigation will first derive the 1D analytical solution for the convection-dispersion equation.The derivation comes from the general advection-dispersion equation. This is shown in Equation 10

$$\frac{\partial(\phi C)}{\partial t} + \nabla \cdot (C\vec{u}) - \nabla \cdot (\phi \vec{D} \nabla C) = 0 \tag{10}$$

where the first term of the left hand sides represents the amount of concentration in the porous medium. The second term is the outflux of concentration due to advection and the third term is the outflux due do dispersive forces. The sum of these three terms is 0 if there is not a source term in the system.

The one dimensional Cartesian system assumes a constant porosity ϕ, a constant Darcy velocity u, as there is an incompressible flow regime, and that there is no source term. This one dimensional reservoir occurs only in the x direction. This leads to the formulation shown in Equation 11

$$\frac{\partial C}{\partial t} + \frac{u_x}{\phi}\frac{\partial C}{\partial x} - D_L \frac{\partial^2 C}{\partial x^2} = 0 \tag{11}$$

where D_L is the longitudinal dispersion and where u_x is the darcy velocity in the x direction. This can be translated into the dimensionless domain, where both time and space are on a scale from 0 to 1.The porosity ϕ and the longitudinal dispersivity D_L are assumed to be constant. The Boundary condtions for this formulation are the following:

$$C_D\left(x_D, 0\right) = 0; C_D\left(0, t_D\right) = 1; C_D\left(\infty, t_D\right) = 0 \tag{12}$$

The conversions from the normal domain to the dimensionless domain are shown:

$$t_D = \frac{u_x t}{\phi L}, x_D = \frac{x}{L}, C_D = \frac{C(x,t) - C_i}{C_j - C_i} \tag{13}$$

where dimensionless time, position and concentration are defined respectively. After rearranging the terms, the non dimensional numbers can be put into this one dimensional formulation as follows:

$$\frac{\partial C_D}{\partial t_D} + \frac{\partial C_D}{\partial x_D} - \frac{1}{\frac{u_x L}{\phi D_L}} \frac{\partial^2 C_D}{\partial x_D^2} = 0 \tag{14}$$

The first two terms represent the change in dimensionless concentration over time t_D and the change in dimensionless concentration over the dimensionless length x_D respectively. The denominator of the multiplier of the third term captures the ratio between advective and diffusive-dispersive forces. This is the non-dimensionless Peclet Number:

$$N_{Pe} = \frac{u_x L}{\phi D_L} \tag{15}$$

A high Peclet Number implies a bigger influence of advective forces in the system. This will have an effect on the length of the mixing zone between the different fluids.

4.4 Static Model

For the base case scenario, a radial model has been constructed based on a model that has been used on investigations performed by EBN , Eikelenboom and Huijskes 2020, Terstappen 2021. A radial model will be used because the injected gas expands homogeneously in every direction, which makes it simple to visualize and compare. All the physical processes that will be compared will be easy to isolate and analyse in a radial model. This radial model is seen in Figure 14.

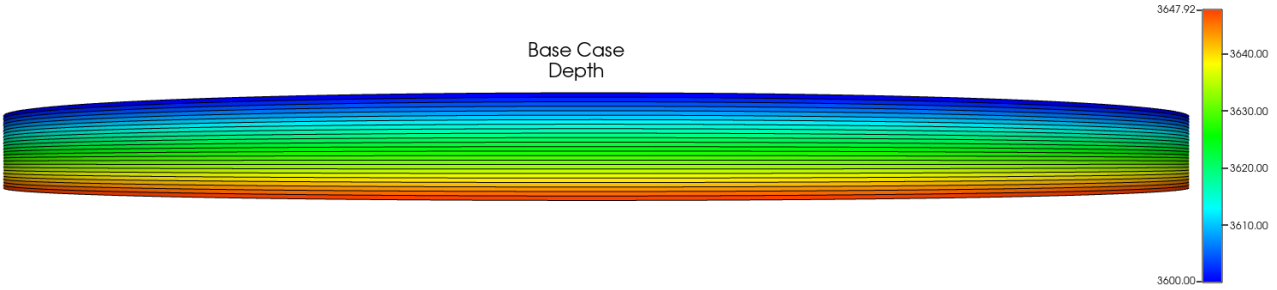

Figure 14: One to One depth map of base case

The base case is a radial model whose basic properties, such as porosity and permeability, are based on average of sandstone Dutch fields Juez-Larré et al. 2019The longitudinal and transverse permeability are defined with the same value, 20mD. The vertical permeability of each individual cell is 10% of the horizontal one as a standard practice. All the grid cells are 10 meter long in the radial direction and have a height of 2.08m. There are 48 horizontal cells and 24 vertical cells. Given that this Is a radial model, the furthermost layers will have a higher volume than the ones nearest to the center of the circle.

The depth (3600m) was chosen based on a typical Dutch reservoir. The maximum pressure during cycling was chosen based on compressor capacity. As a measure to ensure a safe operation, it is important that the maximum average pressure of the reservoir during the cyclic operation does not exceed this maximum pressure. This threshold pressure was set at 250 bar, which is approximately 10% less than the virgin pressure. These basic properties are listed in Table 2

Reservoir Parameter	**Value**	**Unit**
Radius	480	m
Thickness	50	m
Top Depth	3600	m
Temperature	100	°C
Porosity	12	%
Tortuosity	1	-
Horizontal Permeability	20	mD
Vertical Permeability	2	mD
Connate Water Saturation	0.1	-
Gas in Place	CH4	-
Depleted Pressure	20	Bar
Maximum Average Pressure	250	Bar
Gas-Water Contact	3700	m
Dispersivity Value	0	m
Connate Water Saturation	0.15	-

Table 2: Parameters Base Case

Based on a study done by van Gessel et al. 2022, the desired withdrawal period was aimed to be 50 days. This is an estimate for the rate deliverability requirements for a short, seasonal and strategic offshore hydrogen storage. The desired rate, in standard cubic meters per day, established for this base case is 2.5E6. These two will act as a target production values for the base case.

Operation

Figure 15 will be referred throughout this section in order to have a visualization of the following explanations. This radial model is perforated in its innermost cell, and has perforations in each layer. The simulations have three different wells, which all have an individual function and running time in the operation. These three wells will have their own constraints, which will allow them to realize the injection and production cycles. For the sake of simplicity, they will be named $WellA, WellB$ and $WellC$.

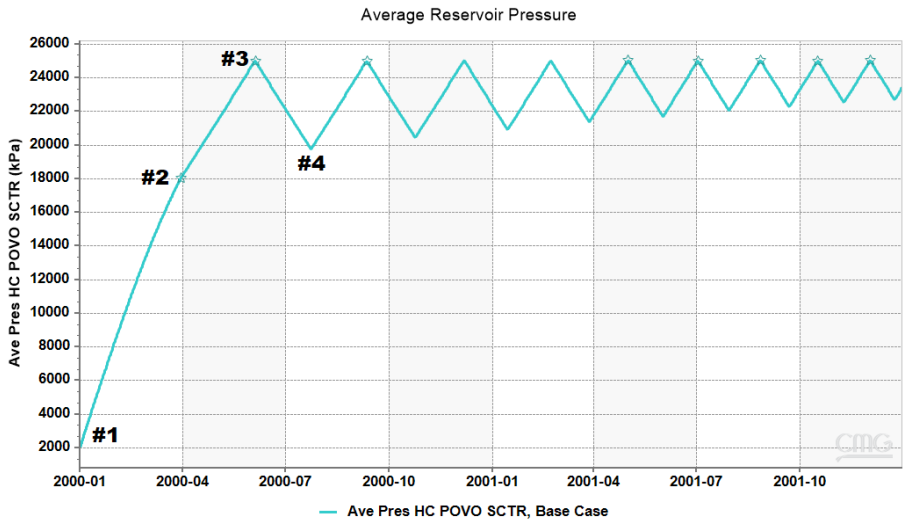

Figure 15: Average Reservoir Pressure of Base case displaying cyclicity

The constraints used in GEM to define a cycle are the following: 98% molar hydrogen purity in the producing well and a minimum production threshold of 98% of the target gas rate at standard conditions. As a side note, this target rate (in cubic meters per day) may vary per simulation. When one of these constraints is reached, the production will finish and injection of new hydrogen will start, which will start a new cycle. This gives an indication of how the simulator starts and ends production.

The simulation starts when the radial model is in a depleted state at 20 Bar. This is marked as point 1. Injection by $WellA$ will start and this loading will continue until an average reservoir pressure of 180 bar is reached. This point is marked as 2. This first injected gas will be either carbon dioxide, nitrogen, methane or hydrogen. This is the only time in the entire simulation that $WellA$ is used.

Point # 2 marks the shut down of $WellA$ and the immediate opening of $WellB$. This well will solely inject H2 into the reservoir. This injection ends when the maximum threshold pressure of 250 bar is reached. This is point #3 in Figure 15 and it marks the end of the first injection of gas into the reservoir. $WellB$ is closed at Point 3.

Point # 3 marks the start of the first production phase. The producing $WellC$ is opened and the extraction of gas of the reservoir starts. This production continues until point #4, which is where one of the production constraints is met. This point marks the end of the first injection and production cycle.

The second injection-production cycle occurs after Point 4. The injection $WellB$ will inject hydrogen, once again, until the upper limit of the average reservoir pressure is reached (250 Bar). Just as in the previous cycle, the hydrogen injection $WellB$ will close and the producing $WellC$ will open. This occurs at Point 5. This second cycle will therefore occur between points 4 and 6. The subsequent cycles are also based on an alternation between injection and production phases.

Apart from the component related constraints, there are also pressure constraints that each well and the reservoir must be kept with. As mentioned in the Background section, a cushion gas has to be injected into the reservoir. This raises the average reservoir pressure, which will later make sure that the production has the desired flow rate. This cushion gas volume is defined by a reservoir pressure at which the difference between

the Bottom Hole Pressure (BHP) and the average reservoir pressure is high enough to sustain the desired rate.

This minimum average reservoir pressure during operation has to be estimated, as the exact values for the future hydrogen network or the requirements for an specific hydrogen field is not yet known. The basic premise is that this minimum pressure has to be higher than the sum of the pressure of the onshore hydrogen network, the pressure needed to transport hydrogen from the field to land and the pressure lost due to friction or transportation.

A report by Gasunie, the Dutch natural gas infrastructure company, states that the natural gas pipelines operate on a usual pressure range of 66 to 80 bars. Gasunie 2015. We must therefore assume that the future hydrogen network will operate at approximately the same range. An assumption of the pressure of an offshore pipeline was settled at 30 Bar, from a personal conversation with the authors of van Gessel et al. 2022. The combination of these two would set a minimum Tubing Head Pressure (THP). The pressure lost by friction also needs to be taken into account for. Finally, because of the low density of hydrogen, the column of hydrogen in the tubing would not have a very high hydrostatic pressure, which would make the BHP slightly higher than the THP. the Bottom Hole Pressure (BHP) must be higher than this pipeline pressure.

These estimates result in a minimum BHP of 100 Bar. Of course, this is a rough estimation of the required minimum BHP. However, it is a parameter that has to be monitored throughout the simulation in order to make sure that there is a positive difference between the BHP and the Tubing Head Pressure.

4.5 Methodology

A sensitivity analysis was done in order to understand the individual effect of certain reservoir parameters in the cyclic storage of hydrogen in gas fields. If these individual effects are better understood in terms of the physical processes that occur in the reservoir, more complex models can be analysed at later stages with more ease. The base case will always be changed one parameter at a time. The reservoir characteristics and perforation intervals that will be changed throughout the sensitivity analysis will be the following:

1. Time step
2. Cell thickness
3. Cell height
4. Cushion gas volume
5. Dispersivity value
6. Diffusion coefficient
7. Location of High Permeability Streak (HPS)
8. Value of HPS
9. Perforation Location
10. Isolation of HPS
11. Volume Cushion with isolation
12. Alternating Permeability

The reasoning behind every sensitivity analysis will be briefly described in the Results & Discussion section, so that the reader may understand why every specific parameter was analysed. As the investigation took place, it became increasingly complicated to compare different scenarios where the reservoir characteristics, as well as the cushion gas, was variable. In order to be able to compare different sensitivity analyses in a systematic, consistent and fair way, some definitions involving the storage process have been conceived.

Originally, It was thought to do a more well-rounded analysis that resembled a real development plan. In the case of developing a UHS project, there must be a technical, economic, environmental and social analysis of the project. Given that this is a sensitivity analysis used to understand the physics of an UHS and not a real

field, the environmental and social aspects will be ignored in the evaluation. A UHS development will have to first choose an existing (depleted) gas field based on reservoir characteristics that seem adequate for a storage project as well with an assessment of the surrounding infrastructure.

This investigation was only aimed to compare results from a technical point of view. However, this would have been a slight dissociation from reality and from the way projects are developed in real life. It was more sound to perform a simplified, but standardized, economic evaluation and combine it with an evaluation of the physical processes that occur in the reservoir.

This volumetric CAPEX analysis allows this investigation to compare the different sensitivities in a more realistic way. The technical attributes of using different cushion gases can be characterized by the degree of mixing, however, if the volumes and rates are changing every time, this comparison would not be fair. If an economic analysis is added, the advantages or drawbacks of using a certain cushion gas can be explained with more depth and arguments, making the analysis more in line with a real development plan.

The suggested comparison is the statement "Per volume of Hydrogen that I can effectively produce, what is the investment in the reservoir". Due to mechanically driven dispersion, molecular diffusion, heterogeneities, and because of density differences between the different components, the well will have earlier breakthrough of cushion gas on every cycle. This means that production cycles become effectively shorter. As the simulator is meant to inject hydrogen into the reservoir when this purity threshold is reached, the injection periods are also reduced.

As shown in Figure 15, the cyclicity period of the base case lowers on each cycle. This decrease is due to the ever-increasing mixing between hydrogen and the cushion gas during the cycling loading. This decrease in cyclicity depends on the degree of heterogeneity of the reservoir, the perforation intervals and the rate of injection and production, something that will be discussed during the results. This mixing leads to an earlier breakthrough of the cushion gas, which makes the cycles shorter and shorter. It is therefore not wise to compare them by a set amount of production days. This would not make an accurate comparison because the times between simulations will not match perfectly.

This effect makes the cycles shorter and shorter, which in turn means that there is less hydrogen being injected and produced in each cycle. Measuring the rate at which these cycles decrease over time can be an interesting finding, because we could quantitatively and qualitatively analyse the effect of heterogeneities and perforation intervals in the reservoir. The quantitative analysis can be done in terms of a percentage reduction in the cycle period and the qualitative analysis can be done by reviewing the movement of the different gases in the reservoir through the cycles.

Given that there is an uneven reduction of cycle period, a comparison of volumes of hydrogen injected per individual cycle throughout the different sensitivity analyses is also not a fair representation. Moreover, even comparing the different cycles of a single run is not representative under a time constraint in production.

Apart from this, it is impractical, simulation wise, to discern between the hydrogen that has been injected on the first cycle than the one on any other cycle, only the cumulative volume of hydrogen injected up until a certain cycle can be known. Therefore, it is useful to see the relationship between the cumulative H2 recovered and injected up until cycle 4. This allows us to compare the mixing behaviour between reservoirs in a consistent manner and that allow a comparison between reservoirs with different dimensions and geological characteristics.

Therefore, this means that for the multiple cycle simulations, "effectively produced" represents the cumulative volume of hydrogen that has been extracted before reaching the purity or rate constraint after 4 cycles. To normalize throughout different reservoirs, a comparison between the ratio of cumulative injected vs the cumulative produced hydrogen can be considered.

The second part of this statement deals with the definition of what is the investment in the reservoir. This CAPEX will only consider the prices of the gases, and not of the pipelines, compressors and other infrastructure to have a UHS system either onshore or offshore.

The investment includes the price of the alternative gas, which is initially injected in the reservoir. The investment in the reservoir will include the difference in price between the cumulative injected and extracted hydrogen after 4 cycles, which is effectively the unrecoverable or lost hydrogen. Therefore, the definition is as

follows:

$$\textit{Investment to effectively store hydrogen} = \textit{Cushion Gas Price} + \textit{Unrecoverable hydrogen after cycle 4}$$

This will be used to compare different reservoirs in a consistent manner. As mentioned, the simulation time is 2 years. If the simulation does not reach the required number of cycles in this period of time, then the results will be removed rom the economic analysis.

4.6 Gas Prices

As mentioned, this investigation will base itself on the investment cost required with different cushion gases for the multiple reservoirs that will be tested. A certain price must be established in order to compare the different reservoir settings. These gas prices will fluctuate over time, however a single number must be established to do a CAPEX analysis. The volume of the reservoir will be constant in all the investigation, which means that the use of different gas prices will have the most effect on the economic evaluation.

In simple terms, gas prices are dependent on the current supply and demand around the world. As of the writing of this report, all of the gas hubs are trading gas at their highest prices ever, this can be seen in Figure 16. The Title Transfer Facility (TTF), the main European gas hub, was trading gas at almost €340 per megawatt hour. The price for methane will be set at €50 per megawatt hour.

Figure 16: TTF future trading prices of the last five years

The study by van Gessel et al. 2022 estimates the price for the production of hydrogen to be €2.7 per kg in an average scenario, and this value will be taken for this investigation.

Nitrogen is an almost inexhaustible resource as it consists of almost 80% of the Earth atmosphere. The price for the industrial separation of nitrogen from air could not be found during this investigation. The assumption will be that nitrogen is one quarter as cheap to produce than hydrogen. This means that the set price for nitrogen will be €0.675 per kg of gas.

Finally, the price for carbon dioxide is established based on the carbon tax imposed by the Netherlands. The carbon tax in this country, for industrial emissions, is on the rise since 2021, as established by the Klimaatakkoord. As of 2022, the tariff is €41.75 per ton of carbon dioxide emitted. This tariff is increasing by €10.87 every year up until 2030, where its price is going to be €128.71. NederlandseEmissieautoritiet 2022. The price carbon dioxide price of this year has been taken for the analysis. This would effectively act as a carbon dioxide storage, meaning that the UHS project would receive money by using this as an alternative gas.

5 Results & Discussion

The results of the different sensitivity analyses will come with an explanation that show their implications for a UHS. The first part of this chapter will describe basic aspects of a reservoir simulator such as the time-step and the grid size and how their refinement will affect the calculations. The second part will try to compare the results from the analytical solution to the results of the simulator. The third part will explain the choice for the different sensitvity analysis as well as discussing the results obtained for each of them.

5.1 Validation of Base case

This validation will base itself on a Nitrogen-Hydrogen scenario. Various reservoir characteristics and numerical issues will be tested so that their effects are better understood and are able to be translated when there are multiple cycles of injection and production.

5.1.1 Cell Size & Time Step

Cell size is a very important parameter in reservoir simulation. The grid size will discretize the reservoir in multiple sections, and the characteristics of each individual cell will be taken into account when the simulator performs the finite difference method. Apart from this a smaller cell size will be able to better capture small scale variabilities in the geology. An example of the grid used in the simulations is shown in Figure 17, where cells extend for 10 meters in the radial direction and have a height of 2 meters.

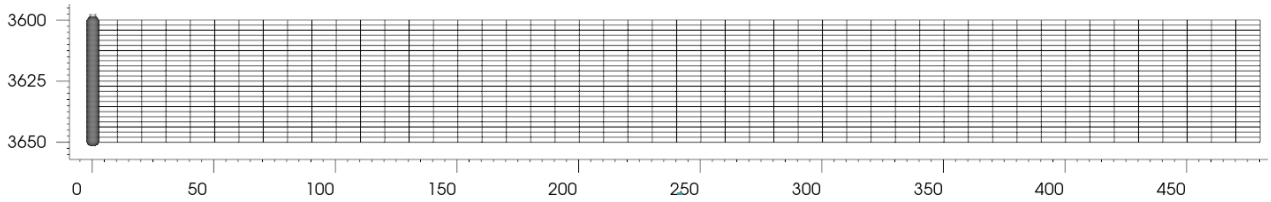

Figure 17: Grid of base case scenario

The truncation error (Δx^2) is, in simple terms, proportional to grid size; the smaller grid size the smaller the calculation error. However, a small grid size means a higher amount of linear equations have to be solved by the simulator. Even in very simple models such as this one, a decrease in grid size will drastically increase the computation time. Therefore, a test on grid size will allow to determine a computational efficient, as well as representative grid size for the remaining simulations. This test will only be done by reducing the cell size but not the time step. The following test will also reduce the time step used,

The main effect of the high cell thickness or height is the fact that the saturation changes between each grid cell becomes more step wise rather than a continuous system. During reservoir simulation, the ideal amount of grids has to be determined in order to run an efficient and accurate simulation.

A coarser grid in a reservoir simulator will mean that the geology is not characterized in a very detailed way. This investigation is dealing with simple, fairly homogeneous reservoirs, where the complicated subsurface does not need to be characterized or up-scaled from well data. However, the gridding will still have an effect on the flow calculations, as numerical errors will arise based on the grid size.

In real life reservoir modelling, there must be a balance between the accuracy of the simulator and static model, which can be done by means of history matching, and the computational time of the simulation. This is due to time and money limitations. This run time directly relates to the grid size of the different cells.

Increasing the number of grids also means that the geology is being represented at a way higher detail than usual. There may not even be sufficient data to populate a reservoir with that degree of accuracy. If there is no sufficient knowledge about the subsurface there is no reason to decrease the grid to a high resolution.

As the cell size is decreased, the smearing of the front between the different gases is reduced until a certain point. The truncation error will decrease as the grid size in both the vertical and horizontal direction decrease.

However, the most important factor here is the length of the cell which is parallel to flow.

Two cases will be shown for a Cell Thickness, the vertical height of each layer. For this test, the cell length is kept at 10 meters. The first case is shown in Figure 18. As seen, the saturation changes between each layer are quite high, and the front cannot be distinguished becuase of the course grid. If an analysis for the gravity number was to be done, it would be difficult to predict a front pattern as the ones shown in Figure 12. The vertical thickness of cells commonly used in reservoir simulators are around 2 to 3 meters, meaning that this value quite big for common standards.

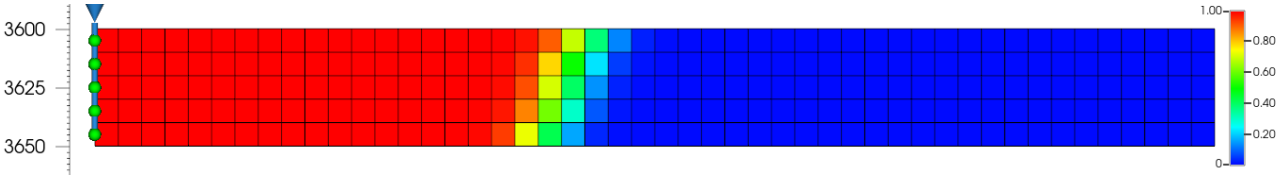

Figure 18: Cell thickness of 10 m. 100% Concentration of nitrogen is shown in red. 100% Concentration of residual methane in blue.

Figure 19 has a cell thickness of 0.4 meters. For visibility, the grid-lines have been taken away. In this example, the effect of gravitational segregation is much clearly seen because of the resolution of the cells. A resolution such as this one will help see the fronts of the components with more ease.

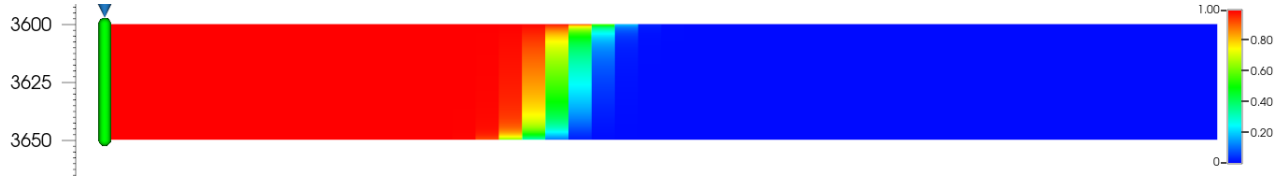

Figure 19: Cell thickness of 0.4 m. 100% Concentration of nitrogen is shown in red. 100% Concentration of residual methane in blue.

Finally, a vertical thickness of 2 meters was chosen and can be seen in Figure 20. The resolution is high enough so that small details are seen as well as having some correlations with cell thicknesses of common reservoir simulators.

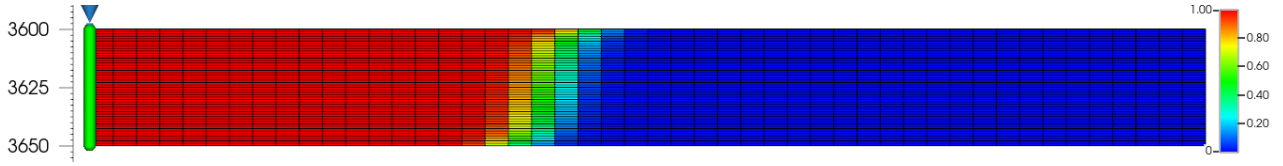

Figure 20: Cell length of 2 m. 100% Concentration of nitrogen is shown in red. 100% Concentration of residual methane in blue.

The following check involves the cell length, which is very important as this is the length of the cell in the direction of flow. The cell thickness in all cases is 2 meters. In the first case, Figure 21, the cell length is set at 100 meters. This is a resolution that some reservoir simulators have. This resolution could be the product of a lack of data or simply because of the size of the reservoir being simulated. As seen, there are massive jumps in concentration between cells. There are only 10 horizontal cells, which reduces vastly the resolution of the reservoir. The length of the mixing zone increases because of the low resolution of the grid.

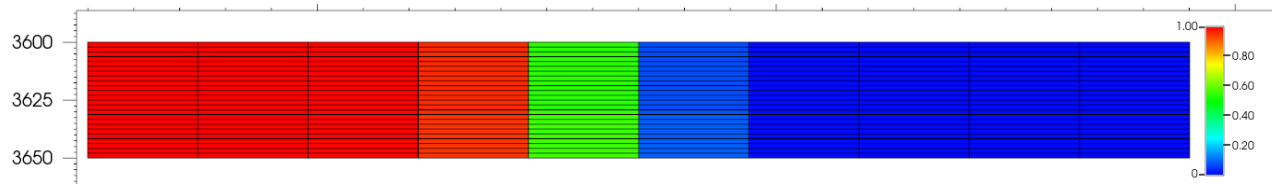

Figure 21: Cell length of 48 m. 100% Concentration of nitrogen is shown in red. 100% Concentration of residual methane in blue.

Figure 22 has a cell length of 0.5 meters. Here, the front between the different components is not fully sharp. This indicates that the effect of numerical dispersion is still present. The front is only around 20 meters in this case. However, a reservoir simulator will not have cells the size of 0.5 meters as the subsurface information is not very detailed. This would also imply an enormous simulation time for reservoirs of great size.

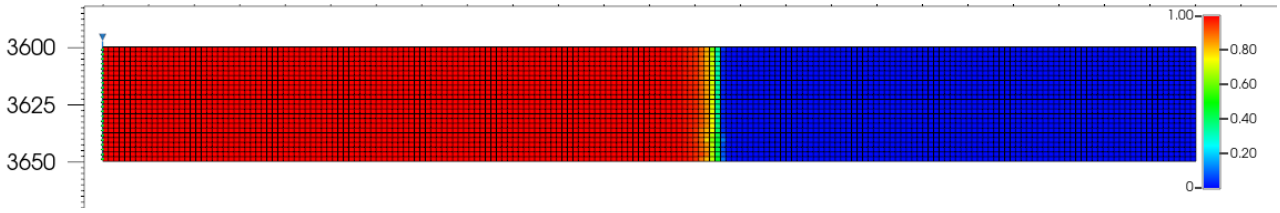

Figure 22: Cell length of 0.5 m. 100% Concentration of nitrogen is shown in red. 100% Concentration of residual methane in blue.

This analysis is only in terms of a single cycle and on the shape of the front between nitrogen and hydrogen. The next section will present the effect of reducing both the time step and the cell size, in order to have a validation of the base case and to be able to know the difference between the results of the base case and the ones where both the grid size and the time step have been reduced.

5.2 Analytical Solution

The idea of attempting a comparison is to provide an indication, even before the simulations are done, of how the system should behave, based on physical laws and not influenced by artifacts created by numerical approximation. Some derivations and governing equations have been provided in the Physics section, which can be solved analytically in order to predict this behaviour.

This brief investigation will deal with the influence of the Peclet number in the reservoir mixing and its development through time and the effect of density differences between the different components in the reservoir. In simple terms, the Peclet number is the ratio between the advective transport and dispersive diffusive transport. As seen in the Physics section the Peclet Number is defined as $N_{Pe} = \frac{U_x L}{\phi D_L}$ an included in equation Equation 15. If this number is large, the advective forces are much larger than the diffusive ones. This means that the last term of this equation can be ignored, as the Peclet Number is in the denominator and therefore reduces the fraction to 0.

A change in the Peclet Number changes the length of the mixing zone that is created when these two fluids mix. As seen in Figure 23 a small Peclet Number, such as 47, will have a diffusive front, which will lead to a higher mixing zone. This small ratio means that the influence from the physical movement of fluid is not higher compared to the dispersive forces. The mixing zone is becoming wider as time increases.

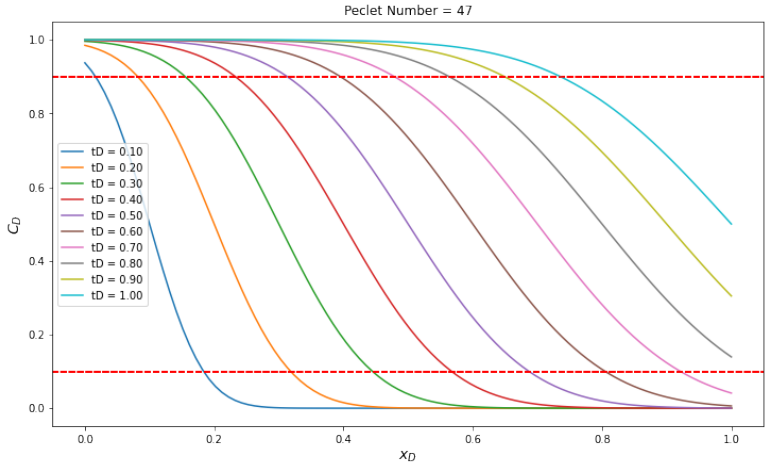

Figure 23: Mixing front between injected and intial concentration over dimensionless time. Red dashed lines at 0.9 and 0.1 C_D indicate the mixing zone

If the Peclet Number is increased to 1000, the advective forces will have a much greater effect. This is characterized by a sharper front, as seen in Figure 24. This figure shows the mixing front at dimensionless time 0.5. The mixing of both components is reduced because of the transport speed in the reservoir. As seen, an increase in Peclet Number decreases the mixing zone and makes a sharp front between components.

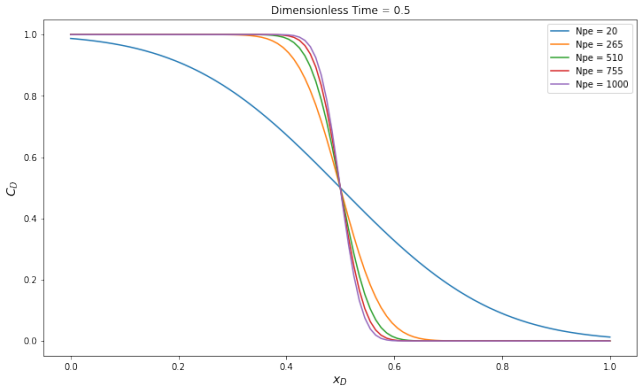

Figure 24: Mixing front between injected and initial concentration at dimensionless time $t_D = 0.5$. Red dashed lines at 0.9 and 0.1 C_D indicate the mixing zone

This can be physically compared to an injection of fluid in a core sample or a reservoir model. If a certain pore volume is flushed through a core sample, the speed at which it is injected will affect the concentration of the fluid measured at either the outlet or at any point in the reservoir at a any given time. A high Peclet Number, will indicate a high velocity of this front of injected fluid will decrease dispersive mixing. A low injection rate will let the dispersive mixing of the components have a greater effect on the concentration pattern.

There must be some considerations to take into account in order to compare this 1D convection-dispersion solution to the results provided by a numerical simulator. In the analytical solution, the concentration that is being injected C_j is 'replacing' the concentration of fluid that is on the system, which is C_i. The solution to the analytical solution in fact have a response depending on the Peclet Number, however it is not dealing with a real physical particle. There is also a constant velocity as an assumption, while there is a decreasing velocity away from the radius of the well and there is also the assumption of incompressible flow

In this no-flow boundary conditions simulator. the injected gas will physically sweep the gas that is currently in the reservoir. A mixing front will develop between the two gases. This front will either be the results of either the effect of numerical or physical dispersion. For this experiment, the cell size and the time step has been decreased in order to reduce the mixing created by numerical dispersion.

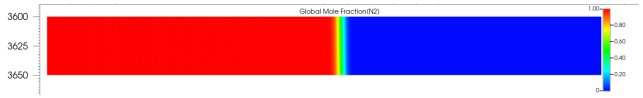

Figure 25: Mixing zone between nitrogen and residual methane midway through injection. 100% Concentration of nitrogen is shown in red. 100% Concentration of residual methane in blue.

Figure 25 shows the distribution of nitrogen when injection of alternative gas midway through injection. The grid lines have been taken out of the picture to increase visibility. The mixing zone is around 15 meters in length.

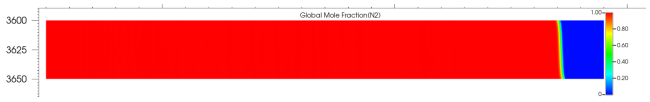

Figure 26: Mixing zone between nitrogen and residual methane showing smaller mixing front. 100% Concentration of nitrogen is shown in red. 100% Concentration of residual methane in blue.

As there is a no-flow boundary the residual methane is pushed to the edge of the reservoir. As seen in Figure 26, this mixing zone has a shorter length. This effect seen in the reservoir simulator cannot be seen in the analytical solution.

The degree of mixing has been investigated in relation to the cell thickness, cell length and time step used. However, the mixing seen is not real physical mixing, it is a numerical error. As seen, reducing these three mentioned factors will reduce the length of the mixing zone, but not fully suppress it. This must be taken into account in the entire analysis.

The next step is to add physical dispersion into the reservoir settings and see its effect on the mixing zone. The previous experiment has reduced the effect of numerical dispersion. A 'dispersivity value' can be added to the simulator in order to try to model real mixing due to advection and dispersion. The dispersivity value will be 1m. Figure 27 shows the front between nitrogen and methane, where the mixing zone has increased significantly compared to Figure 26.

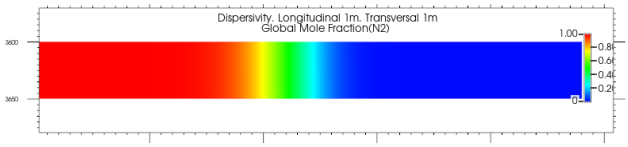

Figure 27: Mixing zone between nitrogen and residual methane with dispersivity value of 1m. 100% Concentration of nitrogen is shown in red. 100% Concentration of residual methane in blue.

Figure 28 shows the mixing front between hydrogen and nitrogen at the right, and the mixing zone between nitrogen and residual methane on the left. Again, the methane has been pushed towards the edge of the reservoir, and its mixing zone is considerably of less length than the one of hydrogen.

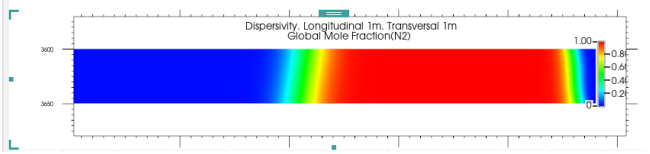

Figure 28: Mixing zone between nitrogen and residual methane with dispersivity value of 1m. 100% Concentration of nitrogen is shown in red.

In the case above, the value for the longitudinal and transversal dispersivity value were the same. Therefore, an experiment with a lower transversal dispersivity was performed. The reason for this was that an equal transversal and longitudinal value as an input to GEM as seen in Equation 2, would cancel the second term of the equation. This would also cancel the remaining tensor components in Equation 3 as the only movement

that would occur would be in the main x,y and z axis.

Although there is not an established ratio between the longitudinal and transverse dispersivity, as well as not being a definite value for the dispersivity in the first place, it is more logical that the longitudinal dispersivity, is higher than the transversal. This is because most of the mixing will occur in the direction of flow and not transversal to it. This will of course vary from reservoir to reservoir. For the simplicity of the experiment, a longitudinal dispersivity value α_{kl} of 1m was established, while a transversal dispersivity value α_{kl} of 0.5m was established.

There was no difference in terms of the mixing zone when an identical or different transversal dispersivity value was used (in the case of the same longitudinal dispersivity value). This is shown in Figure 29 This probably has to do with the fact that the model being used is a radial model, as everything will move towards and away from the well homogeneously while having no variation at any point in the circumference on the reservoir.

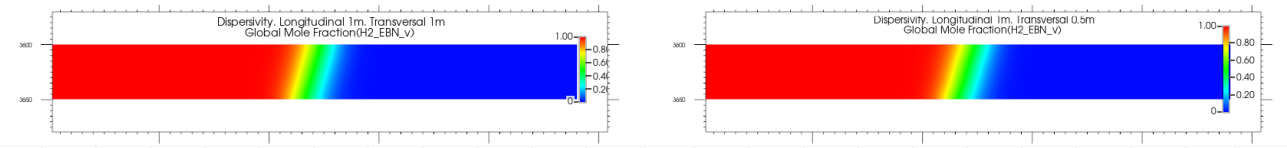

Figure 29: Comparison of mixing zone for a constant longitudinal but different transversal dispersivity

5.3 Multiple Cycle

5.3.1 Rate

It was already established in the formulation of this investigation that the deliverability was aimed at 50 days with a rate of 2.5E6 m^3/day of hydrogen production. The previous section investigated the volume of alternative gas to have this desired deliverability with a given injection and extraction rate. However, it is useful to understand what would happen in the reservoir when different rates are used. As seen in the Physics section, the shape of the front between the different gases will depend on the rate at which it is injected as well as its distance from the well.

A variable rate will translate to a different cyclicity period, and therefore the different cycles cannot be easily compared. However, a change in rate will allow an understanding of the influence of advective and buoyant forces during injection of gas. In this sensitivity analysis, the injection and production rates of the reservoir will change, while the volume of alternative gas will remain constant. This will allow to compare the distribution of hydrogen and alternative gas in the reservoir in respect to the rate which it was injected.

This experiment will try to replicate the results and conclusions that can be derived from the analytical solution. The challenge with this sensitivity are the time scales of the cycles. An analysis of the distribution of hydrogen in the reservoir is meant to be done at the end or start of a certain cycle. However, due to the different injection rates,

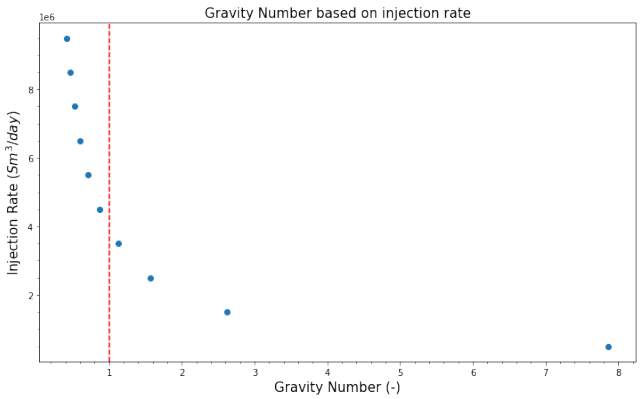

Figure 30: Rate of hydrogen injection against gravity number in reservoir with the characteristics of the base case. Red line at Gravity Number = 1 indicate a balance between gravity and viscous forces

As mentioned in subsection 3.3, large Gravity Numbers (N«1) indicate that gravity forces are dominating in the system while small Gravity Numbers (N»1) indicate that viscous forces dominate. A large N arises from a low injection rate of hydrogen into the reservoir. Injection rates lower than around 4E6 m^3/day will theoretically result in high gravity numbers, where gravity will dominate.

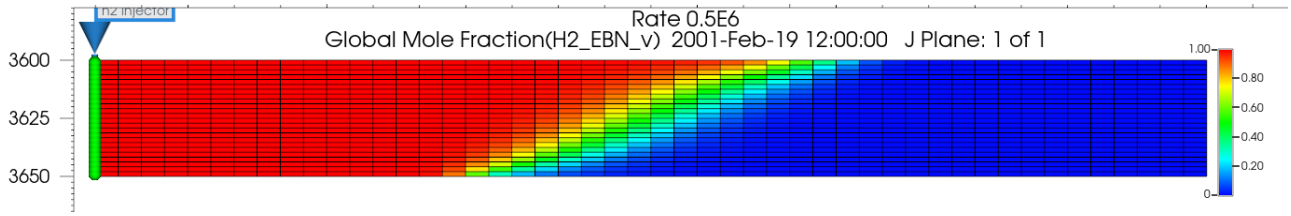

Figure 31: Distribution of hydrogen in the reservoir after injection of nitrogen and hydrogen. 100% hydrogen is displayed as red.

Figure 31 shows the hydrogen distribution after the injection of hydrogen at a rate of 0.5E6 m^3/day. For reference, the simulation start at the start of the year 2000, and shown in the graph, the injection finishes nearly 15 months after this date.

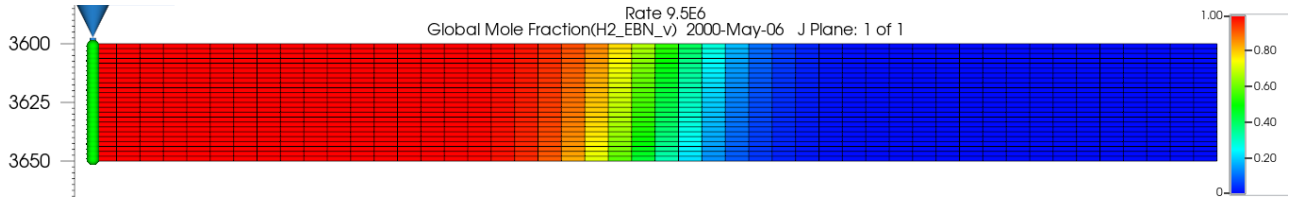

Figure 32: Distribution of hydrogen in the reservoir after injection of nitrogen and hydrogen. 100% hydrogen is displayed as red.

Figure 32 shows the hydrogen distribution after the injection of hydrogen at a rate of 9.5E6 m^3/day. Because of the increased rate, the injection time is lower. There is a clear difference on the shape of the front between both examples. Calculations from the Equation 7 show that there is a gravity dominated system. A lower rate will lead to a smaller γ value, which is characterized by a shallow front between miscible fluids, as seen in Equation 8.

As long as there is movement due to advection, in this case the well injecting fluid, there will be an interplay between gravity and viscous forces. The same volume of hydrogen has been injected in both cases and the distribution of this gas has been analyzed at the end of this injection. When there is no mass transfer due to advection, bouyancy forces will be the ones acting on the fluids.

A slanted front could potentially cause an earlier breakthough of cushion gas by the well. However, this conclusion is taken from a homogeneous test case scenario. The addition of heterogeneities will cause a different distribution of fluids in the reservoir. This will be seen later in the investigation.

5.3.2 Dispersivity Value & Diffusion

As explained in the physics section, the dispersivity value is an optional parameter in this reservoir simulator. The default value for this base case scenario is 0, but the effect of an increasing dispersivity value will be tested and compared to the analytical solution provided. A dispersivity value of 0 would imply a lack of physical dispersion, and therefore mixing. However the mixing seen in the results are purely the results of numerical approximations in the reservoir simulator.

There is no way to quantify the dispersivity of the subsurface on a large scale. This largely depends on the heterogeneity of the subsurface. The dispersivity value is an important parameter in the mass transport equation, which means that it is crucial in reservoir simulator. In this sensitivity analysis, the effect of an increasing dispersivity value is analysed, to see how this would affect the mixing in the reservoir and therefore the effectivity of the system in providing hydrogen with the established requirements.

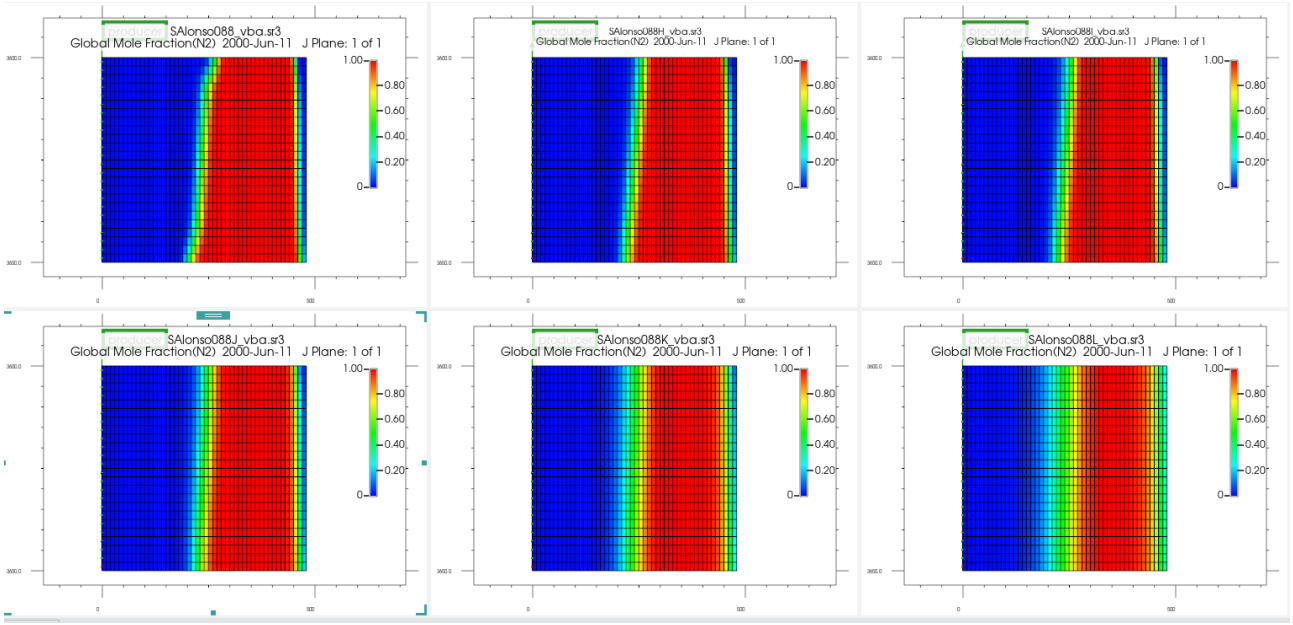

Figure 33: Evaluation of mixing zone during initial production. Concentration of nitrogen is shown in red.

As predicted by theory and by the analytical solution, an increase in the dispersivity value increases the width of the mixing zone, in this case between nitrogen and hydrogen. However, the effect seen in this set of simulations is the combined effect of numerical dispersion and the addition of a real component of dispersion. There does not seem to be any linear relation between the width of this mixing zone and the value of dispersivity. There is an additive or multiplicative effect by the smearing caused by the linear approximations and the addition of physical dispersion. Apart from this, there is no practical manner to discern between the numerical dispersion and the one given by the real dispersion mechanism if the cell size and step size are not decreased to very small values. This was studied by Terstappen 2021 in further detail.

That investigation also showed a very small influence on the mixing zone by the diffusion coefficient compared to the dispersivity value. The diffusion coefficient only had an influence when increased to values which were not realistic. The results of this investigation also show a minuscule effect of the diffusion coefficient in the purity of the extracted hydrogen.

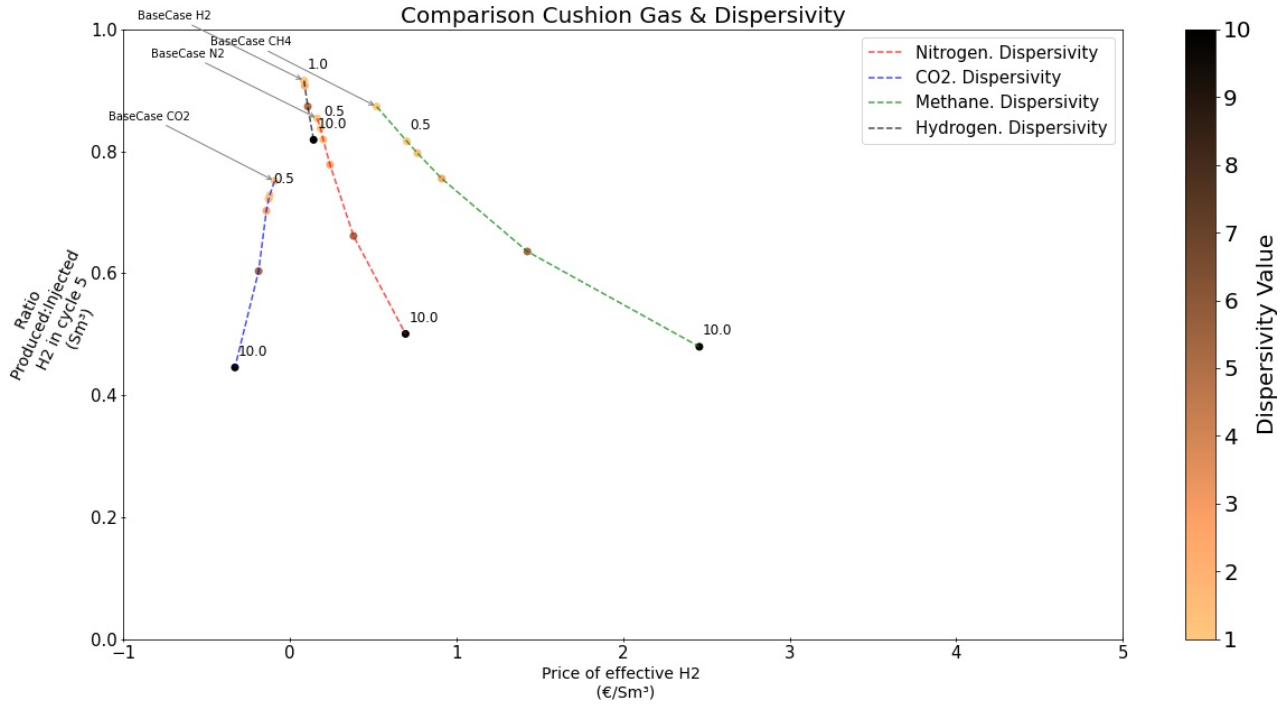

Figure 34: Price evaluation for different dispersivity values and cushion gases

The results show that an increased value for dispersivity makes the UHS system less price effective in the simulations. When a simulation is using a certain alternative gas, it will always inject the same volume. This means that the variations in cost are solely due to how much hydrogen can be recovered.

As mentioned in the Gas Price section, the cost of methane is considerably higher than the one for nitrogen and hydrogen. The use of methane will be high as a cushion gas with the current price. There is a negative price to store hydrogen when using carbon dioxide as the operator would receive money to store the carbon dioxide. It was assumed that the price per cubic meter of nitrogen was lower than the one of hydrogen. However, there is more volume of nitrogen injected into the reservoir, and thus the increased costs. In general the variability of price to effectively store hydrogen will directly come from the volume of unrecoverable hydrogen in the reservoir.

As seen in Table 3, an increasing dispersivity value will have less recovery of hydrogen. At the same time, this recovery will increase along the different cycles for any dispersivity value. This is also the case for all the different alternative gases used. However, the period of every cycle is getting smaller. As previously stated, the objective of this proposed UHS system is that it delivers a certain volume at a certain rate for a given period of time. This decrease of cyclicity period hinders our production goal.

	Percentage Injected:Produced hydrogen										
Dispersivity Value	**Cycle 0**	**Cycle 1**	**Cycle 2**	**Cycle 3**	**Cycle 4**	**Cycle 5**	**Cycle 6**	**Cycle 7**	**Cycle 8**	**Cycle 9**	**Cycle 10**
0.5	69.92%	76.18%	79.14%	81.25%	82.65%	83.75%	84.66%	85.34%	85.87%	85.88%	83.54%
5	45.50%	54.29%	58.90%	62.11%	64.36%	66.12%	67.53%	68.61%	69.71%	70.45%	71.25%
10	31.06%	38.82%	43.24%	46.03%	48.38%	50.06%	51.59%	52.83%	53.98%	54.71%	55.59%

Table 3: Increasing recovery factor of hydrogen as cycles progress. Sensitivity analysis for dispersivity with nitrogen as alternative gas

The conclusion for this certain sensitivity analysis is not the fact that increasing the dispersivity will make the system less cost effective, but that having a certain value for dispersivity will have an effect on the simulations. This will further increase the mixing on the reservoir that at first arises from the truncation error caused by the finite difference method. The combined mixing effect is higher for higher dispersivity values. There is however, no linear relation between the grid size, time step and dispersivity value. This was investigated in the Validation section and also by Terstappen 2021

5.3.3 Heterogeneity

The first heterogeneity test was done with the addition of a High Permeability Streak (HPS) into the base case. This HPS was added at three different locations in the reservoir, as seen in Figure 35. The reservoir perforations are still done in the entire reservoir column. This sensitivity was done in order to see the effect of a HPS in the fluid flow in the reservoir.

This very simple experiment could represent a fracture in a fairly homogeneous reservoir. The majority of the flow would be directed though this medium, and it will be insightful to know how its effect on the cyclicity period and on the distribution of gas in the reservoir. The HPS has a permeability of 40 mD. To keep the formation permeability kh constant, the permeability of the other layers had to be scaled down accordingly. This resulted in the cells having 19.1 mD instead of the 20mD as was established in the base case.

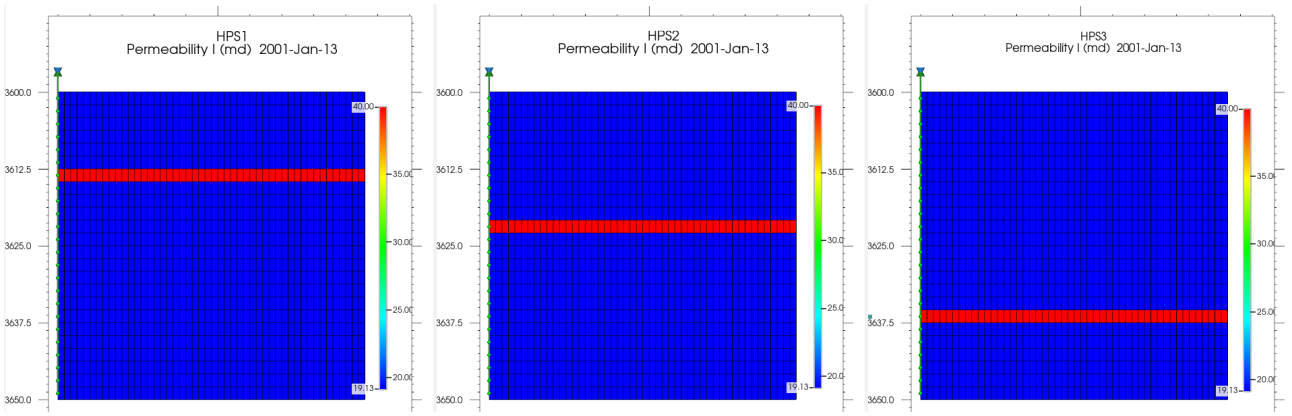

Figure 35: Location of the High Permeability Streak in the reservoir. HPS1, HPS2 and HPS3 respectively. Not to scale

The HPS located near the top of the reservoir is named HPS1, the one placed in the center is HPS2 and the one at the bottom is HPS3. Figure 36 shows the nitrogen distribution in the reservoir halfway through the intial injection of hydrogen. a 100% distribution of nitrogen has a red colour and a 0% concentration is displayed as blue. In this case, the blue in the left part of the reservoir is CH4 while the hydrogen is located on the right part of the reservoir.

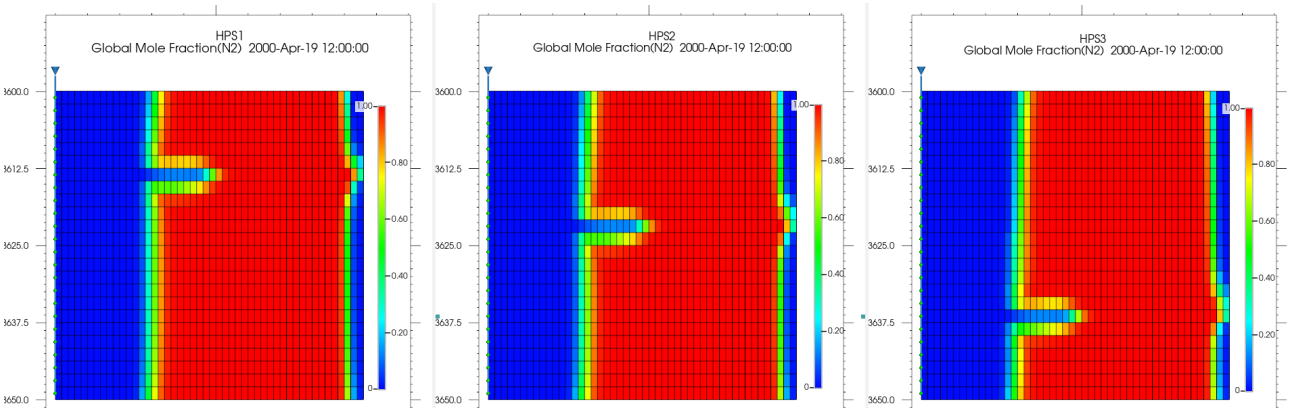

Figure 36: Distribution of nitrogen in the reservoir during the initial injection of hydrogen. Not to scale.

It is clear that the HPS has a effect on the distribution of alternative gas and of the hydrogen. Flow through the HPS (and the layers vertically adjacent to it) is being favoured because of the increased permeability of this layer. The piston like movement of both the alternative gas and the hydrogen is being replaced by a preferential flow by through the HPS. This is the case regardless of the position of the HPS in the reservoir.

The purity of the extracted hydrogen is very different from the one of the base case. As seen in **??**, the addition of a HPS in the system makes the breakthrough of the alternative gas quite early in the process. This flow-path makes the injection of the alternative gas and hydrogen faster and effectively. However, it also has the same effect during production, as this preferential pathway for flow will allow the easy removal of both gases from the reservoir as well. This is detrimental to the system because a high hydrogen purity is obtained for only a short period of time.

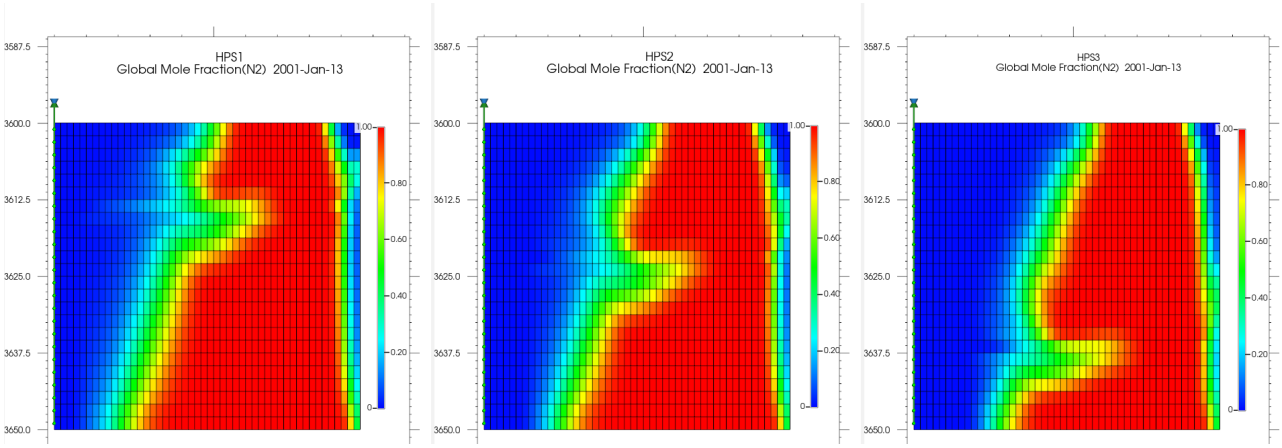

Figure 37: Distribution of nitrogen in the reservoir at the end of cycle 4. Not to scale.

Even with a slight variation in permeability, both Figure 36 and hpsmid clearly show a preferential flow through this streak. The economic results show no major difference in the either the effective produced hydrogen or the price to store it regardless of the location of this HPS. This is the case using all of the different gases. This is shown in Figure 38.

As mentioned, this HPS has only 20mD more permeability than its surroundings. However the HPS has a strong effect on the distribution of gases in the reservoir. Flow through the HPS (and the layers vertically adjacent to it) is being favoured because of the increased permeability of this layer. Mobile hydrogen can be transported in an out of this layer.

The piston like movement of both the alternative gas and the hydrogen (as seen in the base case) is being replaced by a slightly increased preferential flow by through the HPS. The front between the nitrogen and hydrogen is becoming arrow-like near the HPS, as shown in Figure 37. This is the case regardless of the position of the HPS in the reservoir. If the simulation is run for an extended period of time, then the distribution of hydrogen will be slightly different due to accumulation of hydrogen near the higher permeability area.

The effect of the heterogeneity in the reservoir is not very strong as this layer is only 40mD. However, it is clear that a HPS of higher permeability value will have an effect on the distribution of gas in the reservoir.

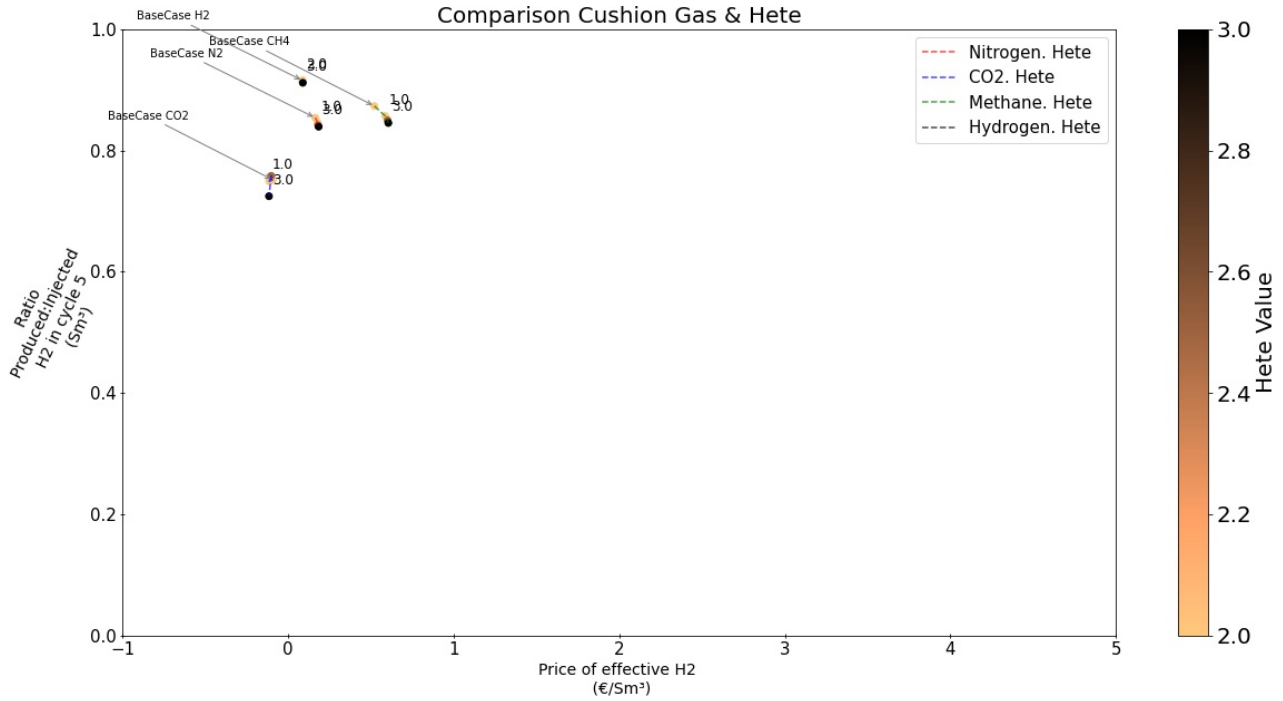

Figure 38: Price evaluation for different locations of HPS

The purity of the extracted hydrogen is slightly different from the one of the base case. As seen in Figure 39, the addition of a HPS in the system makes the breakthrough of the alternative gas early in the process. This flow-path makes the injection of the alternative gas and hydrogen faster and effectively. However, it also has the same effect during production, as this preferential pathway for flow will allow the easy removal of both gases from the reservoir as well.

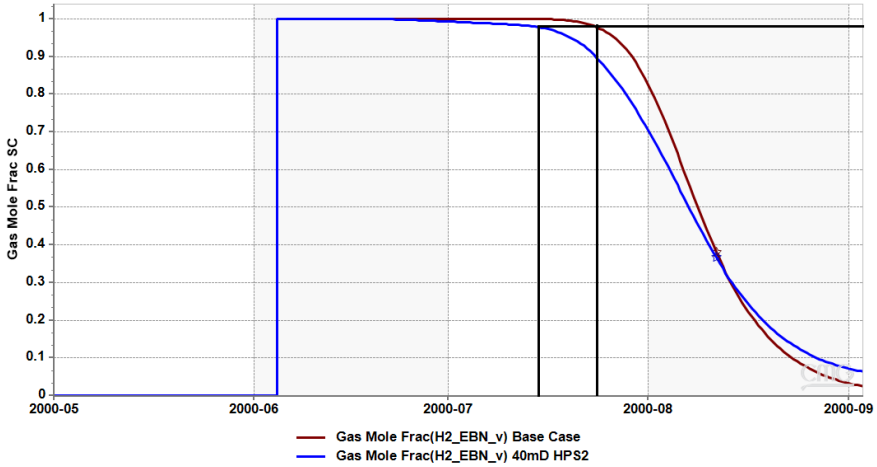

Figure 39: Comparison of hydrogen purity between base case and HPS2 of 40mD. The streak has an earlier breakthrough of alternative gas

This earlier breakthrough is detrimental to the system because a high hydrogen purity is obtained for a shorter period of time. This breakthrough will occur earlier when the system has multiple cycles as well.

5.3.4 Value of HPS

It is clear that a HPS will have an effect on the purity of the extracted hydrogen. As seen in Figure 37, the distribution of hydrogen and alternative gas will vary considerably depending on the location of the streak. In this sensitivity analysis, the value of the HPS is tested in order to see further see the effect of a heterogeneity in the reservoir. The HPS is placed in the middle of the reservoir and the different sensitivity analyses will have

a HPS of increasing values. These values are shown in Table 4. As a note, just as in the previous sensitivity analyses, the permeability of the reservoir had to be scaled down in order to keep the kh of the reservoir constant.

	Case 1	Case 2	Case 3	Case 4
Value HPS (mD)	60.0	100.0	150.0	200.0
Permeability rest of reservoir (mD)	18.3	16.5	14.3	12.2

Table 4: Reservoir permeability in the presence of a HPS

Because of the scaling to keep the permeability thickness constant, the lower the value of the HPS, the more homogeneous the system is, meaning that the movement of the gas in the reservoir will have a piston like behaviour. As shown in Figure 40 the plateau in hydrogen purity is conserved for a longer period of time if the value of the HPS is small. HPS with higher permeabilities will have a breakthrough of alternate gas at a much earlier stage. This standalone HPS has a great effect on the deliverability and capability of this UHS system. However a single HPS in an otherwise homogeneous reservoir can cause a great difference in the purity of the extracted hydrogen.

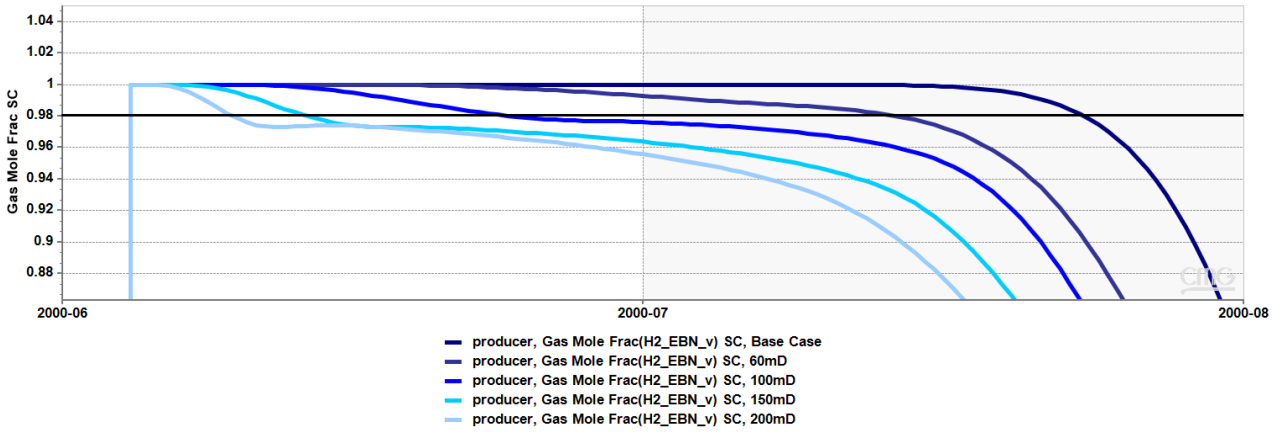

Figure 40: Purity of produced hydrogen showing earlier breakthrough of alternative gas for HPS of higher value

From the economic point of view, the reservoir is less efficient in its recovery of hydrogen as well as it being more expensive to store. The higher value permeabiity streaks are drawing the alternative gas quicker from the reservoir and the period of cyclicity is becoming smaller.

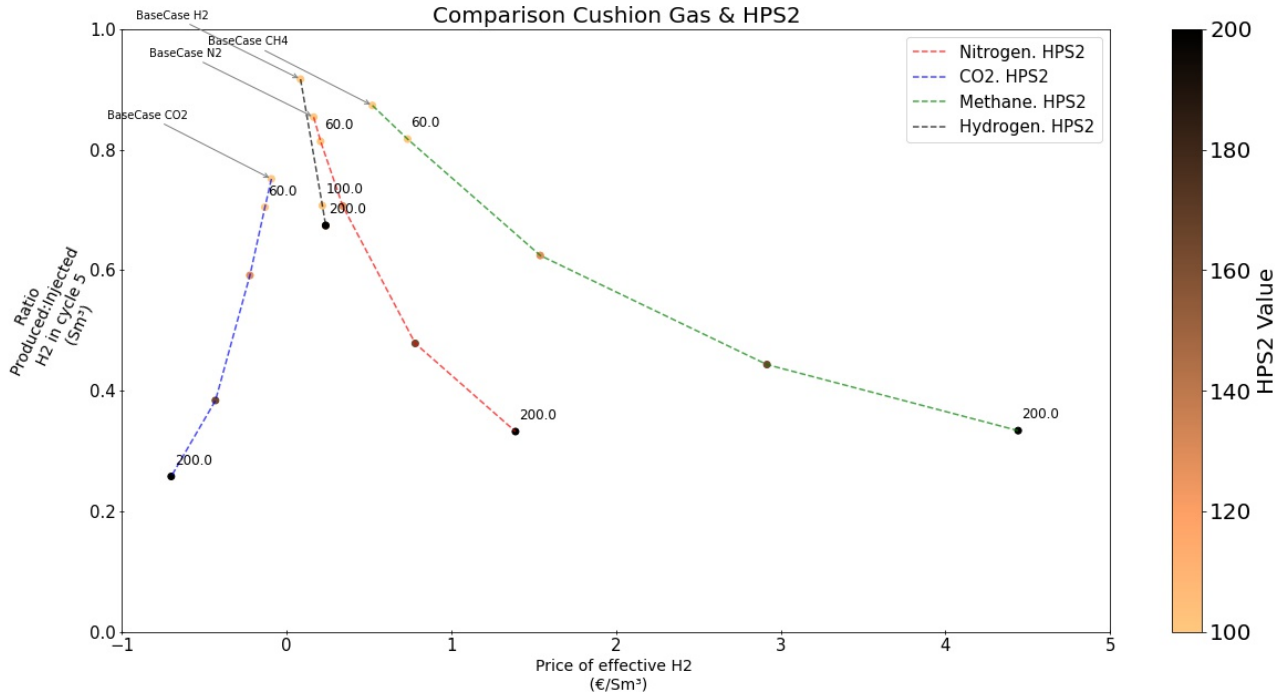

Figure 41: Price evaluation for HPS of different permeabilities. The HPS is located in the middle of the reservoir

Apart from this, there is an amount of unrecoverable hydrogen that is rising from the HPS due to the effect of buoyancy. This can be seen in Figure 42 As the cycles are getting shorter, there is no time or sufficient pressure to produce this hydrogen from that point of the reservoir, which contributes to an inefficient system.

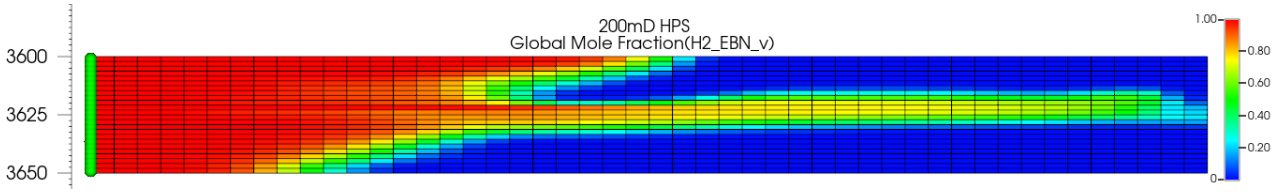

Figure 42: Distribution of hydrogen after 20 cycles showing unrecoverable hydrogen. 100% hydrogen is displayed in red

As seen in Table 5, the cyclicity periods for the case HPS2 200mD do not reduce significantly over time for either of the gases. On the other hand, in the case of a 60mD, the duration of each cycle is decreased substantially.

		Duration of Cycle (days)										
Permeability HPS (mD)	**Alternative Gas**	**0**	**1**	**2**	**3**	**4**	**5**	**6**	**7**	**8**	**9**	**10**
60	N2	40.0	34.5	31.0	28.5	26.0	24.0	22.5	21.0	20.0	18.5	17.5
	CO2	25.0	20.0	17.0	14.0	12.0	11.0	9.0	9.0	8.0	7.0	7.0
	CH4	32.0	31.0	31.0	31.0	29.0	27.0	25.0	23.0	22.0	20.0	19.0
200	N2	5.5	5.0	5.0	5.0	5.0	5.0	4.5	4.5	4.5	4.5	4.5
	CO2	3.9	4.0	3.4	2.7	3.0	3.0	2.8	3.0	2.4	2.4	2.4
	CH4	6.0	5.0	5.0	5.0	5.0	5.0	5.0	5.0	5.0	4.0	5.0

Table 5: Cycle duration in for alternative gases and value of permeability streak

As the permeability thickness of the reservoir was meant to kept constant, a higher HPS value, will represent a decrease in permeability of the rest of the cells in the reservoir. A higher value will also maintain a relatively

constant period of cyclicity. It is clear that most of the flow is going through the HPS. The injected hydrogen is not physically moving across the entire height of the reservoir, but is mainly being transported through the HPS towards the well.

Therefore, it would be insightful to see the effect of this same 200mD permeability streak in the case that the reservoir has a higher permeability thickness. This would model a slightly more 'real' reservoir as in reality, the presence of a HPS will not affect the permeability of the rocks surrounding it. The permeability thickness was kept constant in this sensitivity analysis was done in order to be able to compare the different reservoirs in a fair manner.

This would mean that the remainder of the reservoir would be once again 20mD and there would be a HPS of 200mD, which will increase the kh of the reservoir to 1375mDm. The production periods of multiple cycle are shown in Figure 43

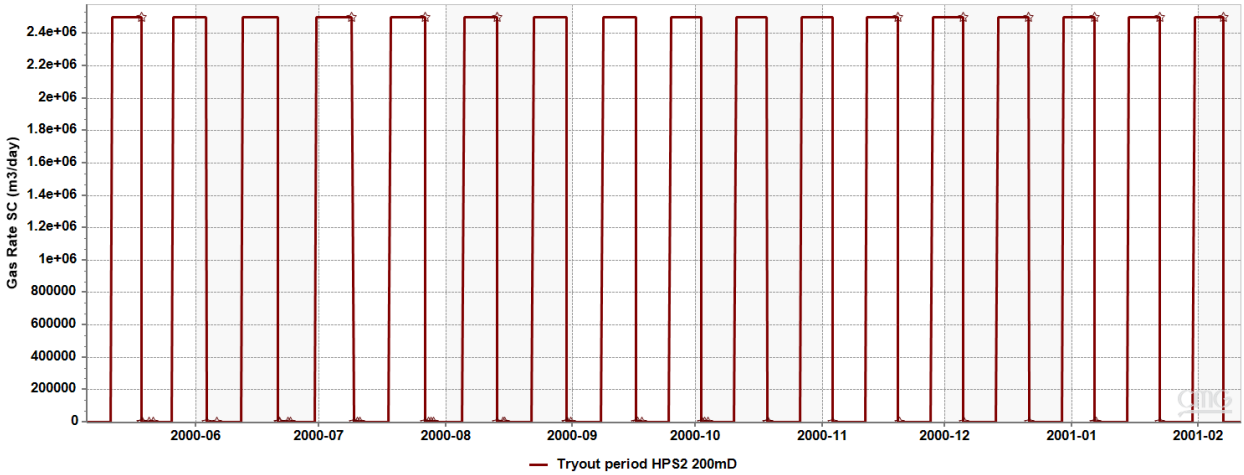

Figure 43: Constant cyclicity over multiple cycles on mentioned experiment

The results show once again that the cyclicity period does not decrease significantly along fifty injection and production cycles. Despite the fact that the period of this system is seven days, a constant period is maintained. This is considerably lower than the target of fifty days, however this gives an indication that the period can be maintained despite a heterogeneous medium.

As the subsurface is a very homogeneous medium, these changes in flow paths, due to higher (or lower) permeabilities, will be spread throughout the entire reservoir, not only in the vertical direction but in a horizontal direction as well. These variabilities will have an impact on the flow and therefore on the ability of the well to extract gas from the subsurface. This reservoir model also does not include any sort of fractures or faults, which are main pathways for fluid flow in reservoirs. Given that a single heterogeneity has a great effect on the extraction purity, it is logical to add more heterogeneities to the reservoir, to see what their effect is.

5.4 Isolation of HPS

The addition of an HPS into an otherwise homogeneous reservoir will add a preferential flowpath that is useful in the injection of gas, as it enhances flow, however it also draws out the alternative gas that has been injected into the reservoir with ease, which is detrimental to the system operational requirements.

This HPS can be isolated by means of different perforation intervals, in order to reduce the influence of flow of this high permeable zone. This will change the pathflow of the gases and therefore have an effect on the cyclicity period, pressures in the well and purity of the extracted hydrogen. In terms of the simulator, these perforations intervals translate into perforated cells. These can be turned on and off to stop or allow flow. The different sensitivity analyses will isolate the surrounding 1,3,5,7 and 9 cells around the HPS. A single cell is roughly 2 meters.

An increasing amount of isolation means that the gases will enter the reservoir through a reduced space. This will have an effect on the bottom hole pressure and on the flow paths of gas in the reservoir, as well as the time

it takes to reach a certain average reservoir pressure.

The permeability of the HPS in these sensitivity analysis will be 200mD, which corresponds to Case 4 of the previous section. As stated, the cyclicity period decreased at a lesser extent as the permeability of this streak was increased. An isolation of five cells will be used which roughly translates to an isolation 10 meters below and above the HPS. Figure 44 shows that the distribution of hydrogen in the reservoir at the end of injection is fairly similar to the one shown in Figure 44. The main difference between the normal and the isolation case is the time taken to load the reservoir with both hydrogen and the alternative gas.

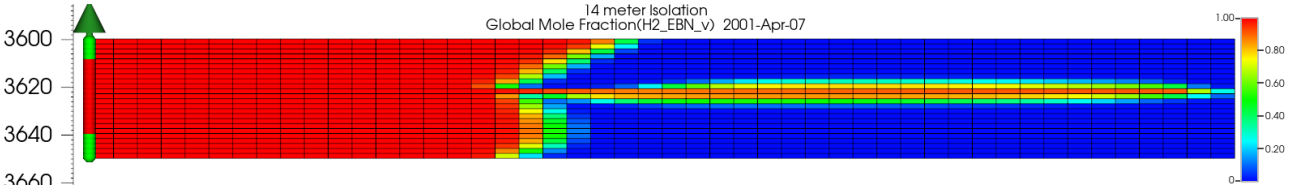

Figure 44: Distribution of hydrogen after initial injection. 100% hydrogen is displayed in red

However, the distribution of hydrogen at the end of the first production is very different, as shown in Figure 45. The flow path of the gas has changed completely. There is a triangular shaped mixing zone that stems from the interval that has not been perforated towards the HPS. This is due to the different pathway of flow that the gas needs to take in order to travel in and out of the reservoir.

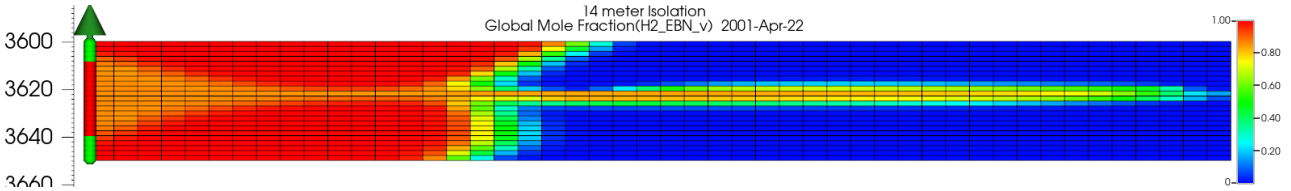

Figure 45: Distribution of hydrogen after initial production. 100% hydrogen is displayed in red

In terms of the effectivity of storing hydrogen, there is a trend between the degree of isolation and the cost of to store hydrogen. However, if the cyclicity period is analyzed, there is a trade off for this decrease in price. As seen in Table 6, as the isolation of the HPS increases, the initial period increases however, the reduction of this period is also higher. For example, an isolation of approximately four meters, which is the equivalent of 2 vertical cells, has an initial period of 9 days and becomes 7 days after 10 cycles, which is a decrease of 23%. On the other hand, a 9 cell isolation has in initial period of 14 days, but this becomes only 7 days after 10 cycles, which is a 50% decrease.

	Duration of Cycle (days)										
Meters of perforation around HPS	**0**	**1**	**2**	**3**	**4**	**5**	**6**	**7**	**8**	**9**	**10**
0	6	5	5	5	5	4	5	4	4	5	4
4	9	8	7	7	7	7	7	7	7	7	7
6	11	10	9	9	9	8	8	8	8	8	8
10	12	11	10	10	10	9	9	9	9	9	9
14	13	12	11	11	11	10	10	10	10	10	9
18	14	13	12	12	11	11	11	10	9	8	7

Table 6: Cycle duration for a system with isolation around a 200mD HPS located in the center of the reservoir.

This time around, the decrease of the period of the cycles is not being solely caused by the purity of hydrogen in the reservoir, but by an operational constraint. The isolation is reducing the entrance and exit point for the

gas. In the cases with less isolation, the purity constraint is the bottleneck, while the bottleneck on the higher isolation cases is the bottom hole pressure.

This operational interaction has an interplay with the requirements of the system in terms of cyclicity and the effectivity of the reservoir of delivering hydrogen. The price evaluation for this sensitivity analysis is shown in Figure 46. There is a trade-off between reducing the effect of the HPS and being able to efficiently inject and produce hydrogen from the subsurface. It seems like there is a clear trend: a higher isolation will have a higher recovery of hydrogen as well as a reduced volumetric price.

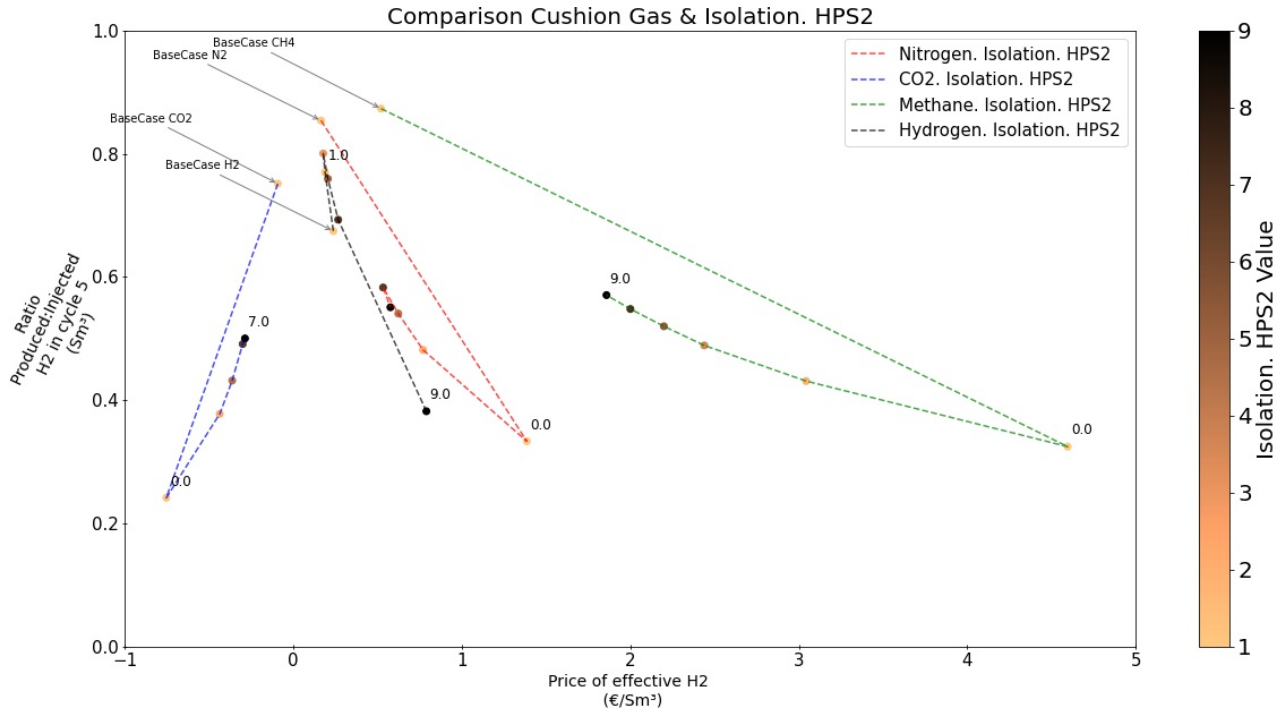

Figure 46: Price evaluation for different locations of HPS

If analysed more thoroughly, the period of cyclicity will reduce rapidly the more isolation there is. Apart from this, the higher isolation cases will not meet the desired production rates established. A higher isolation will decrease or increase drastically the bottom hole pressure. The system will try to inject the established 2.5E6 m3/day but the reservoir permeability is low. The physical response is a bottom hole pressure increasing, however this cannot be higher than 250 Bar. Therefore, the gas rate taht is delivered to the reservoir is reduced. As seen in Figure 47, the injection rate of hydrogen is under the daily target. This is portrayed by the blue line. The injection time of hydrogen is slower than its non perforated counterpart. Apart from this, the production phase, as seen in the dark red line, is done after only four days. The permeability of the perforated zones cannot withstand such high rates, and therefore the gas rate declines rapidly, which is detrimental to the system.

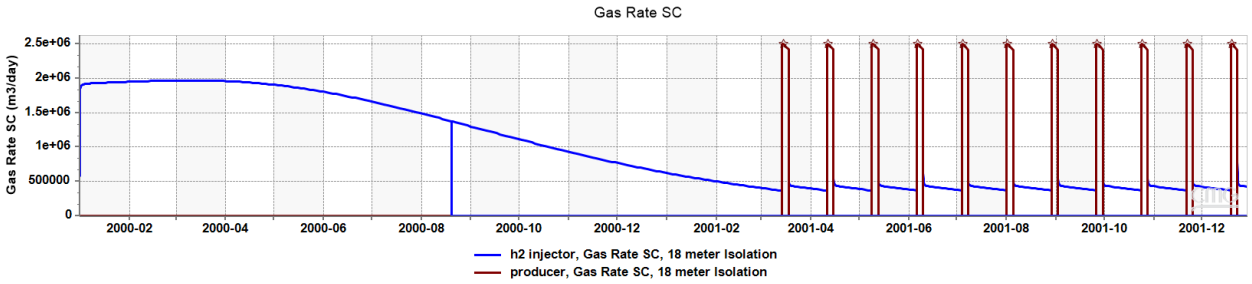

Figure 47: Injection rates of reservoir under the desired production and injection rates.

5.4.1 Isolation with Alternative Gas

The isolation of an HPS can help on reducing its effect on the pathway of flow in the reservoir. Knowing this, the volume of alternative gas can be modified, in order to see its effect on the mixing. As it is usually the case, more volume of alternative gas will result in higher cyclicity periods. This sensitivity analysis is helpful to see how to further reduce the effect of a HPS in a reservoir. Again, there will be a balance between the price of the alternative gas, the mixing in the reservoir, and the period of cyclicity.

There will be an isolation of 10 meters around the HPS, which is the same isolation used to explain the previous sensitivity analysis. The HPS will have a permeability of 200mD. Again, the HPS is placed in location 2, which is in the middle of the reservoir. The distribution of hydrogen looks exactly like Figure 45 from the previous subsection, as the pathway of hydrogen will be the same.

The result for the three alternative gases is that increasing the volume of alternative gas will increase the effectivity of the system to extracted hydrogen. However, this ratio does not increase massively between the different cases. In the case of methane, case 5 and Case 6 require the most investment because of the high price of methane, meaning that the extra investment in methane is not very beneficial. Reducing the injected carbon dioxide that has been injected makes the CAPEX higher, as the carbon dioxide reduces the price of the investment. The results for nitrogen show a slight increase in in the ratio of extracted hydrogen but not much change in price.

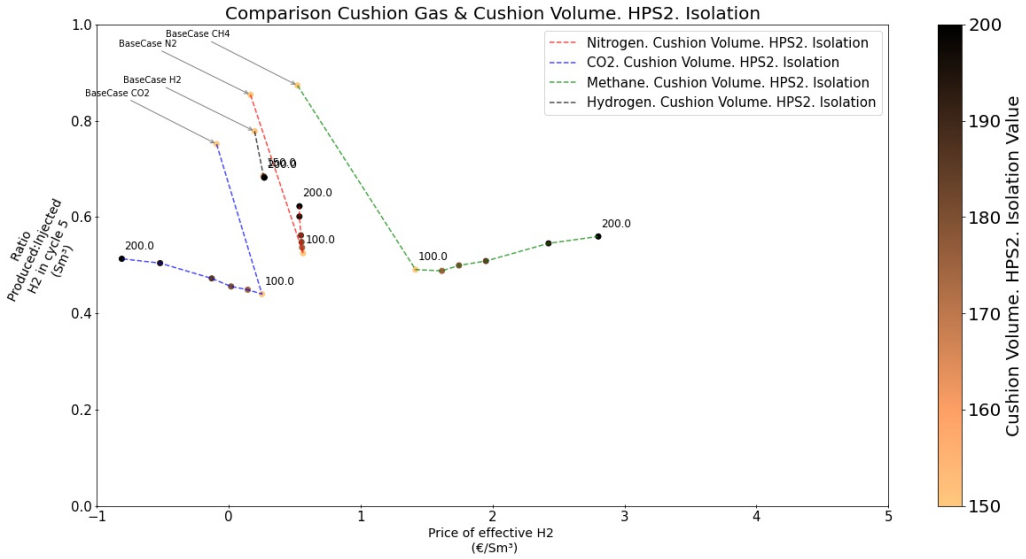

Figure 48: Price evaluation for the reservoir with two heterogeneities

As seen in previous analysis, the higher the volume of injected alternative gas, the smaller the period of hydrogen. In this case, here is no reason for a change in the degree of mixing in the reservoir, as the rates are exactly the same. However, ratio of injected to produced is higher with more alternative cushion gas. The main reason for this is that the unrecoverable hydrogen is less. As seen in Figure 49, the injected hydrogen does not reach the end of the reservoir, which means that it can be extracted more easily. This the higher injected to produced ratio.

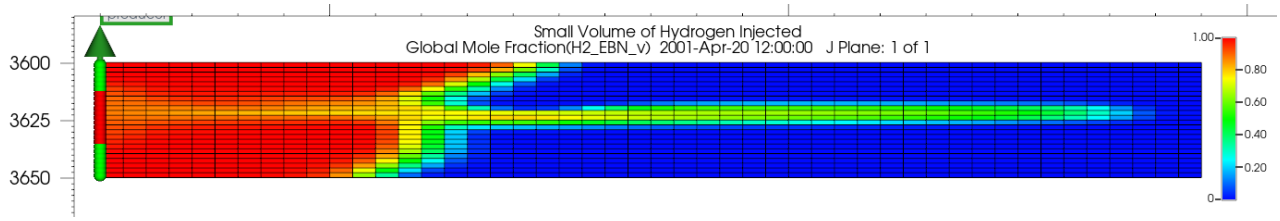

Figure 49: Distribution of hydrogen after initial production. 100% hydrogen is displayed in red. Hydrogen does not travel as much as it does in Figure 45

5.5 Alternating Permeability

As a follow up of the HPS sensitivity, a pancake reservoir model with alternating permeabilities was constructed. This was done so that the effect of the preferential pathways for flow are analysed in the presence of a bigger number of hetereogeneities. There were three different studies done, one where the reservoir was subdivided in two, four and six parts. This can be seen in Figure 50. Once again, the permeability thickness of the reservoir was kept constant in order for the results to be comparable. This was done by increasing and decreasing the permeabilities of the different sections of the reservoir.

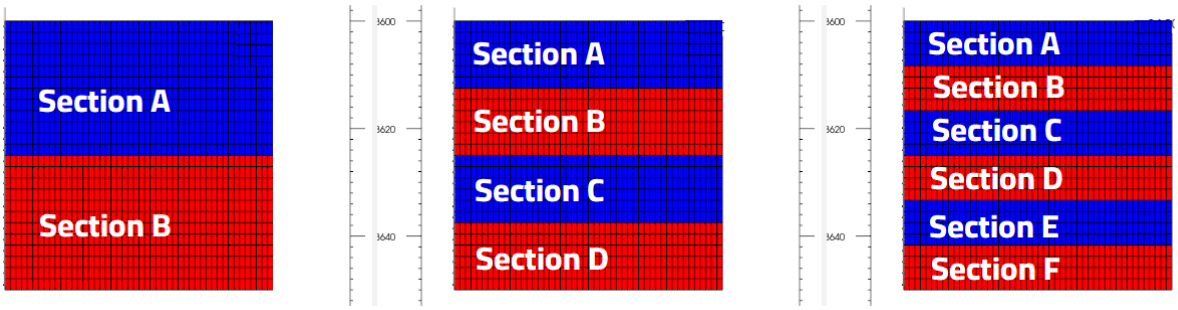

Figure 50: Three different heterogeneities, where the reservoir is divided in two, four and six parts respectively. Not to scale

In all of the three alternating cases, the permeabilities of the different sections were varied but kept the total permeability thickness of 1000 mDm was kept constant. There are 8 cases per alternating sensitivity analysis, as shown in Table 7. This shows the permeability of the different sections of the 'Six Heterogeneity' analysis. This table shows that for Case 1, the entire Section A (as seen in Figure 50c) has a permeability of 4mD, the entire section B has a permeability of 36mD and subsequently until section F. The setup of the four and two divisions will be shown in Appendix Section 1.

As a note, due to injection and production in very low permeable zones, the desired rates could not be injected in the simulation time of 2 years. As the comparison is done on the fourth cycle of every simulation, these data points are taken away from the final price evaluation chart. This however, does give an indication of the minimum permeability that this reservoir should have in order to inject and produce with these certain operational constraints.

		Horizontal Permeability of different cases (mD)							
Section	Perforation YES/NO	1	2	3	4	5	6	7	8
A	YES	4	8	12	16	24	28	32	36
	YES	4	8	12	16	24	28	32	36
	YES	4	8	12	16	24	28	32	36
	YES	4	8	12	16	24	28	32	36
B	NO	36	32	28	24	16	12	8	4
	NO	36	32	28	24	16	12	8	4
	NO	36	32	28	24	16	12	8	4
	NO	36	32	28	24	16	12	8	4
C	YES	4	8	12	16	24	28	32	36
	YES	4	8	12	16	24	28	32	36
	YES	4	8	12	16	24	28	32	36
	YES	4	8	12	16	24	28	32	36
D	NO	36	32	28	24	16	12	8	4
	NO	36	32	28	24	16	12	8	4
	NO	36	32	28	24	16	12	8	4
	NO	36	32	28	24	16	12	8	4
E	YES	4	8	12	16	24	28	32	36
	YES	4	8	12	16	24	28	32	36
	YES	4	8	12	16	24	28	32	36
	YES	4	8	12	16	24	28	32	36
F	NO	36	32	28	24	16	12	8	4
	NO	36	32	28	24	16	12	8	4
	NO	36	32	28	24	16	12	8	4
	NO	36	32	28	24	16	12	8	4

Table 7: Permeability distribution for 'Six Heterogeneity' sensitivity analysis.

As all of the cases in the three sensitivity analysis cannot be described fully, only the results for Case 2 and Case 7 will be analysed in the following sections as a representative of the entire system. These will be named Example 1 and Example 2 respectively.

The perforations will be located in alternating layers as well, and in the case of 'Six Hetereogeneity' the open perforations are located in Section A, C and E. The perforation intervals for the injection and production wells are the same. The permeability of the different sections of the reservoir are changing with the different cases, meaning that sometimes the perforations were done on a very impermeable zone, while on other occasions the perforation was done on a zone of high permeability. Of course, this has an impact on the distribution of the hydrogen and alternative gas in the reservoir, and will be discussed throughout this section. The location of the perforations will be constantly shown, to help the reader understand their impact. Open perforations are shown as a green ball, while closed perforations are seen as a red ball.

5.5.1 Two Heterogeneities

The first pancake model will be divided in two Sections, Section A and Section B. Only section A of the reservoir was perforated in order to see the effect of this varying heterogeneity in the cyclic injection and extraction. This is shown in Figure 51.

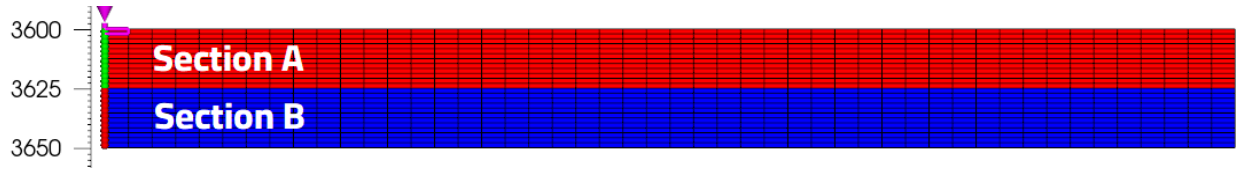

Figure 51: Division of reservoir based on halves. Perforations are always done in section A

Example 1a

In Example 1a, the high permeability zone, of 32mD, is section B while the low one has a permeability of 8mD and is located at section A, the top of the reservoir. The open perforations are done at section A. Hydrogen is slowly pushed through section A while it quickly migrates to part B. Even after one cycle, the effect of gravity segregation is seen. The nitrogen, as displayed in blue colour, is sinking from section A into the advancing hydrogen that located in section B. This is creating a finger-like distribution, as shown in Figure 52.

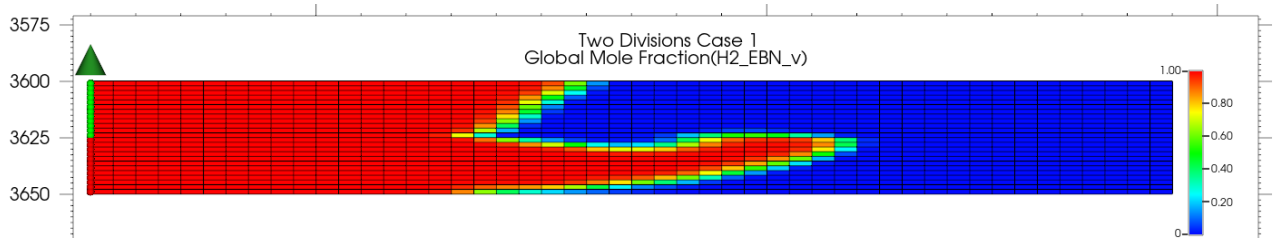

Figure 52: Example 1a. Distribution of hydrogen in the reservoir moments before the first production cycle. 100% saturation of hydrogen is marked as red

This finger-like shape is developing further into the reservoir as cycles progress. This is seen in Figure 53, where the distribution of hydrogen is shown at the end of production of the third cycle. There are two observations to note here. First, The hydrogen located at the bottom half of the reservoir is rising due to the buoyancy difference, which is making some hydrogen unrecoverable. Second, the shape of the front between in section A and section B do not have the same inclination, which is an effect derived from the permeability of the zone.

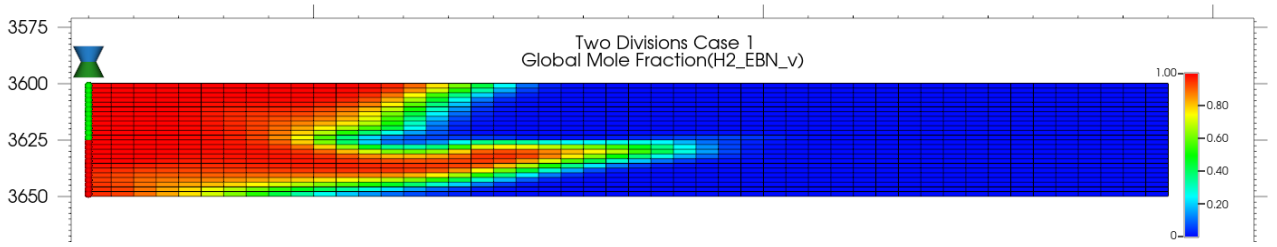

Figure 53: Example 1a. Distribution of hydrogen in the reservoir after the third injection production cycle. 100% saturation of hydrogen is marked as red

As defined earlier, the vertical permeability is a function of the horizontal permeability. A higher vertical permeability will lead to an easier vertical transport of gas, meaning that the effect of gravity segregation will be stronger.

This can also be checked with Equation 9, where a higher permeability, when having the other parameters constant, will lead to a lower gamma value. As seen in Figure 12, a lower value will cause a more curved front shape. This example matches quite well a proposed analytical solution.

As a follow up to the previous assessment, the simulator was left to run longer, for five years instead of two. This allows for more injection production cycles to occur, as shown in Figure 54. This average reservoir pressure graphs indirectly shows that the period of the cycles are getting shorter along time. This indicates an increase in the degree of mixing in the reservoir. The shorter cycles means that there is less time for the reservoir to produce the hydrogen that has been injected previously.

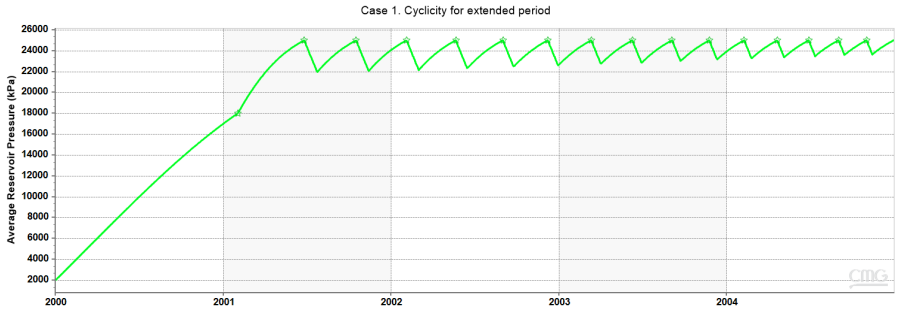

Figure 54: Example 1a. Average reservoir pressure in Example of extended simulation time

The distribution of hydrogen is also changing considerably. After a few cycles, the hydrogen has expanded laterally through section A, as shown in Figure 55. A complete bubble of hydrogen has formed from the finger-like behaviour showcased in Figure 52. This creates an unrecoverable volume of hydrogen that is slowly rising and mixing through the layers of this reservoir. The increase in mixing in the reservoir is causing a decrease in cycle period. This has been the case in all of the previous simulations as well.

The earlier breakthrough of the alternative gas, is causing the cyles to be increasingly shorter. The hydrogen that has been injected does not have time to travel towards the well.

The effect of gravity segregation is not helping the production of hydrogen in this system. Hydrogen is slowly advancing through section A, which is relatively impermeably and getting stuck and there is a bubble of unrecoverable hydrogen, which was created from the finger-like distribution of hydrogen. This is making the reservoir less effective in delivering hydrogen.

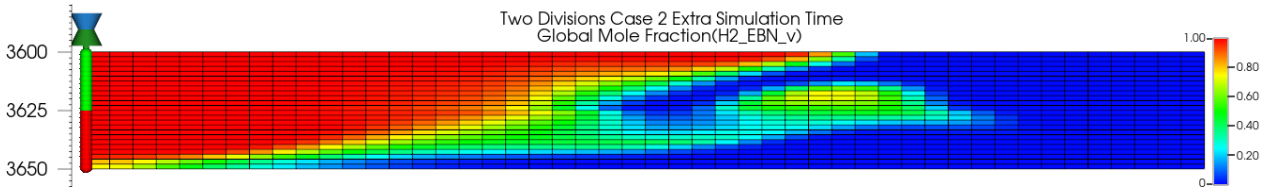

Figure 55: Example 1a. Distribution of hydrogen in the reservoir after 15 cycles, which is almost 5 years. 100% saturation of hydrogen is marked as red

Example 2a

The perforations in Example 2a are still done in section A. Section A is now a high permeability zone. Because of the easier flow through this layer, hydrogen mostly moves through section A of the reservoir. Hydrogen is also laterally extending through section B but at a lower rate. This is seen in Figure 56, which is a snapshot of the reservoir during the first injection.

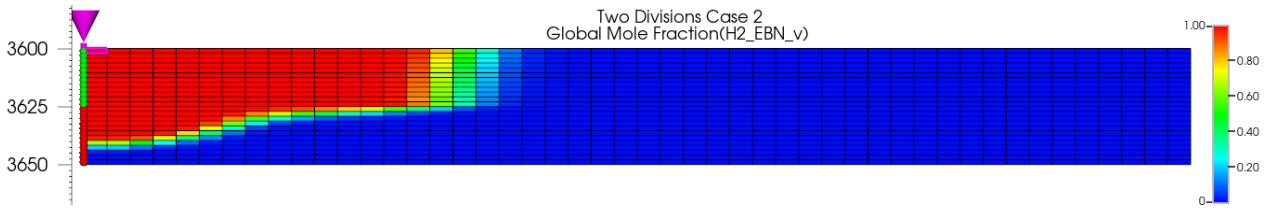

Figure 56: Example 2a. Distribution of hydrogen in the reservoir during the first injection production cycle. 100% saturation of hydrogen is marked as red

Figure 56 also shows the difference in front shape and width in the two sections. The hydrogen injected in section A, the high permeable one, is having almost a vertical front against the alternative gas, which is nitrogen in this case. At the same time, section B has a shallow angle of front between the two gases.Equation 9 shows that the shape of the front is dependant on the flow going though the layer as well as the permeability of the layer

itself. This will raise the gamma factor, thus making the front more vertical, as shown in Figure 12. Advective forces will make the front have a piston like behaviour, as seen in the base case scenario for example and gravity forces will result in a shallower front.
This gamma value is inversely proportional to the distance from the well. This is because there is less influence and velocity farther away from the well. Figure 57 shows the distribution of hydrogen at the end of the first injection cycle. Here, the front in the high permeability zone also has a shallow angle. The gamma value is a function of the distance against from the well, and this front will become shallower and shallower the further the distance away from the well. The front will be more gravity dominated the further away from the well, as the velocity of the gases will be increasingly lower.

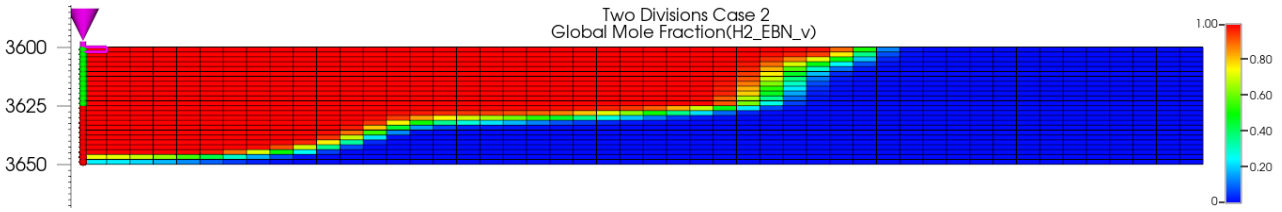

Figure 57: Example 2a. Distribution of hydrogen in the reservoir at the end of the first injection production cycle. 100% saturation of hydrogen is marked as red

The main findings and differences for the pancake models with two layers are mainly the position of the heterogeneities. Example 1a shows the creation of an unrecoverable hydrogen bubble due to the fast movement of hydrogen through section B and later rise towards section A due to buoyancy. This is detrimental to the system from a technical point of view. In the case where the perforation is done in the high permeability zone, most of the flow will go through this zone and the distribution of hydrogen be mostly on this layer.

The economic evaluation shows that there is no clear trend between the different sensitivities. The different permeabilities imply that the hydrogen or the alternative gas will be able to not only flow, but to segregate quickly due to changes in density between the gases. However, The full effect of this gravity segregation is only seen at longer time scales. As seen, there are small differences in volumetric price to store hydrogen within the different gases but that is due to the effects of, for example, creation of unrecoverable bubbles. These will have different volumes and location depending on the permeability of the system.

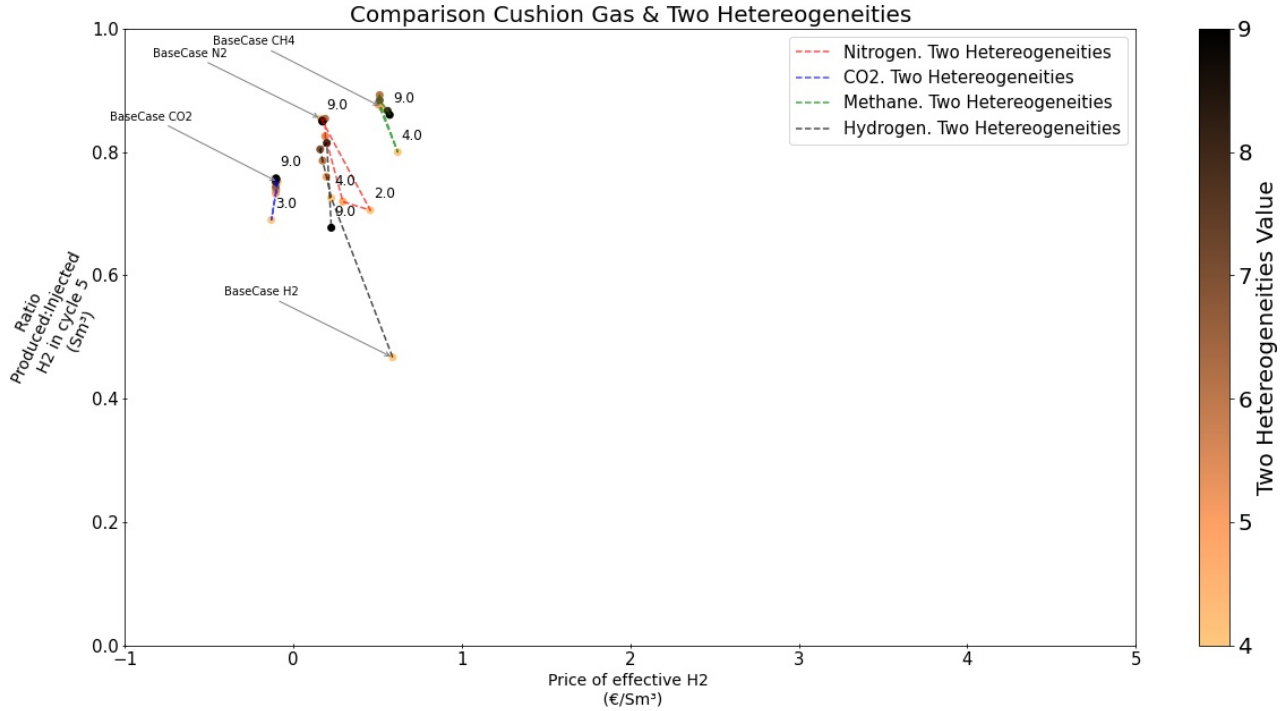

Figure 58: Price evaluation for the reservoir with two heterogeneities

5.5.2 Four Heterogeneities

In this study, the reservoir is subdivided into four sections. Once again, the formation permeability is kept the same and the higher permeability zones are 32mD and the low ones will be 8mD.

Example 1b is perforated in the lower permeability zone. This is clear because the injected hydrogen has not laterally advanced through the reservoir even though the perforations are done in this layer. The hydrogen has migrated to the higher permeability zone and has spread laterally more than halfway through the reservoir, as shown in Figure 61. There are four different fronts that have developed, which already show the buoyancy difference between the nitrogen and hydrogen during the first stage of injection.

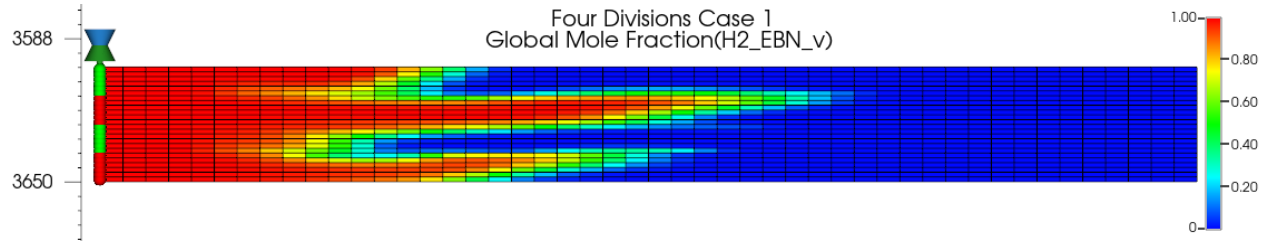

Figure 59: Example 1b. Distribution of hydrogen in the reservoir after the first injection production cycle. 100% saturation of hydrogen is marked as red

The distribution of hydrogen in the reservoir after the second injection cycle, as shown in Figure 60 is quite similar to the one after a single cycle. Again, the higher permeability zones have enhanced flow through them, allowing the gas to move easily. It is good to note as well that the lateral extent of the mixing zones in both the high and low permeability zones are quite similar.

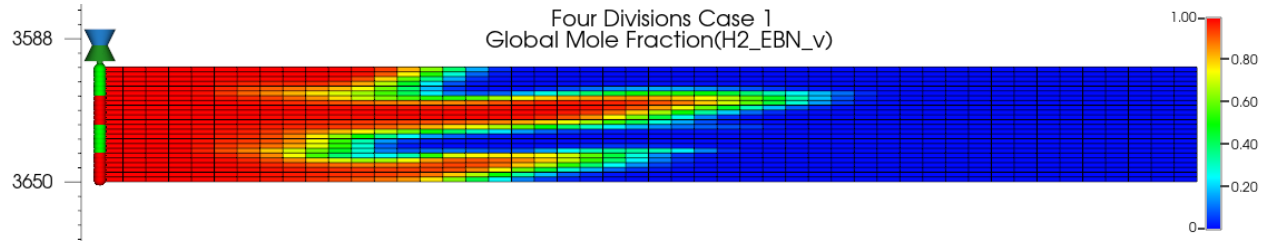

Figure 60: Example 1b. Distribution of hydrogen in the reservoir after the second injection production cycle. 100% saturation of hydrogen is marked as red

The perforations in Example 2b are done in the high permeability zone. Figure 61 shows the hydrogen, once again, has preferentially moved through the higher permeability zones. The low permeability zone has not been invaded as much as in the previous case, as most of the gas will simply flow through the zone with the higher permeability. In the case shown in Figure 59, hydrogen had to migrate to the high permeability zone from the low permeability zone. There was more trapping of hydrogen in the low permeability zone as well.

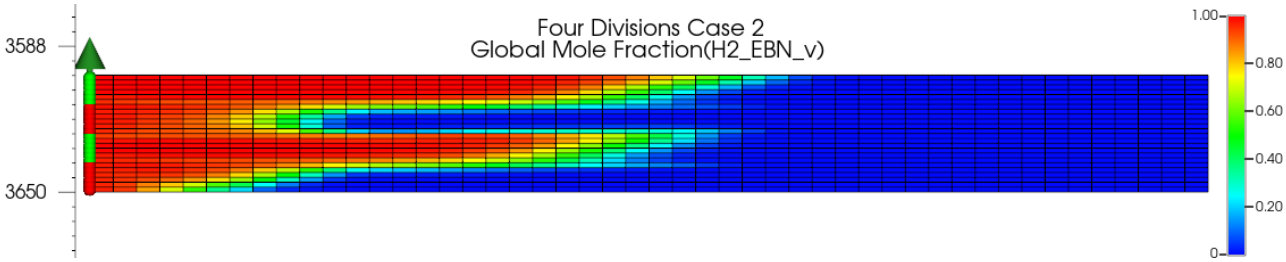

Figure 61: Example 2b. Distribution of hydrogen in the reservoir after the first injection production cycle. 100% saturation of hydrogen is marked as red

Figure 62 shows that after four cycles, the hydrogen has spread laterally further through the reservoir. The distribution of hydrogen in the low permeable layers is comparable to the one in Figure 61. The effect of buoyancy is starting to be visible in the middle layer, where the hydrogen is slowly seeping into the low permeability

layer. This is marked with number 1. Given that hydrogen is slowly entering a low permeability layer, it will require more of a pressure difference to be extracted from the reservoir. This hydrogen is also located around 250 meters away from the well, meaning that this could mean an increase in unrecoverable hydrogen in the reservoir.

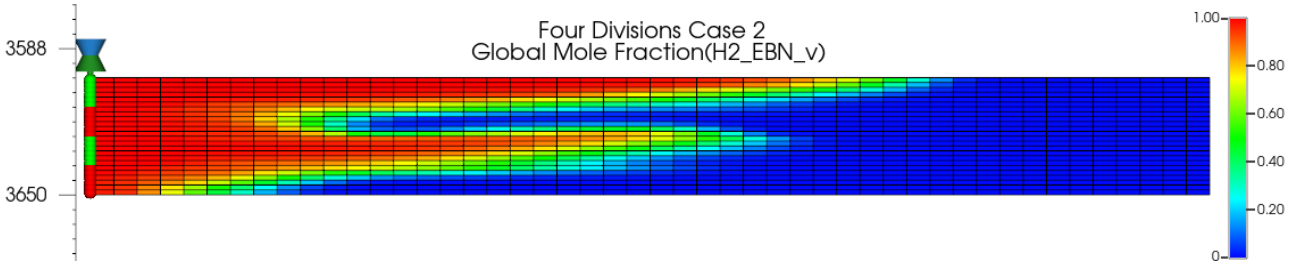

Figure 62: Example 2b. Distribution of hydrogen in the reservoir after the fourth injection production cycle. 100% saturation of hydrogen is marked as red

Again, the mixing zone in both high and low permeable zones seems to have the same lateral extent. As stated earlier, all these simulations do not have the optional dispersivity value. As stated, the dispersion is a function of the Darcy velocity in the cell, which is a function of the permeability. Therefore, it would be expected that the mixing zone in the high permeability zones have a greater width.

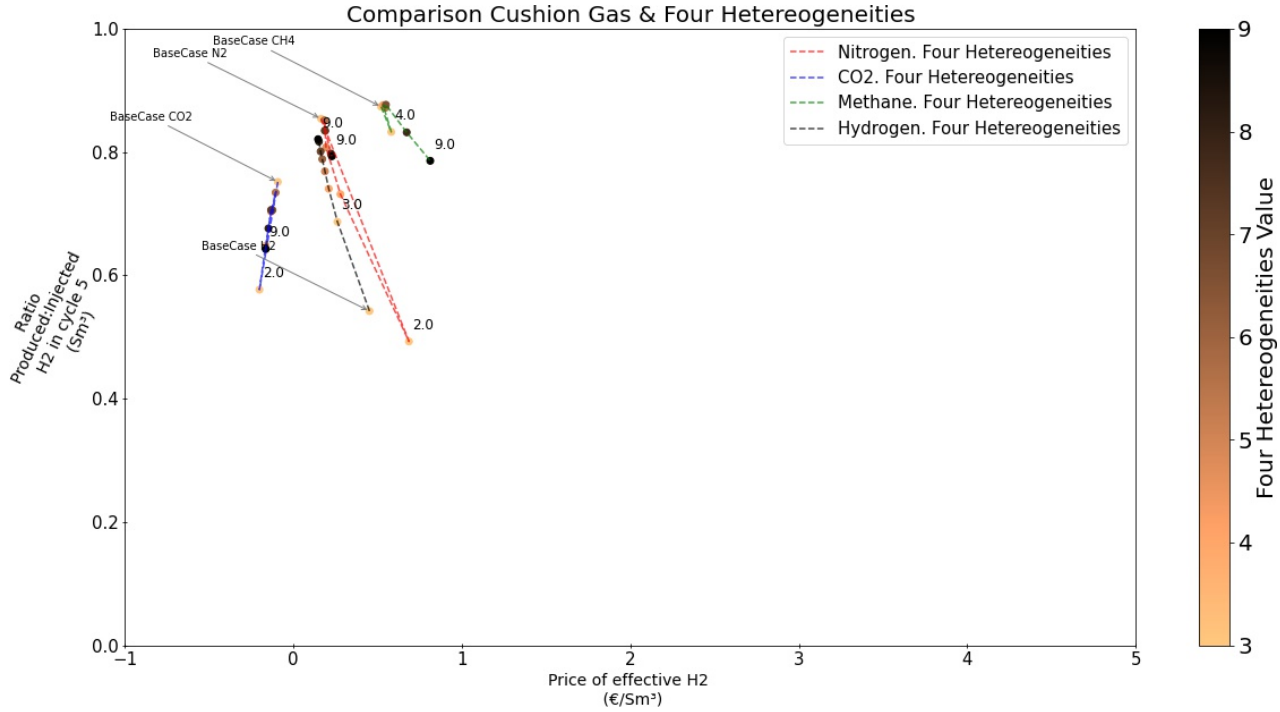

Figure 63: Price evaluation for the reservoir with four heterogeneities

Once again, there is not a clear trend between the different pancake layer model. There are some outliers within the individual gases but no clear trend. Increasing the degree of heterogeneity is not causing a major change in the ability of the system to effectively produce hydrogen from the subsurface. The distribution of hydrogen in the reservoir will be different, but the overall the efficiency is similar.

5.5.3 Six Heterogeneities

In this sensitivity analysis, the reservoir is sub-dived further into six different domains. As seen from the other two heterogeneities trials, the well has trouble injecting and producing gas when the perforations are done in low permeability zones. However, the gas will eventually reach the higher permeability zones, where it could potentially flow with more ease. However, the results of the two previous analyses implied a trapping of hydrogen in the reservoir instead of an improvement to flow.

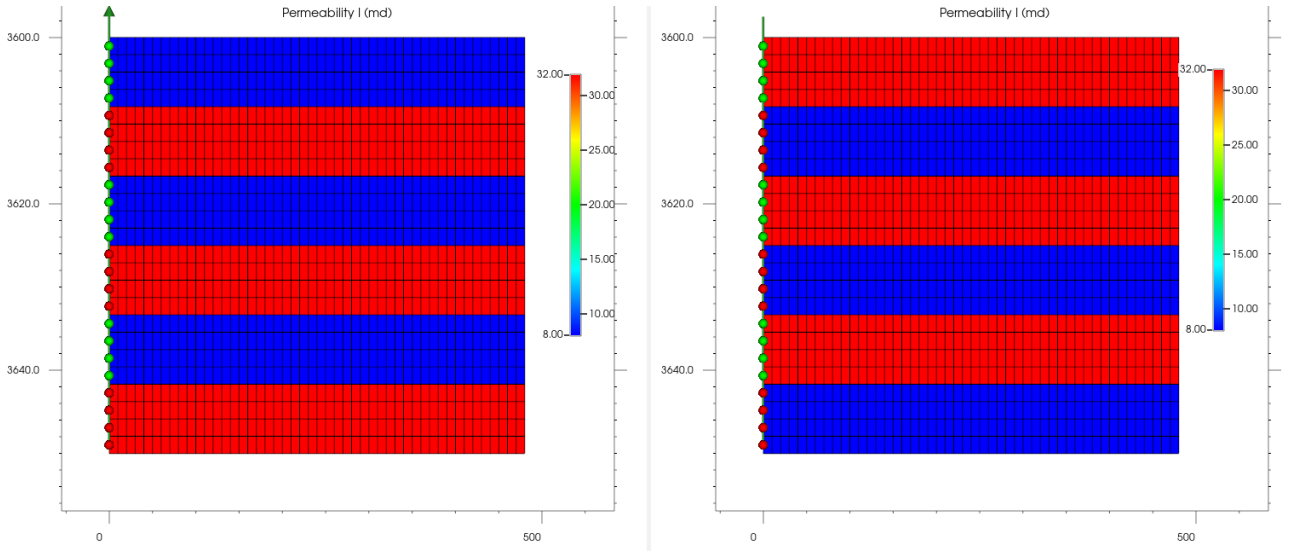

Figure 64: Open perforations in green. Closed perforations in red. Two set ups of alternating permeabilities. Example 3a and Example 3b respectively.

The results for the examples in Figure 64 differ quite a lot in terms of distribution of gases in the reservoir. As the reservoir is more heterogeneous than the last two examples, the interactions will be different and occur at different scales.
Case 1 has been perforated in Section 1, 3 and 5. These are the lower permeability zones. As seen from Figure 65, hydrogen has extended laterally past halfway the reservoir. The spread in the section 2 has advanced more than the one at section 4 or section 6.

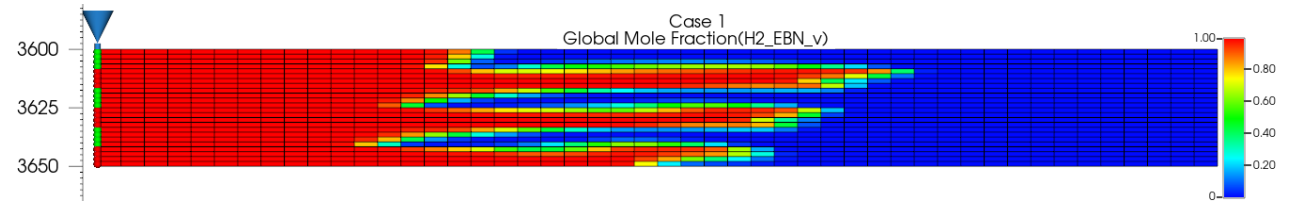

Figure 65: Example 3a. Hydrogen distribution at the end of primary injection

By the end of the first production cycle, some of the hydrogen is left behind in the reservoir in these far stretching fingers that have been created. This is seen in Figure 66. This effect will reduce the hydrogen effectivity of extraction. The hydrogen will become increasingly less inaccessible by reach of the well.

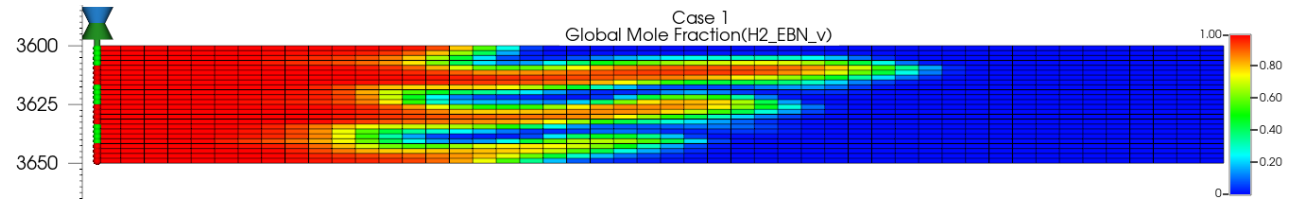

Figure 66: Case 2. Hydrogen distribution at the end of first production

As seen in Figure 67, there is now a considerable amount of unrecoverable hydrogen in the reservoir. Due to buoyancy, hydrogen has migrated through the multiple layers and has spread diagonally across the reservoir. The production period has become only five days, where at the start the system could produce pure hydrogen for 23 days.

There is of course still a preferential flow through the higher permeability layers, and this is causing the earlier breakthrough of the alternative gas. This is detrimental to the economics of the system. Figure 67 shows the distribution of hydrogen after an extended period of time. Hydrogen has risen through the the high and low permeable layers and now extends throughout the entire reservoir.

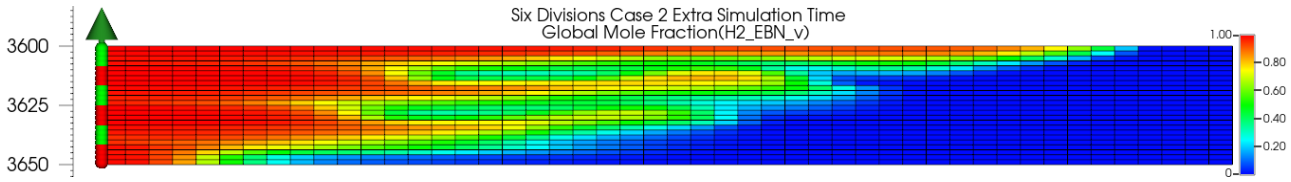

Figure 67: Case 2. Hydrogen distribution after 45 cycles.

Over time, hydrogen will rise due to buoyancy differences and eventually move through the reservoir. The recovery of this hydrogen will depend on where it is located and if it can be drawn out by the well.

In terms of the economic analysis, as seen in Figure 68, there is not much difference between the different sensitivity analysis within the individual gases. There is not a clear correlation between the pancake layers with different permabilities. The column is being perforated a the same locations each time. As the pancake model has a higher degree of heterogeneity, there will be simply pathways where flow can occur with more ease.

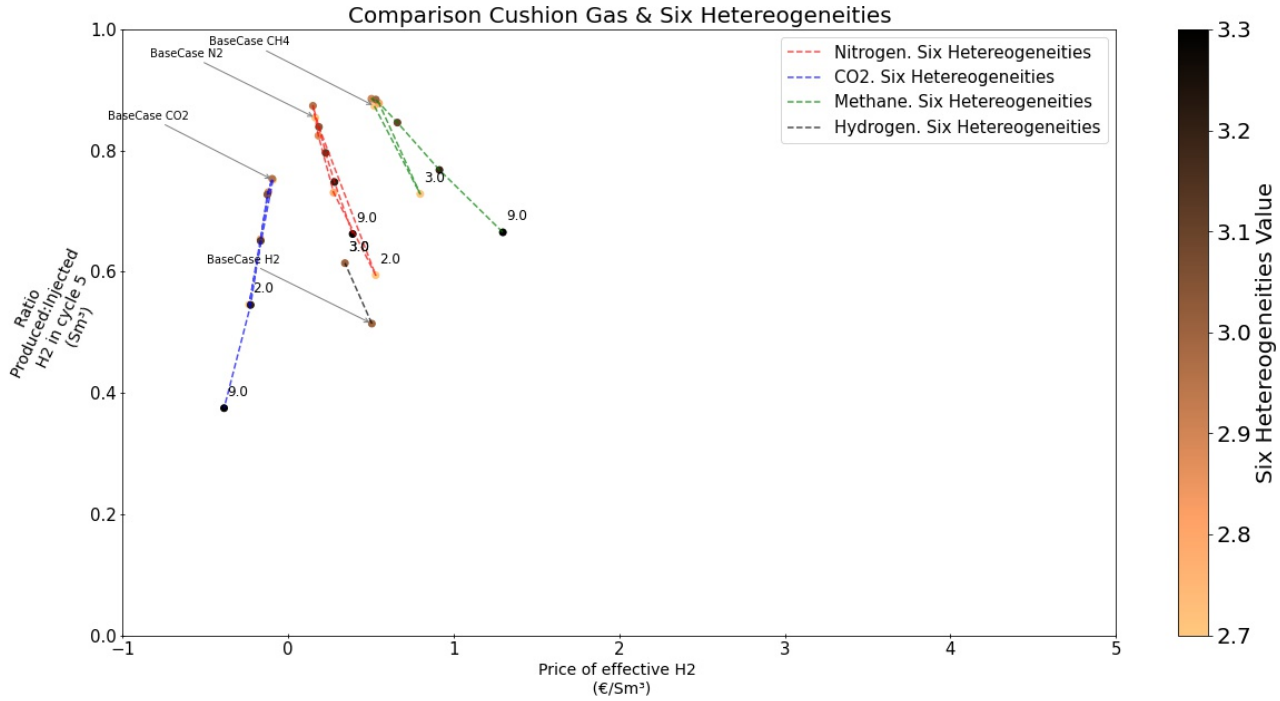

Figure 68: Price evaluation for the reservoir with six heterogeneities

The layered heterogeneities are not making much of a difference in the economic evaluation. However, as seen in the previous sections, the distribution of gas will change depending if the hydrogen is injected in high or low permeable layers. Some results had to be removed from the analysis as the simulations did not reach the fourth cycle.

As the heterogeneity of this pancake model is increased, the high and low permeability layers become thinner, which will allow easier vertical movement of particles. Although this movement depends on the permeability and connectivity of the subsurface, eventually hydrogen will rise easily due to its particle size and mobility.

6 Limitations

The relative permeability and capillary pressure curves for hydrogen have to be better understood in order to be able to upscale them into a reservoir model. As mentioned, the relative permeability curves are taken from Yekta et al. 2018 and there is in fact only one study that characterizes the contact angle of the hydrogen-water system.

As mentioned, the GWC has been set below this reservoir. If there was to be a GWC present, the operation of injection and production would have to change completely. Injecting hydrogen into water can potentially cause

viscous fingering, low hydrogen recovery, and dissolution of hydrogen, as mentioned by **?**. The presence of bodies of water in the reservoir will have an impact on the location of the perforations in the single or multiple wells used.

As seen from the sensitivity analysis, the system is very susceptible to heterogeneities. Layers of high permeability effectively acted like hydraulic fractures, and most of the flow of fluid occurred through these. Most of the flow in reservoirs will occur through these high permeable fractures, that are unevenly distributed throughout the reservoir. Apart from this, these sensitivity analyses do not have a fracture network. The addition of a fracture network will have an impact on the flow pathways as well as the effectivity of the system in delivering and injecting gas, depending on the orientation of the fractures.
One limitation to this investigation is the lack of a geomechanical model. In a real reservoir model, the different lithologies present will have different rock properties which will define their behaviour under stress. It is important to ensure cap rock integrity in the system, if not the system will to leak and cause hydrogen loss. The reservoir will undergo cyclic loading due to the injection and production cycles and there will be deformation in the rock which is a function of the rate of stress change. A geomechanical model forms an important part of a reservoir simulator

7 Conclusion

The conclusions of this investigation will summarize the insights obtained with the sensitivity analysis. The four sub-questions have been approached by the different sensitivities and will be useful to give a concrete answer to the main research question. These are the main conclusions for the different sub-questions:

1. How will the working volume/cushion gas ratio be with different gases?

The final analysis compared the ratio of cumulative injected to produced hydrogen against the price per $Sm3$ that was invested to store this hydrogen. The system effectivity was measured in the ratio of recoverable hydrogen after five cycles.

Because of the compressibility and density differences of the alternative gases, not the same volume in Sm^3 is injected in the reservoir. This will have a direct impact on the investment that has to be made for the alternative gas.

The molecular diffusion term did not have an effect in the effectiveness of the system. Both nitrogen and methane mixed with hydrogen at approximately the same rate. The most important factor that enhances mixing is the dispersivity value. This actually simulates real mixing of gases. All the mixing that is seen throughout the simulations are due to truncation errors in numerical approximations.

The mixing of hydrogen with super critical carbon dioxide is not a very well known topic in terms of thermodynamics or kinetics. The simulator shows that there is substantially more mixing when carbon dioxide is present, however this has not been backed up by any field or laboratory experiments yet.

2. What is the optimal perforation interval depending on the cushion gas?

The initial tests for heterogeneities involved the addition of high permeability streaks into the reservoir. These streaks, that effectively acted as hydraulic fractures, made preferential pathways for flow of fluids. The addition of a HPS led to an earlier breakthrough of the alternative gas.

A solution for this early breakthrough is to isolate the HPS, in order to reduce its impact on the flow path of the fluids in the reservoir. This isolation increased the effectivity of the system by increasing the injection-production period as well as increasing the recoverable hydrogen from the reservoir. This means that it is perhaps preferential to avoid injection in very high permeability zones, as the mixing and breakthrough of alternative gas will occur quicker.

3. How do heterogeneities affect the multi-component flow?

In the case of a use of an alternative gas, a rapid decrease in the injection-production cycles is inevitable due to the ever increasing mixing in the reservoir. This is mostly caused by dispersive forces as well as the effect of buoyancy, which sometimes will move the alternative gas closer and closer to the well. As seen, high permeable

areas will facilitate both the injection and production of alternative gas, which is mostly detrimental to the system.

Due to its low viscosity, hydrogen is able to easily travel through porous media. The presence of a HPS will enhance the quick extraction of hydrogen which will make the breakthrough of alternative gas earlier. As seen, isolating these permeable pathways, by means of perforation intervals, is an option, as they reduce the effect of this streak. However, this can result in decreased rates of extraction, which also hinders the effectivity of the system.

4. Is there an optimal injection rate to ensure the maximum purity of hydrogen?

The injection rates in the reservoir are directly to the distribution of hydrogen in the subsurface. There are two main forces that will cause a different distribution of hydrogen or any gas in the reservoir. These are the effects of gravity and viscosity. The ratio between these two changes based on the distance away from the well and because of the fluid and reservoir properties.

The direct effect of rate was only seen in one sensitivity analysis. This showed that a low rate of injection resulted in a shallower mixing front between hydrogen and an alternative gas. This was a gravity dominated system. On the other hand, the mixing front for a high rate of injection resulted in a piston like behaviour of the gas, where the front after injection was relatively vertical.

The indirect effect of rate can be indirectly seen in the hydrogen distributions of the pancake models. The mixing fronts in the higher and lower permeability zones have different shapes, which depend on the permeability of the layer as well as its distance from the well.

Finally, the main research question of this investigation was:
"Which is the most ideal cushion gas that can be used in an Underground Hydrogen Storage?"

In a compositional simulator, the mixing of the different components is a combination of numerical and physical (real) dispersion. Numerical dispersion is caused by the truncation error that arises due to the use of the finite difference method while physical dispersion is caused by mass transfer processes. If an alternative gas such as methane, carbon dioxide or nitrogen is used, there will be an increased dispersive mixing in the reservoir. The recovery of hydrogen will increase as cycles progress, however the injection and production cycles will decrease. Although distinguishing numerical and physical dispersion is not straightforward, it is clear and logical that there is mixing in the reservoir, which is detrimental for the system.

From an economical point of view, it is ideal to reduce investment costs, have the ability to store the highest volume of hydrogen, and at the same time, produce a high percentage of the injected hydrogen. This will also depend on the size and shape of the reservoir. If the system is able to produce the majority of hydrogen that has been injected to the reservoir, the price to *effectively store* a cubic meter of hydrogen will decrease regardless of the choice of cushion gas. At the same time, a great percentage of this investment will depend on the price of the alternative gas that has been used, and there is a great variability of price between all of the used gases.

Therefore, it is technically and economically more feasible to use a hydrogen as a cushion gas for Underground Hydrogen Storage in depleted gas fields. This system would only have mixing of hydrogen with the remaining gas in the reservoir, instead of two fronts of mixing. This reduces the problematic effects in the distribution of hydrogen in the reservoir caused by gravitational segregation and the ever increasing mixing of hydrogen and the alternative gas.

Although the volume of cushion gas will account for a great percentage of the investment for a project like this, a much higher volume of hydrogen in the reservoir will lead to production cycles of the desired length as well as a decrease of mixing. The heterogeneities and early breakthrough of alternative gas will not be an issue when using hydrogen as a cushion gas.

7.1 Recommendation

The next direct step on this investigation would be to translate the findings of this investigation to a cartesian grid. This will allow the addition of multiple wells, as well as having the possibility of a more realistic geology. As the static model of an existing gas field is already known, the perforations in the wells can be optimized based on the permeability of the layers.

In the case of the economic evaluation, a more detailed study could be done in the process of separating gases in the platform. If this is economically and technically possible, then the purity issue stops being the main bottleneck of an operation as this one. The hydrogen could be separated and used, and the alternative gas that has been extracted can be re-injected to the reservoir to keep the operating pressure.

Last, but not least it is of great importance to quantify the large-scale mixing and transport processes that occur in geological media as a result of mass transfer processes and the heterogeneity of the subsurface. As seen, it is already troublesome to identify the mixing of the reservoir due to numerical errors and the physical, miscible displacement of gases. If there is a better quantification of the mixing due to real processes, large scale simulations will provide more accurate prediction of this subsurface operation.

References

A. Arya, T. A. Hewett, R. G. Larson, and L. W. Lake. Dispersion and reservoir heterogeneity. *SPE Reservoir Engineering*, 3:139–148, 2 1988. ISSN 0885-9248. doi: 10.2118/14364-PA. URL https://onepetro.org/RE/article/3/01/139/75327/Dispersion-and-Reservoir-Heterogeneity.

M. Boon and H. Hajibeygi. Experimental characterization of $${\text {h}}_2$$/water multiphase flow in heterogeneous sandstone rock at the core scale relevant for underground hydrogen storage (uhs). *Scientific Reports*, 12(1):14604, 2022. doi: 10.1038/s41598-022-18759-8. URL https://doi.org/10.1038/s41598-022-18759-8.

Z. Cai, K. Zhang, and C. Guo. Development of a novel simulator for modelling underground hydrogen and gas mixture storage. *International Journal of Hydrogen Energy*, 47:8929–8942, 2 2022. ISSN 03603199. doi: 10.1016/J.IJHYDENE.2021.12.224.

M. Dentz and D. M. Tartakovsky. Abrupt-interface solution for carbon dioxide injection into porous media. *Transport in Porous Media 2008 79:1*, 79:15–27, 8 2008. ISSN 1573-1634. doi: 10.1007/S11242-008-9268-Y. URL https://link.springer.com/article/10.1007/s11242-008-9268-y.

W. Eikelenboom and T. Huijskes. H2 storage in gas fields. *GET 2020*, 11 2020.

EuropeanCommission. Repowereu plan, 5 .

F. Feldmann, B. Hagemann, L. Ganzer, and M. Panfilov. Numerical simulation of hydrodynamic and gas mixing processes in underground hydrogen storages. *Environmental Earth Sciences*, 75, 8 2016. ISSN 18666299. doi: 10.1007/S12665-016-5948-Z.

Gasunie. Werken met hoge druk, 2015.

L. W. Gelhar, C. Welty, and K. R. Rehfeldt. A critical review of data on field-scale dispersion in aquifers. *Water Resources Research*, 28:1955–1974, 7 1992. ISSN 1944-7973. doi: 10.1029/92WR00607. URL https://onlinelibrary.wiley.com/doi/full/10.1029/92WR00607https://onlinelibrary.wiley.com/doi/abs/10.1029/92WR00607https://agupubs.onlinelibrary.wiley.com/doi/10.1029/92WR00607.

C. M. Group. Manualgem, 2022.

N. Gutierrez. Aspects of transverse dispersion in porous media. *Geologica Ultraiectina, Departement Aardwetenschappen*, 2009.

B. Hagemann. Numerical and analytical modeling of gas mixing and bio-reactive transport during underground hydrogen storage, 8 2017.

L. Hashemi, M. Blunt, and H. Hajibeygi. Pore-scale modelling and sensitivity analyses of hydrogen-brine multiphase flow in geological porous media. *Scientific Reports*, 11:8348, 2021a. ISSN 2045-2322. doi: 10.1038/s41598-021-87490-7. URL https://doi.org/10.1038/s41598-021-87490-7.

L. Hashemi, W. Glerum, R. Farajzadeh, and H. Hajibeygi. Contact angle measurement for hydrogen/brine/sandstone system using captive-bubble method relevant for underground hydrogen storage. *Advances in Water Resources*, 154:103964, 8 2021b. ISSN 0309-1708. doi: 10.1016/J.ADVWATRES.2021.103964.

L. Hashemi, W. Glerum, R. Farajzadeh, and H. Hajibeygi. Contact angle measurement for hydrogen/brine/sandstone system using captive-bubble method relevant for underground hydrogen storage. *Advances in Water Resources*, 154:103964, 2021c. ISSN 0309-1708. doi: https://doi.org/10.1016/j.advwatres.2021.103964. URL https://www.sciencedirect.com/science/article/pii/S0309170821001196.

L. Hashemi, M. Boon, W. Glerum, R. Farajzadeh, and H. Hajibeygi. A comparative study for h2–ch4 mixture wettability in sandstone porous rocks relevant to underground hydrogen storage. *Advances in Water Resources*, 163:104165, 2022. ISSN 0309-1708. doi: https://doi.org/10.1016/j.advwatres.2022.104165. URL https://www.sciencedirect.com/science/article/pii/S0309170822000410.

N. Heinemann, J. Alcalde, J. M. Miocic, S. J. Hangx, J. Kallmeyer, C. Ostertag-Henning, A. Hassanpouryouzband, E. M. Thaysen, G. J. Strobel, C. Schmidt-Hattenberger, K. Edlmann, M. Wilkinson, M. Bentham, R. S. Haszeldine, R. Carbonell, and A. Rudloff. Enabling large-scale hydrogen storage in porous media – the scientific challenges. *Energy Environmental Science*, 14:853–864, 2 2021. ISSN 1754-5706. doi: 10.1039/D0EE03536J. URL https://pubs.rsc.org/en/content/articlehtml/2021/ee/d0ee03536jhttps://pubs.rsc.org/en/content/articlelanding/2021/ee/d0ee03536j.

IEA. The future of hydrogen, 2019.

Z. Jangda, H. Menke, A. Busch, S. Geiger, T. Bultreys, H. Lewis, and K. Singh. Pore-scale visualization of hydrogen storage in a sandstone at subsurface pressure and temperature conditions: Trapping, dissolution and wettability. *Journal of Colloid and Interface Science*, 629:316–325, 1 2023. doi: 10.1016/j.jcis.2022.09.082. URL https://doi.org/10.1016%2Fj.jcis.2022.09.082.

J. Juez-Larré, S. F. Gessel, R. Dalman, G. Remmelts, and R. Groenenberg. Assessment of underground energy storage potential to support the energy transition in the netherlands. *First Break*, 37:57, 10 2019. doi: 10.3997/1365-2397.n0039.

L. Kopal, P. Cizek, and J. Milička. Geological model of lobodice underground gas storage facility based on 3d seismic interpretation. *Contributions to Geophysics and Geodesy*, 46:125–135, 6 2016. ISSN 1338-0540. doi: 10.1515/CONGEO-2016-0009. URL https://journal.geo.sav.sk/cgg/article/view/149.

M. Lysyy, M. Fernø, and G. Ersland. Seasonal hydrogen storage in a depleted oil and gas field. 2021. doi: 10.1016/j.ijhydene.2021.05.030. URL www.sciencedirect.com.

M. H. McCay. Chapter 23 - hydrogen: An energy carrier, 2014. URL https://www.sciencedirect.com/science/article/pii/B9780080994246000235.

F. Molz. Advection, dispersion, and confusion. *Groundwater*, 53:348–353, 5 2015. ISSN 1745-6584. doi: 10.1111/GWAT.12338. URL https://onlinelibrary.wiley.com/doi/full/10.1111/gwat.12338https://onlinelibrary.wiley.com/doi/abs/10.1111/gwat.12338https://ngwa.onlinelibrary.wiley.com/doi/10.1111/gwat.12338.

NAM. Norg ugs fault reactivation study and implications for seismic threat, 2016.

NederlandseEmissieautoritiet. Tarieven co2-heffing, 2022.

K. Nordahl, C. Messina, H. Berland, A. B. Rustad, and E. Rimstad. Impact of multiscale modelling on predicted porosity and permeability distributions in the fluvial deposits of the upper lunde member (snorre field, norwegian continental shelf). *Geological Society, London, Special Publications*, 387:85–109, 1 2014. ISSN 0305-8719. doi: 10.1144/SP387.10.

M. Panfilov and M. Panfilov. Underground storage of hydrogen: In situ self-organisation and methane generation. *Transport in Porous Media 2010 85:3*, 85:841–865, 6 2010. ISSN 1573-1634. doi: 10.1007/S11242-010-9595-7. URL https://link.springer.com/article/10.1007/s11242-010-9595-7.

A. Perez and S. Dupraz. Patagonia wind - hydrogen project: Underground storage and methanation. *21st World Hydrogen Energy Conference*, 2016.

RAG. Underground sun storage 2030, 2021.

K. Ramesh Kumar and H. Hajibeygi. Multiscale simulation of inelastic creep deformation for geological rocks. *Journal of Computational Physics*, 440:110439, sep 2021. ISSN 00219991. doi: 10.1016/j.jcp.2021.110439. URL https://linkinghub.elsevier.com/retrieve/pii/S002199912100334X.

K. Ramesh Kumar, A. Makhmutov, C. J. Spiers, and H. Hajibeygi. Geomechanical simulation of energy storage in salt formations. *Scientific Reports 2021 11:1*, 11(1):1–24, oct 2021. ISSN 2045-2322. doi: 10.1038/s41598-021-99161-8. URL https://www.nature.com/articles/s41598-021-99161-8.

Rijksoverheid. *Klimaatakkoord*. 2019.

V. K. Shrivastava. Physical dispersion in compositional reservoir simulation, 2003. URL https://prism.ucalgary.ca/handle/1880/39841.

G. Strobel, B. Hagemann, T. M. Huppertz, and L. Ganzer. Underground bio-methanation: Concept and potential. *Renewable and Sustainable Energy Reviews*, 123:109747, 5 2020. ISSN 1364-0321. doi: 10.1016/J.RSER.2020.109747.

R. Tarkowski. Underground hydrogen storage: Characteristics and prospects. *Renewable and Sustainable Energy Reviews*, 105:86–94, 5 2019. ISSN 1364-0321. doi: 10.1016/J.RSER.2019.01.051.

R. Terstappen. Analysis of mixing during hydrogen storage in gas reservoir, 9 2021.

E. M. Thaysen, S. McMahon, G. J. Strobel, I. B. Butler, B. T. Ngwenya, N. Heinemann, M. Wilkinson, A. Hassanpouryouzband, C. I. McDermott, and K. Edlmann. Estimating microbial growth and hydrogen consumption in hydrogen storage in porous media. *Renewable and Sustainable Energy Reviews*, 151:111481, 11 2021. ISSN 1364-0321. doi: 10.1016/J.RSER.2021.111481.

S. van Gessel, B. Jaarsma, W. Eikelenboom, and R. Groenenberg. Haalbaarheidsstudie offshore ondergrondse waterstofopslag, 7 2022. URL https://www.rijksoverheid.nl/documenten/rapporten/2022/07/01/22286281bijlage-1-haalbaarheidsstudie-offshore-ondergrondse-waterstofopslag.

W. van Rooijen, L. Hashemi, M. Boon, R. Farajzadeh, and H. Hajibeygi. Microfluidics-based analysis of dynamic contact angles relevant for underground hydrogen storage. *Advances in Water Resources*, 164: 104221, 2022. ISSN 0309-1708. doi: https://doi.org/10.1016/j.advwatres.2022.104221. URL https://www.sciencedirect.com/science/article/pii/S0309170822000938.

G. Wang, G. Pickup, K. Sorbie, and E. Mackay. Scaling analysis of hydrogen flow with carbon dioxide cushion gas in subsurface heterogeneous porous media. 2021. doi: 10.1016/j.ijhydene.2021.10.224. URL www.sciencedirect.com.

A. E. Yekta, J.-C. Manceau, S. Gaboreau, M. Pichavant, P. Audigane, and B. A. E. Yekta. Determination of hydrogen-water relative permeability and capillary pressure in sandstone: Application to underground hydrogen injection in sedimentary formations. *Transport in Porous Media*, 122:333–356, 2018. doi: 10.1007/s11242-018-1004-7. URL https://doi.org/10.1007/s11242-018-1004-7.